SYNTHESIS AND CHARACTERIZATION OF CONJUGATED POLYMERS WITH POLYHEDRAL OLIGOMERIC SILSESQUIOXANE PENDANT GROUPS

A THESIS SUBMITTED TO
THE GRADUATE SCHOOL OF NATURAL AND APPLIED SCIENCES
OF
MIDDLE EAST TECHNICAL UNIVERSITY

BY

SALİH ERTAN

IN PARTIAL FULFILLMENT OF THE REQUIREMENTS
FOR
THE DEGREE OF DOCTOR OF PHILOSOPHY
IN
POLYMER SCIENCE AND TECHNOLOGY

DECEMBER 2017

Approval of the thesis:

SYNTHESIS AND CHARACTERIZATION OF CONJUGATED POLYMERS WITH POLYHEDRAL OLIGOMERIC SILSESQUIOXANE PENDANT GROUPS

submitted by **SALİH ERTAN** in partial fulfillment of the requirements for the degree of **Doctor of Philosophy in Polymer Science and Technology Department, Middle East Technical University by**,

Prof. Dr. Gülbin Dural Ünver
Dean, Graduate School of **Natural and Applied Sciences** _____

Prof. Dr. Necati Özkan
Head of Department, **Polymer Science and Technology** _____

Prof. Dr. Cevdet Kaynak
Supervisor, **Metallurgical and Materials Eng. Dept., METU** _____

Prof. Dr. Atilla Cihaner
Co-Supervisor, **Chemical Eng. and Applied Chemistry Dept., Atılım University** _____

Examining Committee Members:

Prof. Dr. Ahmet M. Önal _____
Chemistry Dept., METU

Prof. Dr. Cevdet Kaynak _____
Chemistry Dept., METU

Prof. Dr. Ali Çırpan _____
Chemistry Dept., METU

Assoc. Prof. Dr. Seha Tirkeş _____
Chemical Eng. and Applied Chemistry Dept.,
Atılım University

Assoc. Prof. Dr. Murat Kaya _____
Chemical Eng. and Applied Chemistry Dept.,
Atılım University

Date: 20.12.2017

I hereby declare that all information in this document has been obtained and presented in accordance with academic rules and ethical conduct. I also declare that, as required by these rules and conduct, I have fully cited and referenced all material and results that are not original to this work.

Name, Last name : Salih Ertan

Signature :

ABSTRACT

SYNTHESIS AND CHARACTERIZATION OF CONJUGATED POLYMERS WITH POLYHEDRAL OLIGOMERIC SILSESQUIOXANE PENDANT GROUPS

Ertan, Salih

Ph.D., Department of Polymer Science and Technology

Supervisor: Prof. Dr. Cevdet Kaynak

Co-Supervisor: Prof. Dr. Atilla Cihaner

December 2017, 151 pages

In this thesis, a series of monomers covalently bonded to polyhedral oligomeric silsesquioxane (POSS) pendant group was designed and synthesized. POSS group is a hybrid organic-inorganic nanostructure with 1 to 3 nm diameter. POSS which has a cage structure is mainly composed of silicon (Si) (at vertices) and oxygen (O) (in the middle of the edge). POSS nanostructure can be modified through the vertices with organic functional groups. POSS groups provide different properties, such as thermal robustness, mechanical endurance, electrochemical stability etc. to the matrices in which they are added. These groups are attached to the monomers chemically and the possible effects of the POSS units on electrochemical and optical behaviors, thermal stability and solubility of the polymers have been investigated.

Alkyl-substituted POSS cage is combined with 3,4-ethylenedioxythiophene (EDOT-POSS), 3,4-propylenedioxythiophene (ProDOT-POSS) and 3,4-ethylenedioxyselenophene (EDOS-POSS). Chemical and electrochemical polymerizations of EDOT-POSS monomer were achieved successfully and the resulting polymers (PEDOT-POSS) were found to be soluble. Both chemically and electrochemically obtained polymers are soluble in common organic solvents like

dichloromethane, chloroform, tetrahydrofuran etc. PEDOT-POSS has somewhat higher band gap (1.71 eV with λ_{max}= 618 nm) than its parent PEDOT (1.60 eV with λ_{max}= 627 nm) and as expected PEDOT-POSS exhibits higher optical contrast (74% at 618 nm) and coloration efficiency (582 cm^2/C for 100% switching), lower switching time (0.9 s), higher electrochemical stability (93% of its electroactivity retains after 5000 cycles under ambient conditions) when compared to PEDOT. Photocatalytic activity of PEDOT-POSS polymer on dye removal was also investigated. When compared to parent PEDOT polymer, PEDOT-POSS showed better performance on removal of dye in shorter exposure time to UV light. While PEDOT can remove 95% of the dye in an hour, PEDOT-POSS can remove nearly all the dye in the same period of time.

In addition, ProDOT-POSS was also polymerized chemically and electrochemically resulting in soluble polymers (PProDOT-POSS). Both chemically and electrochemically obtained polymers were completely soluble in common organic solvents like toluene, dichloromethane, chloroform, tetrahydrofuran, etc. It is possible to dope and dedope the polymers successfully in film and solution forms via both chemical and electrochemical methods. Electroactive polymer film has a band gap of 1.95 eV with a maximum absorption band at 555 nm. Also, soluble polymers have a reddish orange emission centered at 605 nm in toluene solution. Furthermore, PProDOT-POSS polymers have a percent transmittance change of 55% at 555 nm, high transparency at oxidized state, low switching time (~1.0 s) and high coloration efficiency (504 cm^2/C for 95% switching).

Finally, electroactive EDOS-POSS monomer was successfully polymerized via both chemical and electrochemical methods. The obtained polymer called PEDOS-POSS was solution-processable and soluble in common organic solvents like tetrahydrofuran, toluene, dichloromethane, chloroform, etc. PEDOS-POSS polymer exhibited electrochromic behavior: pure blue when neutralized and highly

transparent when oxidized. When compared to the parent PEDOS (1.40 eV with λ_{max}= 673 nm), the polymer film has a somewhat higher band gap (1.50 eV with λ_{max}= 668 nm and 724 nm). Also, PEDOS-POSS exhibited high optical contrast ratio (59%) and coloration efficiency (593 cm^2/C for 95% switching) with a low switching time (0.9 s) due to the presence of POSS cage in the polymer backbone. Furthermore, the polymers exhibited fluorescent properties and exhibited a pinkish orange emission centered about at 640 nm.

Keywords: Conjugated polymers, conductive polymers, Polyhedral oligomeric silsesquioxane, POSS, 3,4-ethylenedioxthiophene, EDOT, poly(3,4-ethylenedioxythiophene), PEDOT, poly(3,4-propylenedioxythiophene), PProDOT, 3,4-ethylenedioxyselenophene, EDOS, poly(3,4-ethylenedioxyselenophene), PEDOS, electrochromism, electrochromic device, photocatalysis, dye removal.

ÖZ

POLİHEDRAL OLİGOMERİK SİLSESKUOKZAN GRUPLARI ASILI KONJÜGE POLİMERLERİN SENTEZİ VE KARAKTERİZASYONU

Ertan, Salih

Doktora, Polimer Bilim ve Teknolojisi Bölümü

Tez Yöneticisi: Prof. Dr. Cevdet Kaynak

Eş Danışman: Prof. Dr. Atilla Cihaner

Aralık 2017, 151 sayfa

Bu tezde, kovalent bağ ile bağlı polihedral oligomerik silseskuokzan (POSS) sarkıt grupları asılı monomerler tasarlanmış ve sentezlenmiştir. POSS grubu 1nm'den 3 nm'ye kadar çapa sahip hibrit organik-anorganik bir yapıdır. Kafes yapısına sahip POSS genellikle köşelerinde silicon (Si) ve kenar ortalarında oksijen (O) atomlarından oluşmaktadır. POSS yapıların köşelerinden bağlanabilen organik fonksiyonel gruplar ile çeşitlendirilebilir. POSS yapıları katıldıkları matrise termal dayanıklılık, mekanik dayanım, elektrokimyasal kararlılık gibi farklı özellikler sunarlar. Bu gruplar monomerlere kimyasal olarak bağlanmış ve POSS biriminin polimerlerin elektrokimyasal ve optiksel davranımına, termal kararlılığına ve çözünürlüğe olan olası etkileri incelenmiştir.

Alkil sübstitüeli POSS kafes yapısı 3,4-etilendioksitiyofen (EDOT-POSS), 3,4-propilendioksitiyofen (ProDOT-POSS) ve 3,4-etilendioksiselenofen (PEDOS-POSS) ile birleştirilmiştir. EDOT-POSS monomerinin kimyasal ve de elektrokimyasal yollarla polimeri (PEDOT-POSS) elde edilmiş ve ilgili polimelerin çözünür olduğu bulunmuştur. Hem kimyasal hem de elektrokimyasal olarak elde edilen polimerlerin diklorometan, kloroform, tetrahidrofuran gibi genel organik çözücülerde çözünür olduğu görülmüştür. PEDOT-POSS (1.71 eV, λ_{maks}= 618 nm) PEDOT'a göre (1.60 eV, λ_{maks}= 627 nm) bir miktar yüksek bant aralığına sahip çıkmıştır ve PEDOT-

POSS, PEDOT ile kıyaslandığında beklenildiği gibi daha yüksek optik zıtlık (618 nm'de 74%) ve renklenme etkinliği (582 cm^2/C, 100% anahtarlanmada), daha düşük anahtarlanma süresi (0,9 saniye), daha yüksek elektrokimyasal kararlılık (normal çevre koşullarında 5000 döngü sonrası elektroaktivitesinin %93'ünü korumuştur. Bunlara ek olarak PEDOT-POSS polimerinin fotokatalitik aktivitesi de araştırılmıştır. Boya giderimi çalışmasında daha kısa süre mor ötesi ışığa maruz bırakılarak PEDOT ana polimerine kıyasla daha iyi sonuç verdiği gözlenmiştir. PEDOT polimeri 1 saat içerisinde %95 giderim sağlarken PEDOT-POSS polimeri boyanın neredeyse tamamını gidermiştir.

Ayrıca, ProDOT-POSS kimyasal ve elektrokimyasal olarak polimerleştirilmiş ve elde edilen polimerlerin çözünür oldukları görülmüştür. Kimyasal ve elektrokimyasal olarak elde edilen polimerler tolüen, diklorometan ve kloroform vb. gibi genel organik çözücülerde tamamen çözünürdürler. Polimerlerin film halinde ya da çözelti halinde hem elektrokimyasal hem de kimyasal olarak katkılanması ve katkılanmaması mümkündür. Elekroaktif polimer 555 nm maksimum soğurma bandı ile 1.95 eV bant aralığına sahiptir. Çözünür polimer tolüen içerisinde 605 nm'de merkezlenmiş kırmızımsı turuncu emisyona sahiptir. Bunlara ek olarak PProDOT-POSS polimeri 555 nm'de %55 yüzde geçirgenlik değerine, yükseltgen halde yüksek saydamlığa, düşük anahtarlanma süresine (~1.0 s) ve yüksek renklenme etkinliğine (504 cm^2/C, 95% anahtarlanma) sahiptir.

Son olarak, elektroaktif EDOS-POSS monomeri kimyasal ve elektrokimyasal yöntemler ile başarılı bir şekilde polimerleştirilmiştir. Hem kimyasal hem de elektrokimyasal polimerlerin tetrahidrofuran, tolüen, diklorometan ve kloroform vb. gibi genel organik çözücülerde çözünür olduğu gözlemlenmiştir. PEDOS-POSS polimeri nötr halde saf mavi, yükseltgen halde ise oldukça saydam elektrokromik davranım göstermiştir. Ana PEDOS polimeri (λ_{maks}= 673 nm'de 1,40 eV) ile kıyaslandığında PEDOS-POSS polimeri (λ_{maks}= 668 nm and 724 nm'de 1,50 eV) bir

miktar yüksek bant aralığına sahip olduğu gözlemlenmiştir. Polimer iskeletinde bulundurduğu POSS kafes yapıları sayesinde PEDOS-POSS %59 optik zıtlık, %95 anahtarlanmada 593 cm^2/C renklenme etkinliği ve 0,7 saniye anahtarlanma süresine sahiptir. Ayrıca polimer pembemsi turuncu emisyon ile floresan özellik de göstermiştir.

Anahtar Kelimeler: Konjüge polimer, İletken Polimer, Polihedral oligomerik silseskuokzan, POSS, 3,4-etilendioksitiyofen, EDOT, poli(3,4-etilendioksitiyofen), PEDOT, poli(3,4-propilendioksitiyofen), PProPOT, 3,4-etilendioksiselenofen, EDOS, poli(3,4-etilendioksiselenofen), PEDOS, elektrokromizm, elektrokromik cihaz, foto-kataliz, boya giderimi.

To my parents and my wife,

ACKNOWLEDGMENTS

I would like to thank my supervisor Prof. Dr. Cevdet Kaynak for his support, understanding and patience. I also thank him for giving me a chance to work in distance.

I would like to give my sincere thanks to my co-advisor Prof. Dr. Atilla Cihaner for everything he provided me not only academically but also mentally. He has been a great role model to me and I am sure he will be too. I also thank him for being always my side for every obstacle that I have faced with during these years.

I also want to thank my former and present lab-mates Emine Gül Cansu Ergün, Barış and Canan Karabay, Saad Mahmood Saeed Al-Ogaidi, Dheyaa Dawood Salman Al-Mahdawi, Mohammed Al_Jumaili, Mohammed Salman and Muhammed Ayad for the mostly-enjoyable time that we spent together.

I also want to thank people of Atilim University, Chemical Engineering and Applied Chemistry Department especially Belgin İşgör, Seha Tirkeş and Murat Kaya and, former and present colleagues Ceyhan, Seda, Ceren, Zuhal, Gözde, Elif and Tuğçe for their support.

I would like to thanks to a member of Önal Group, Deniz Çakal for her help and friendly attitude for every time I need.

I also thank Tuğrul Akpolat for his friendship, patience and help during the preparation of this thesis.

I would like to thank to my friends from Northwestern University and Chicago, Kezban, Gürkan, Taner, Timur, Ahmet, Constanza, Reddy, Matthew, Brain, and Ferdinand.

I want to thank to my parents for supporting me through my long education years and giving me their endless love.

Last but not least, I do thank to my wife Gülçin for her support, patience and understanding during these years. She always believed in me and pushed me to go further. Her love has been the greatest motivation for me. I want to repeat one more time, her love, touching my heart, makes me a Don Quixote for every challenge in my life.

TABLE OF CONTENTS

LIST OF FIGURES

FIGURES

LIST OF SCHEMES

SCHEMES

LIST OF TABLES

ABBREVIATIONS

ACN Acetonitrile

Ar Argon

CB Conducting band

CE Coloration efficiency

CIE Commission Internationale de I'Eclairge

CP Conducting polymer

CV Cyclic voltammetry

DCM Dichloromethane

ECD Electrochromic device

EDOS 3,4-Ethylenedioxyselenophene

EDOT 3,4-Ethylenedioxythiophene

E_g Band gap

GPC Gel permeation chromatography

HOMO Highest Occupied Molecular Orbital

HRMS High-resolution mass spectrometry

ITO Indium tin oxide

LUMO Lowest Unoccupied Molecular Orbital

MEH-PPV Poly(2-methoxy-5-(2′-ethyl-hexyloxy)-1,4-phenylene vinylene))

NMR Nuclear Magnetic Resonance

PAc Polyacetylene

PANI Polyaniline

PC Propylene carbonate

PEDOT Poly(2,3-dihydrothieno[3,4-b][1,4]dioxine)

PMMA Poly(methyl methacrylate)

POSS Polyhedra oligomeric silsesquioxane

PPy Polypyrrole

PRODOT 3,4-propylenedioxythiophene

Pt Platinum

PXDOT Poly(alkylenethiophene)

RGB Red-green-blue

TBABF4 Tetrabutyl ammonium tetrafluoroborate

TBAH Tetrabutylammonium hexafluorophosphate

THF Tetrahydrofuran

TLC Thin layer chromatography

TMS Tetramethylsilane

VB Valence band

CHAPTER 1

INTRODUCTION

Organic polymers or plastics had been known as poor electronic conductors and excellent insulators so that they have been used as insulators in any electrical and electronical applications. After a discovery demonstrates that the electrical conductivity of organic conjugated polymers can be increased in significant order through oxidation and reduction, an interesting phenomenon uprose that the idea of possibility of producing plastics as conductive as metals is not a dream anymore [1-4]. A material, called as a synthetic metal [5], with flexible character and metal conductivity created a new field of application named as "Organic Electronics" which contain electrochromic devices, organic photovoltaics, organic and polymer light emitting diodes and sensor, etc. [6-12].

1.1 Conjugated Polymers

The interest on conjugated polymers showed a sharp peak after the discovery of Nobel Laureates Heeger, MacDiarmid and Shirakawa [13, 14] but to construct a solid background, it is necessary to mention about the forerunners of the field. Letheby accomplished to produce polyaniline electrochemically and showed that the powder polyaniline is colorless at reduced state and blue at its oxidized state [15]. After Letheby, Buvet and Jozefowicz carried out detailed studies and succeded to

produce polyaniline in emeraldine form by chemical oxidative polymerization [16, 17]. Besides polyaniline, polypyrrole was introduced to literature by Donald Weiss as it is synthesized from its halogenated form [18]. Poypyrrole products were insoluble black powder with good conductivity and resistivity [19]. In the same period, Natta managed to produce polyacetylene, using a coordination catalyst which is used to polymerize ethylene and propylene. In 1960s, semiconductor behavior of polyacetylene was revealed by treating it with different dopants such as boron trifluoride and ammonia [20-22].

In 1970's, Shirakawa, Heeger and MacDiarmid studied concurrently on improving the conductivity of polyacetylene film by the halogen vapor exposure resulting in an increase over a 12 order of magnitude [23]. There are some different oxidizing and reducing agents introduced by other research groups to get highly conductive polyacetylene films [24,25]. However, troubles stemming from high reactivity and handling problem of the chemical dopants made these methods not applicable for polyacetylene polymers. After a short time, Diaz et al. succeeded to produce polypyrrole film electrochemically and showed that the film is air stable with the conductivity of 100 $\Omega^{-1}cm^{-1}$ [26, 27] by benefiting from Dall'Olio's findings. On the contrary to Dall'Olio's powdery in soluble precipitate, the film could be peeled off from the surface of the platinum electrode [28]. This method also showed not only the electrochemical polymerization of pyrrole onto electrode surface is achievable but also the electrochemical characterization of the film (switch between neutral and oxidized states) is possible on the electrode.

In today's knowledge, creating a conducting polymer having desired band gaps, soluble, stable and high performance is possible. Chemical architecture can be designed according to the need for the applications like electrochromic devices, polymer light emitting diodes, organic photovoltaics, organic field effect transistors and sensors etc. [1, 4, 6-12, 29-32].

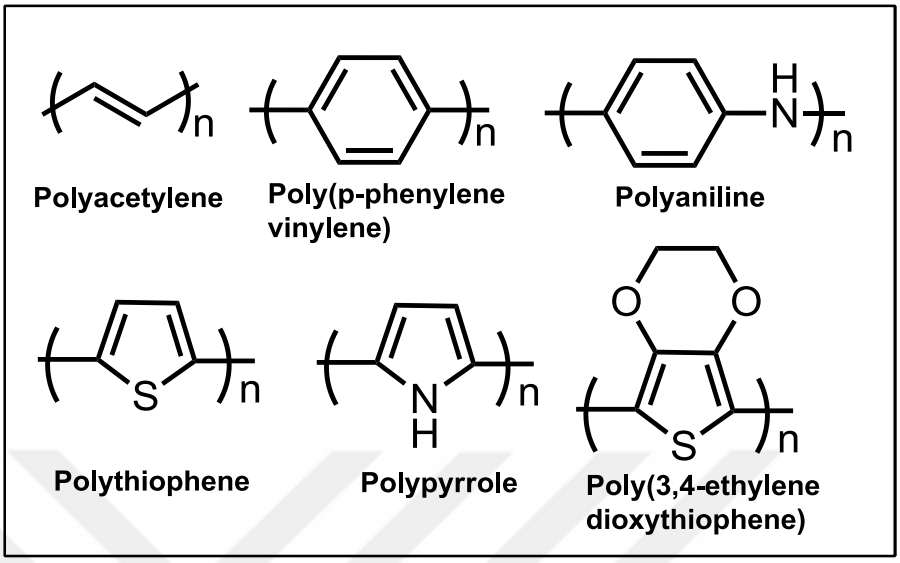

Figure 1.1. Common and mostly used conjugated polymers from the literature.

1.2 Band Gap Theory

Conduction characteristics of insulators, semiconductors and metals have been described by band gap theory. Theory defines the band gap (E_g) as the difference between Lowest Unoccupied Molecular Orbital (LUMO) which is named as the conduction band and Highest Occupied Molecular Orbital (HOMO) which is named as the valence band. Metals have excellent electrical conductivity since band gap or energy gap in metals is very low (E_g~0) or they have extra electrons in valence band. The band gap in semi-conductors is close enough to get reasonable conductivity (E_g< 3.0 eV) with a small push for electrons to reach valence band. However, in insulator case the energy gap is large (E_g> 3.0 eV) and due to that electron movement from conduction band to valence band is not possible. [33]

In organic semi-conductors band gap depends on effective conjugation length. While the conjugation length increases which means addition of repeating units to polymer backbone, the difference between HOMO and LUMO level decreases due to the formation of new energy levels (π-π* orbitals). Figure 1.2 shows newly formed molecular orbitals by monomer addition to the backbone and hence the emerging of valence and conduction bands.

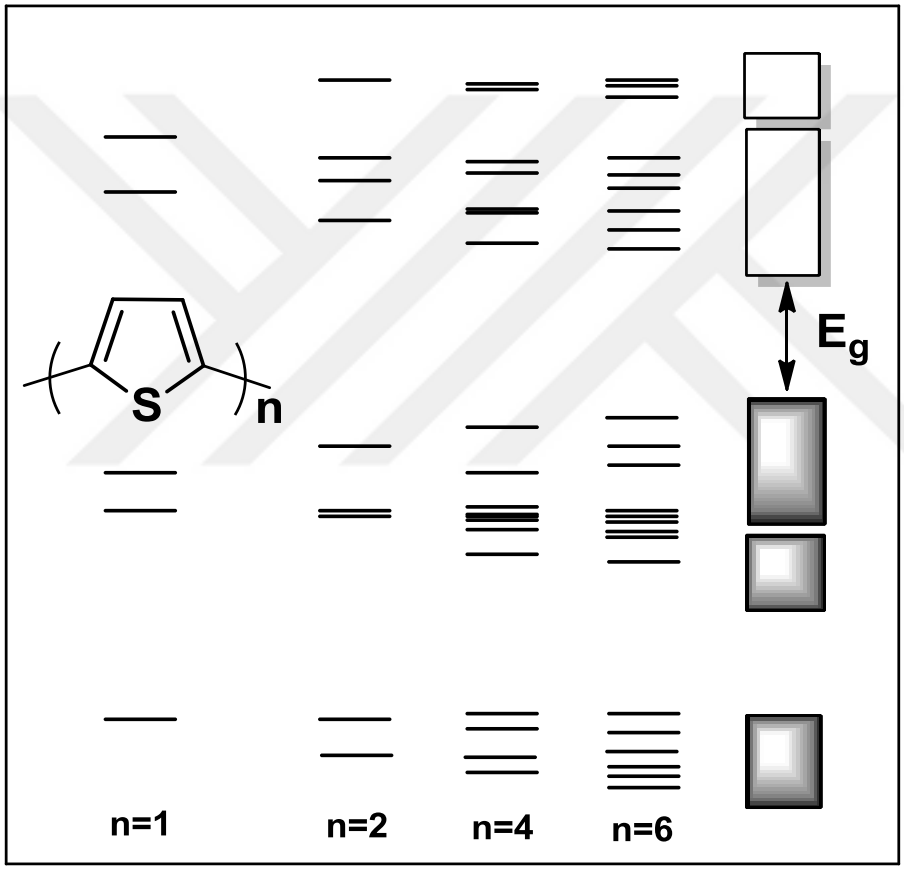

Figure 1.2. Molecular orbital and band formation during polymerization.

The gap between energy bands can generally be determined in two different ways via electrochemically or optically. In electrochemical way, the potentials for removal of an electron from HOMO and the arrival to LUMO level are determined [34-36]. Another and more common method for the band gap calculation is through

determining electro-optical behavior of the neutral state of the conducting polymer. In electronic absorption spectra, the energy gap between HOMO and LUMO is specified as the onset point for the π-π^* transition [37].

The population of electrons in the empty conduction band can be increased by exciting the electrons with thermal or photochemical interventions to overcome the band gap. In order to do this, chemical or electrochemical doping can be applied to semiconductors and hence better conductivity can be achieved. During doping process, charge carriers, which are named as holes and electrons, are generated [38].

1.3 Doping Process

Doping process occurs by injection and ejection of charges upon disturbing the structure of conducting polymers (CPs) resulting in creation of a hole and an electron. If there is a removal of an electron from the material, it is called as p-type doping and if there is an addition of an electron, it is called as n-type doping (Figure 1.3).

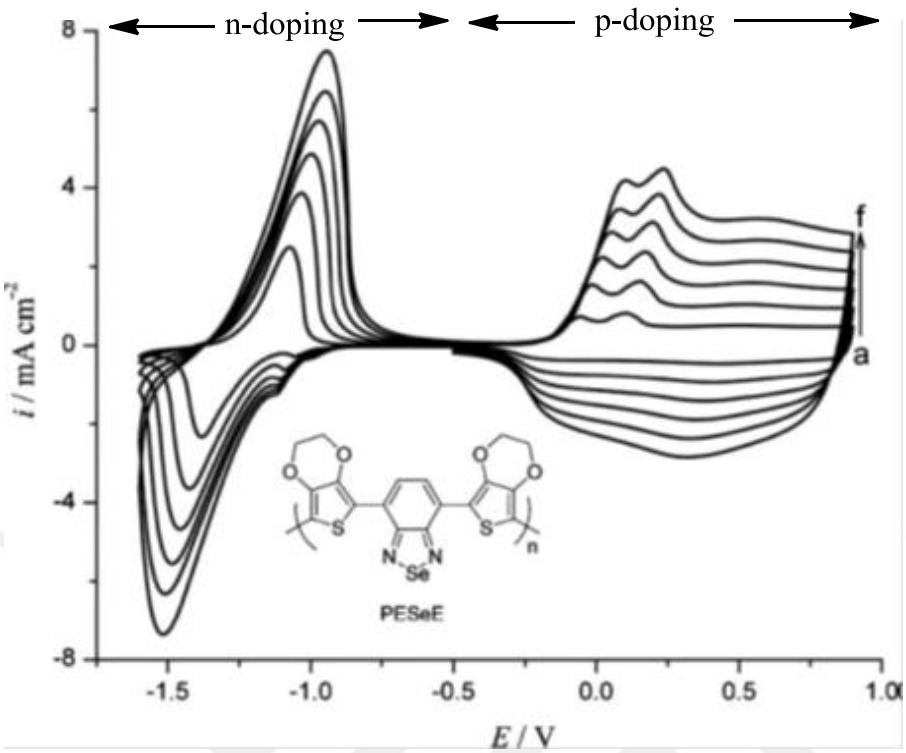

Figure 1.3. Cyclic voltammograms of n- and p-doped Poly(4,7-di-2,3 dihydrothieno[3,4-b][1,4]dioxin-5-yl-2,1,3-benzoselenadiazole) film in tetrabutylammonium hexafluorophosphate in dichloro methane solution at different scan rates [39].

The study on conductivity of polyacetylene by exposure to iodine proved that the conductivity of conjugated polymers can be increased in significant orders upon chemical doping. Chemical doping can be achieved by the exposure to I_2, Br_2, SbF_5 [40] etc. and the rate of doping can be kept under control by changing the parameters like concentration of dopant or exposure time to dopant. On the other hand, after a time chemical doping started to seem as a problematic method in utilizing the conducting polymers due to the high reactivity and handling problems of dopants. These problems drove scientists to find a better way to dope conducting polymers and finally Nigrey and coworkers showed that reversible electrochemical doping of

polyacetylene is achievable. [41] In addition to that, Diaz et al. performed an experiment and accomplished not only the reversible switch between the neutral and oxidized state of the polymer, but also electrochemical polymerization of a heterocyclic polymer “polypyrrole” [26, 27].

Figure 1.4 shows the allowed electronic transition states in poly(3,4-ethylenedioxythiophene) (PEDOT) occurring during doping. When the polymer is oxidized, electron movement starts from valence band of the conjugated polymer resulting in a formation of a radical cation (polaron). This process induces the creation of half-filled polaron levels between valence and conduction bands. Oxidation of the conjugated polymer by doping causes changes in the molecular structure at the same time due to facilitated charge transfer along the backbone, and the resulting geometry is called as quinoid-like structure. In order to preserve the electroneutrality, anions start to diffuse into conjugated polymer film. Further doping causes more electron ejection from the polymer chain and hence dications (bipolaron) are formed. While polaron formation continues upon doping, the generation of new energy levels between valence and conduction bands increases.

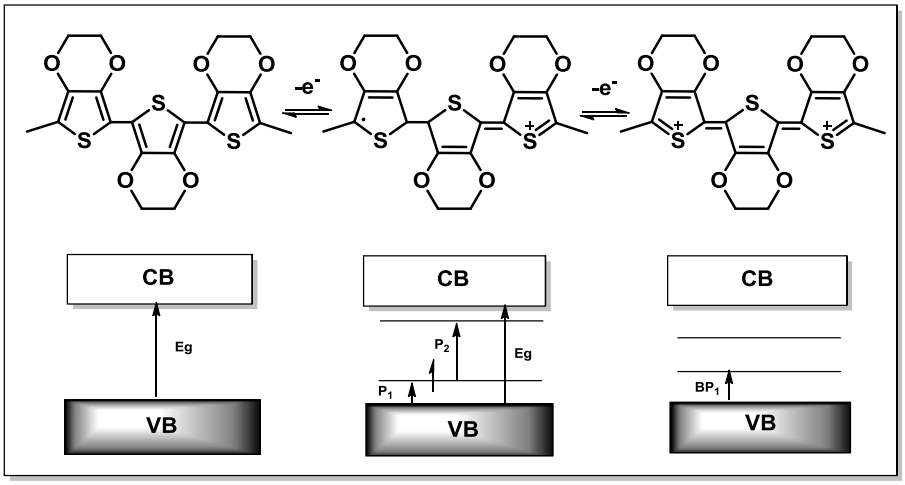

Figure 1.4. Doping mechanism and polaron and bipolaron formation on poly(3,4-ethylenedioxythiophene).

During doping process, optical changes in the polymer film accompany the chemical changes as well. As shown in Figure 1.5, when oxidation starts, a significant decrease is observed from 400 nm to 700 nm, which corresponds to the creation of charge carriers (polarons) in PEDOT polymer chain, and by further oxidation a peak arises beyond 800 nm, which is related to the creation of low-energy charge carriers (bipolarons). PEDOT exhibits dark blue color at neutral state with a band gap of 1.65 electron volts (eV) and starts to bleach upon oxidation to give sky blue color.

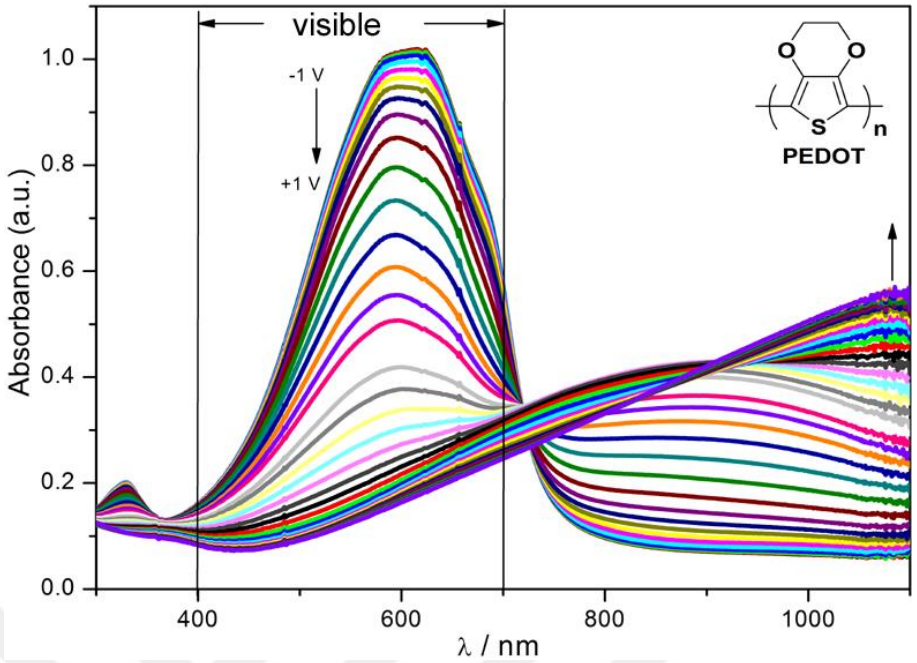

Figure 1.5. UV-Vis spectra of PEDOT polymer film under applied external potential in 0.1 M tetrabutylammonium hexafluorophosphate /acetonitrile.

1.4 Band Gap Engineering

The band gap of conjugated polymers depends on certain parameters involving intramolecular and intermolecular interactions. While intramolecular parameters stem from substituents composing polymer chain and the stereochemistry of the functional groups on the chain, intermolecular parameters are the result of interactions between chains. In a nut shell, these parameters are the manifestations resulting from interchain interactions, aromatic resonance energy, substituents, bond alternation and coplanarity deviation [42].

Bond length alteration arises from the difference in the length of single and double bond. It can also be defined as the density of aromatic and quinoid character in the

conjugated polymer chain. When compared to aromatic form, quinoidal form exhibits lower band gap [43,44]. More specifically, heterocyclic conjugated polymers such as polypyrrole and polythiophene have nondegenerate ground state forms including both aromatic and quinoid structure.

Coplanarity deviation results from the twist of the single bond connecting the aromatic rings. The rotation around the single bond bridging the aromatic rings prevents the π orbitals from overlapping which causes a decrease in the effective conjugation length. A decrease in the effective conjugation length is fundamentally a reason for an increase in the band gap [45-49]. In order to overcome this, to an aromatic monomer like polythiophene a flexible side chain groups can be attached [50]. However, if the regioregularity trough the polymer chain cannot be obtained, the deviation in the planarity increases due to the steric interaction resulting in an increase in the band gap.

Resonance energy of the monomer is another key point especially in the case of poly(aromatics). The changes in the aromaticity originating from resonance are the challenge between π-electron delocalization through the polymer chain and their confinement in the aromatic ring. Consequently, an increase will be observed when the resonance stabilization energy increases which causes a decrease in the delocalization of π-electro [51].

It also known that electrochemical and optical properties of conjugated polymers depend on the interactions between polymer chains. The band gap can shift significantly when strong π-stacking interactions are observed regarding the relative orientations of the neighboring polymer chains [52,53].

One of the most important parameters is the inductive and mesomeric effect of substituents for band gap engineering. As it seen in Figure 1.6, introduction of electron withdrawing substituents decreases the LUMO level energy and hence causes a reduction in the band gap energy. In addition to that, electron donating

groups increase the HOMO level energy, which causes a decrease in the band gap as well.

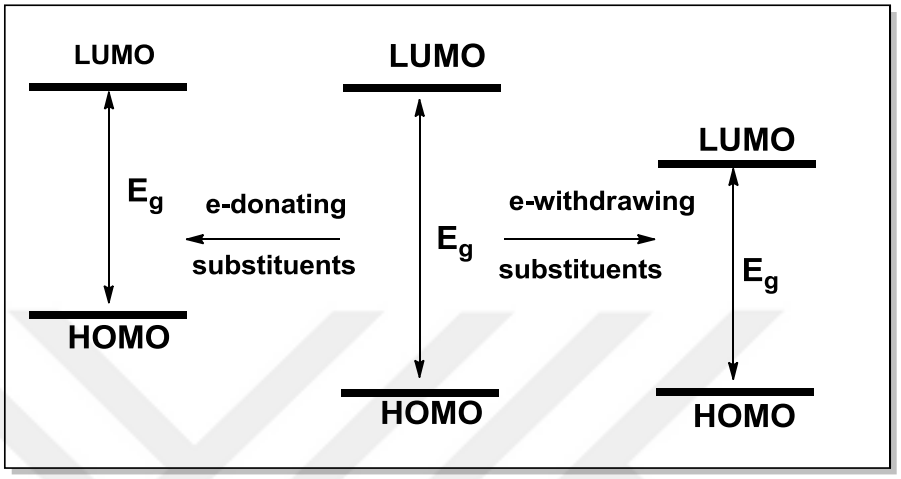

Figure 1.6. Substituents effects on the HOMO and LUMO level energies.

The substituent effect allows scientist to tune the band gap of conjugated polymers by playing the HOMO and LUMO level energies. One of the best examples showing donor substituents effect is poly(alkylenedioxythiophenes) (PXDOTs). By introducing oxygens on thiphene ring from 3- and 4- positions with an alkyl bridge on top, lone pair electrons can start flowing to thiophene ring. Consequently, a decrease is observed in the band gap following the raise in the HOMO level. In addition to that, oxidation onset potential of PXDOTs compared to thiophene shifts to lower potentials. For example, for neutral PEDOT, HOMO level energy is at -4.1 eV and band gap energy is around 1.65 eV.

PEDOT is one of the most important and mostly used polymers in the conducting polymer family. PEDOT exhibits superior properties when compared to thiophene and most of its derivatives. PEDOT has high conductivity, relatively low HOMO

level and band gap energy, optical reversibility, high stability at doped state, remarkable stability against air humidity and durability over multiple switches, etc. However, PEDOT polymer is not soluble in organic solvents and water and this problem limits its use in industrial application like spray coating ink printing and spin coating [54].

In order to overcome solubility problem of PEDOT, there are some methods utilized like functionalization of the ethylene bridge with alkyl chain and facilitating different surfactants and dispersants (e.g. polystyrenesulfonate (PSS^-)). [55-58] Functionalization through the bridge causes some changes in the electrochemical and optical properties of the obtained polymers [55,58]. Moreover, PSS^- containing PEDOT which is water-soluble may contain excess immobilized counterion preventing PEDOT from reducing fully to its neutral form. This limits utilization of PEDOT as an active material in electrochemical devices.

1.5 A Different Type of Heterocyclic Polymers; Polyselenophenes

As it is stated above, the band gap of the polymers can be tuned by different approaches. One of these approaches is the replacement of the heteroatom in the heterocyclic polymer backbone. EDOT and its derivatives were discussed in the previous section. The sulfur in the heterocyclic thiophene group can be replaced with different atoms such as selenium [59-62] and tellurium [63-66].

Selenium atom provides some different properties when compared to sulfur. Selenium with more-metallic character has larger atomic radius and lower electronegativity and shows greater polarizability. These properties created an

expectation that the possibility of producing a superior heterocyclic monomer and as a result production of a new class of conjugated polymers [67]. After the obstacles in producing selenophene derivatives were overcome, different types of polyselenophenes were synthesized and used in different applications. Results showed that the replacement of sulfur with selenium atom caused electrochemical and optical changes in the corresponding polymers. Polyselenophene derivatives provide better interchain charge transfer because of Se-Se interactions which allows more charge accommodation during doping. As a result the band gap is lowered and due to this reason the optical properties of polyselenophenes differ from polythiophenes. In addition to that, the quinoid structure is favored in polyselenophenes which have shorter distance (C-C bond length) between selenophene rings resulting in greater twisting energy when compared to polythiophenes. Furthermore, due to the lower aromaticity of selenophene ring, polyselenophenes have a tendency to show lower redox potential than polythiophenes [68-73].

As mentioned above, like PEDOT, poly(3,4-ethylenedioxyselenophene) (PEDOS) has a solubility problem. It is found that electrochemically synthesized PEDOS is not soluble in common solvents. Aqad et al. showed that chemically synthesized PEDOS is moderately soluble in common organic solvents which indicates that resulting product contains relatively short oligomers [74]. To overcome this insolubility problem of PEDOS, Bendikov et al. produced a series of EDOS derivatives (EDOS-C_n where n=2, 4, 6, 8, 12) by integrating alkyl chains with different chain lengths (Figure 1.6). They investigated the effect of chain length on electrochemical and optical properties of the resulting polymers. PEDOS-C_6 showed the best results with high optical contrast (ΔT= 89%), high coloration efficiency (CE= 715 cm^2/C) and highly promising optical stability (60% after 10000 cycles) [75,76]. Unfortunately, they couldn't successfully synthesized soluble polymers.

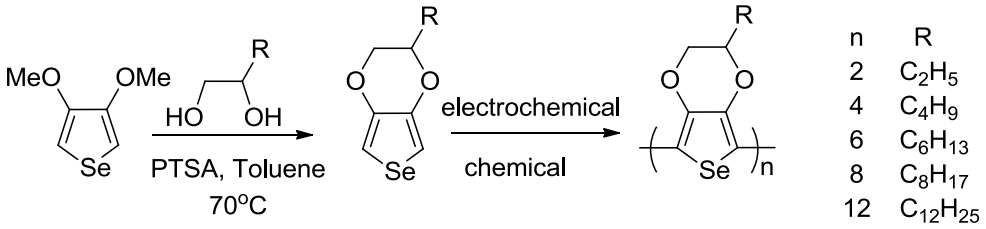

Figure 1.7. Synthesis and polymerization of EDOS-Cn derivatives [75,76].

1.6 Conducting Polymer Nanocomposites

Due to the promising results obtained from nanotechnology applications, nanomaterials gained the attention of polymer scientists. Polymer nanocomposites consisting of polymer matrix and the nano-sized filler can show superior properties when they compared to their neat analogues. Conducting polymer nanocomposites can be prepared by direct blending or in situ synthesis of polymer. They contain nano-fillers such as single or multi-walled carbon nanotubes, fullerene, graphene, metal or ceramic nanoparticles. By addition of these nano-fillers, these novel polymer nanocomposites have gained great attention since they exhibit advantages like good electroactivity, tunable band gaps and good processability [77-79].

One of the most studied nano-fillers is carbon nanotube which is known as one-dimensional filler. Addition of carbon nanotubes to conducting polymers for example polyanilines, polythiophenes and polypyrroles has been found to show quite good enhancements due to electronic interactions among the components. Polyaniline prepared by in situ polymerization [80,81] and polythiophene analogue attached covalently to carbon nanotubes [82] exhibited higher conductivities. In addition, polypyrrole coated carbon nanotubes [83,84] showed enhanced charge capacity which allows them to be used as capacitors and high performance electrodes for rechargeable batteries.

Fullerenes are nano-fillers with different incorporation on conducting polymers such as side-chain, main-chain, star-shaped, crosslinked and so on [85]. One of the most important usages of fullerenes is utilization as acceptor unit in bulk-heterojunction solar cells. Yu et al. showed that by blending fullerene, as an accepetor unit, with (poly(2-methoxy-5-(2′-ethyl-hexyloxy)-1,4-phenylene vinylene)), the incident photon to electron conversion efficiency achieved to raise 10 fold when it is compared to conventional donor–acceptor bilayer devices [86].

Graphene is a two-dimensional carbon nanofiller with a thickness of an atom. Graphene has been used as nano-filler for conducting polymers in various applications such as energy storage, sensors, high temperature electrodes and organic photovoltaic applications like solar cells [87]. Zhao and his collogue showed that graphene containing PEDOT, polyaniline and polypyrrole exhibited superior capacitive performance [88].

Metal nanoparticles with one dimensional character have been used to add different properties for conducting polymers. Ti, Ni, W and Ir as oxides and Ag and Au as in metallic form were utilized as metal nano-fillers in electrochromic conductive polymers. For example, Au-CdSe nanoparticle containing PEDOT nanocomposite exhibited higher coloration efficiency and faster kinetic response [89].

Another nano-filler is polyhedral oligomeric silsesquioxane (POSS) which has been used in different applications of conducting polymers. The thesis is about POSS containing conducting polymer so it is a necessity to open a new sub-chapter for this topic.

1.6.1 POSS Containing Conjugated Polymeric Nanocomposites

Silsesquioxanes are nano-size materials with $RSiO_{1.5}$ simple formula where R can be hydrogen atom, alkyl, alkylene, acrylate, hydroxyl, epoxy etc. functional groups. Silsesquioxanes are named as random, ladder, incomplete and complete cages

(Figure 1.8) according to the number of Si atoms and the arrangement of these atoms in space [90-94].

Inorganic POSSs with silicon-oxygen inner-center have 1 to 3 nm sizes and modifiable organic side groups. Due to these properties, they are accepted as one of the most suitable nano-fillers. The side functional groups on POSS unit can be modified according to any purpose. Moreover, by these functional groups the compatibility with the matrix that they are intended to mix can be increased. POSS units can be added directly to the matrix or can be attached to the structure by the help of covalent bonds [90,93,94]. Figure 1.8 represents the possible architectures of POSS with different functionalities. As it is mentioned above, POSS can be used as it is in the network or polymer chain matrix without any bound. It can be modified to have one functional side and it can be used as an endcap group and also it can be a pendant group attached to a polymer chain. Moreover, POSS can have two functional side groups which enable it to be used like bead on a polymer chain. Furthermore, POSS can be modified from all its corners to have a star-like geometry and from those points it can be polymerized in network structure [90,93,95,96].

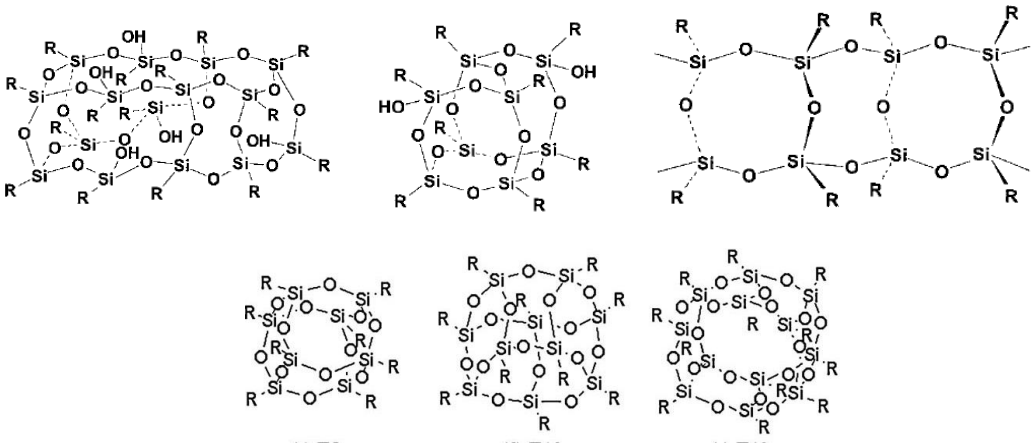

Figure 1.8. Different arrangements of POSS units: a) Random, b) Incomplete cage, c) Ladder and d) Complete cage.

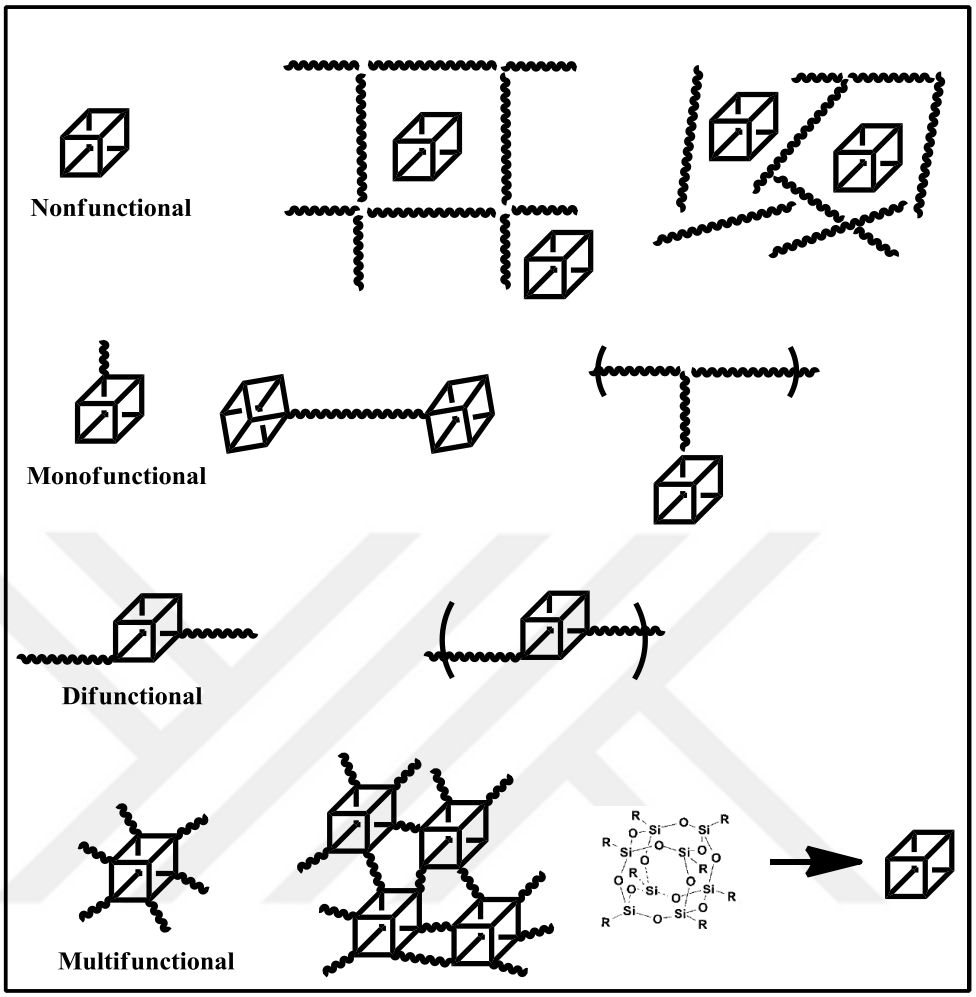

Figure 1.9. POSS functionalities used in polymer matrix.

POSS units introduced into the polymer matrix with physical or chemical interactions have abilities to enhance varieties of properties. For nearly all polymer matrices, they can affect thermal behavior like increased glass transition [97] and decomposition temperature [98], reduce viscosity [99], change mechanical behaviors like modulus and strength [100], reduce flammability [101], increase gas permeability [102], increase oxidation resistance [103], provide hydrophobic property [104], etc. Specific to conducting polymers, there are many studies showed that the incorporation of POSS units exhibits improvements in thermal, electrochemical and optical stability [90, 93, 97, 105, 106].

There are lots of studies conducted on conjugated polymers due to their potential high fluorescence quantum efficiency on light emitting diodes applications. However, there is a tendency of aggregation and/or excimer formation between chains during device applications for some soluble conjugated polymers. As it known, although polyfluorene type polymers have been used for blue light source in light emitting diodes, they exhibit undesired green light emission (keto effect) because of the oxidation occurring on thermally unstable polyfluorene backbone. In order to overcome this problem, Chen and Shim realized the integration of POSS unit on polyfluorene backbone resulting in reducing the formation of aggregates and increasing the thermal stability. Resulting POSS/Polyfluorene (Figure 1.10(a)) based electroluminescent devices showed twice better performance when compared to neat polyfluorene containing devices [107]. In this study, it is concluded that the integration of POSS groups on polymer backbone is not only significantly reducing the aggregation but also increasing the thermal stability. As in Chen's study, Shim et al. showed that the presence of bulky POSS units (Figure 1.10(b)) reduced the aggregate/excimer formation since they prevented the interactions between chains.

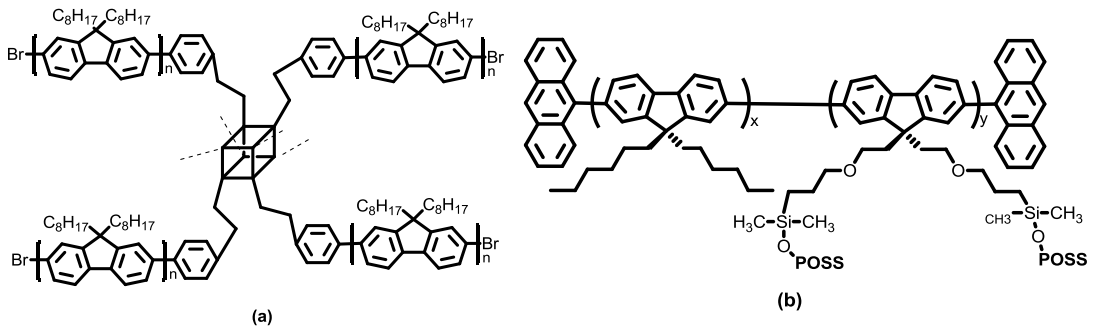

Figure 1.10. POSS containing polyfluorene derivatives synthesized by Chen et al. and Shim et al. [107]

In literature, there are some studies related with the effects of POSS units on polyaniline. polyaniline copolymers (Figure 1.9) obtained in star-like structure by facilitating each corner of POSS unit showed higher ionic conductivity than that of polyaniline because POSS units among the copolymer chains allows faster ionic diffusion by increasing the distance between the chains [108,109]. Also, it is found that these copolymers exhibited 40% enhancement in optical contrast when compared to polyaniline. In addition to those, POSS units in the center of star-like polyaniline copolymers showed improvement in the electrochemical stability.

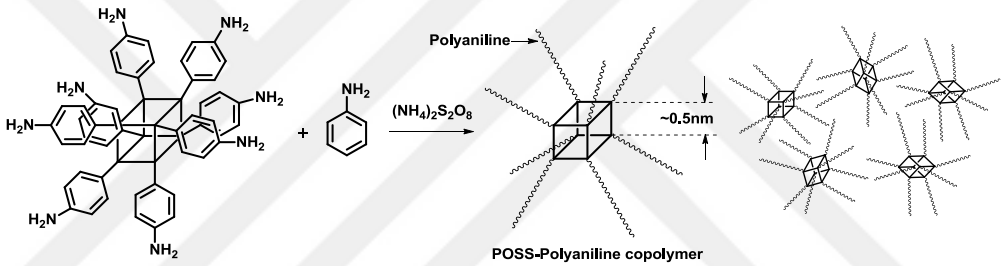

Figure 1.11. Star-like POSS based polyaniline copolymer synthesized by chemical polymerization, POSS-Polyaniline.

In another study, Toppare et al. synthesized a hybrid monomer containing POSS unit and thiophene containing organic functional groups (Figure 1.12) but they could not achieved to polymerize it [110]. The copolymer of this material with pyrrole was synthesized and this copolymer showed higher optical contrast ratio and faster switching time when compared to polypyrrole.

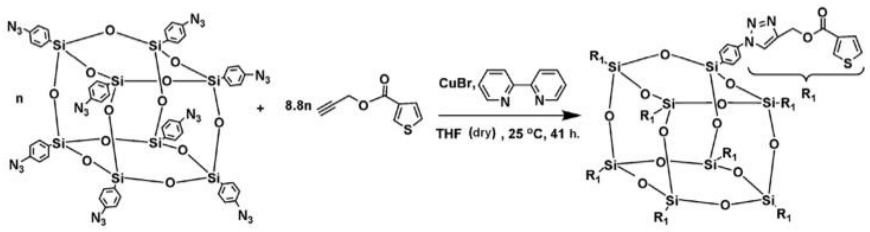

Figure 1.12. Synthesis of POSS and thiophene containing hybrid monomer.

Heeger et al. used POSS units as end-capping reagents in two different polymers poly(2-methoxy-5-(2-ethylhexyloxy)-1,4-phenylenevinylene) and poly(9,9-dihexylfluorenyl-2,7diyl) (Figure 1.11) [106]. Device application results showed that POSS containing polymers have better thermal stabilities without showing any difference in absorption, photoluminescent and electroluminescent spectra when compared to parent polymers. poly(2-methoxy-5-(2-ethylhexyloxy)-1,4-phenylenevinylene) polymer exhibited higher brightness and external quantum efficiency. poly(9,9-dihexylfluorenyl-2,7diyl) also showed higher external quantum efficiency and improved blue electroluminescent emission.

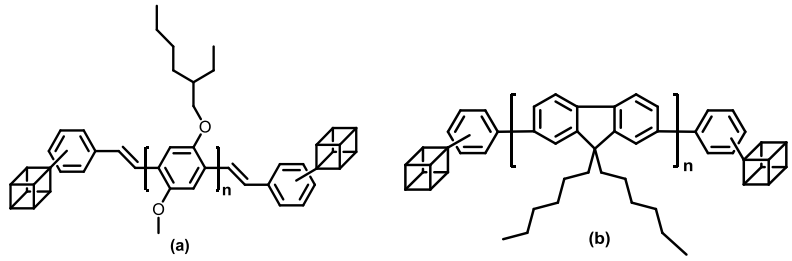

Figure 1.13. Structural appearances polymers (a) poly(2-methoxy-5-(2-ethylhexyloxy)-1,4-phenylenevinylene) and (b) poly(9,9-dihexylfluorenyl-2,7diyl)end-capped with POSS units.

In a recent study, octa-ProDOT-POSS (Figure 1.14) unit was synthesized and its PEDOT copolymer was characterized and studied [111]. Homopolymer of this unit could not be achieved. It was shown that PEDOT-co-ProDOT-POSS copolymer exhibited slightly increased impedance and significantly increased electrochemical stability on metal electrodes even with a quite low octa-ProDOT-POSS molar ratio.

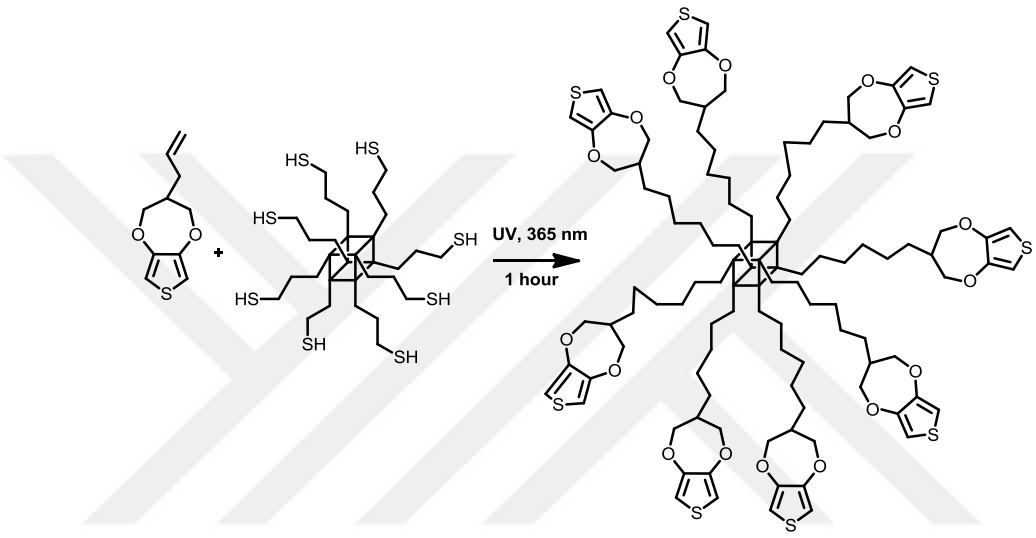

Figure 1.14. Synthesis of octa-ProDOT-POSS unit as crosslinking agent [111].

1.7 Photo-Catalysis Application of Conjugated Polymers

Heterogeneous photo-catalysis is one of the attractive methods when their promising potential in energy and environment issues is taken into account. Among the many others, it can be stated that photocatalytic process is one of the effective mechanisms for organic pollutants elimination. This process has an ability to yield good results under ambient conditions such as room temperature by using sunlight as energy source and due to these reasons photocatalysis can be considered as a good choice

[112]. Up to now, metallic precursors like Ga, In, Nb, Ta, W and Bi have been used with or without TiO_2 support [113-115].

Due to the potential application areas and the promising results, the search for a cheap and sustainable photocatalyst has been going on. Besides metallic ones, there are many studies to develop an organic photocatalyst due to their advantages such as low production costs, availability of resources, and the capability of absorbing light [116].

Conjugated polymers have ability to absorb both visible and ultraviolet light due to presence of unsaturated bonds on their backbone. In addition to that linear conjugated polymers having band gap values ranging from 2.0 eV to 5 eV depending on the conjugation length can be good candidates for ultra violet and visible light photocatalytic applications [117].

1.8 Aim of Study

Because of its properties and promising applications like organic light-emitting diodes, organic photovoltaic devices, electrochromic displays and devices, transistors, chemical sensors, PEDOT has attracted the interest of many scientists. Today, many research papers and patents have been published on the synthesis and applications of PEDOT and its derivatives. It can be easy to understand its importance in chemistry and material science areas by searching on 'PEDOT' in the search engine *Web of Science* (date: December 14th, 2017). There were more than 10000 published works cited more than 200.000 in 2017.

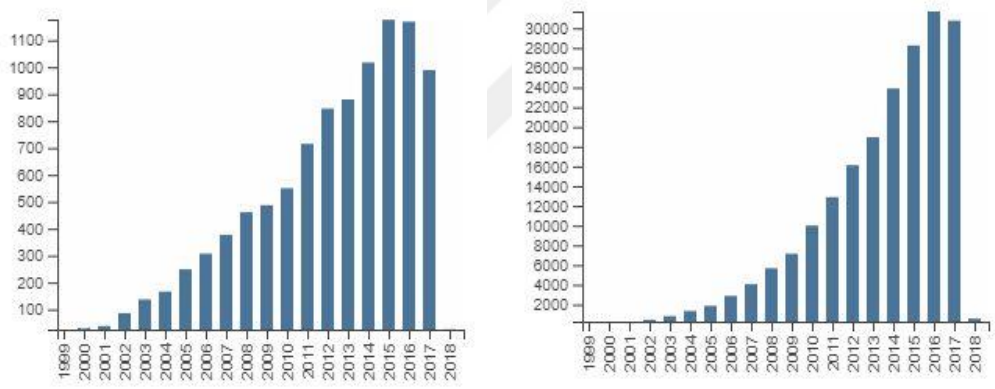

Figure 1.15. The growth in the annual numbers of research publications on poly(3,4-ethylenedioxythiophene) (PEDOT) (left-hand graph), and the number of citations to papers (right-hand graph), as obtained by searching on 'PEDOT' in the search engine *Web of Science* (date: December, 2017).

On the other hand, in this study, as it is mentioned above in order to remove insolubility problem, to make PEDOS polymer more advantageous than PEDOT and to favor the research on PEDOS to be able to make it a real competitor to take the place of PEDOT, PEDOS must be soluble in common organic solvents.

With the help of alkyl substituted POSS units, chemically and electrochemically synthesized polymers called PEDOT-POSS, PProDOT-POSS and PEDOS-POSS (Schemes 1.1 and 1.2) will not only be soluble but also will be possible to create some gaps between polymer chains due to the presence of nano sized POSS cages. By the help of these gaps it will be easier to enter counter ions in the polymer structure. Therefore, when compared to the parent aromatic rings, it will be possible to get the polymers with higher optical contrast and coloration efficiency as well as shorter switching time since ion injection into the polymer structure will be much easier during doping process.

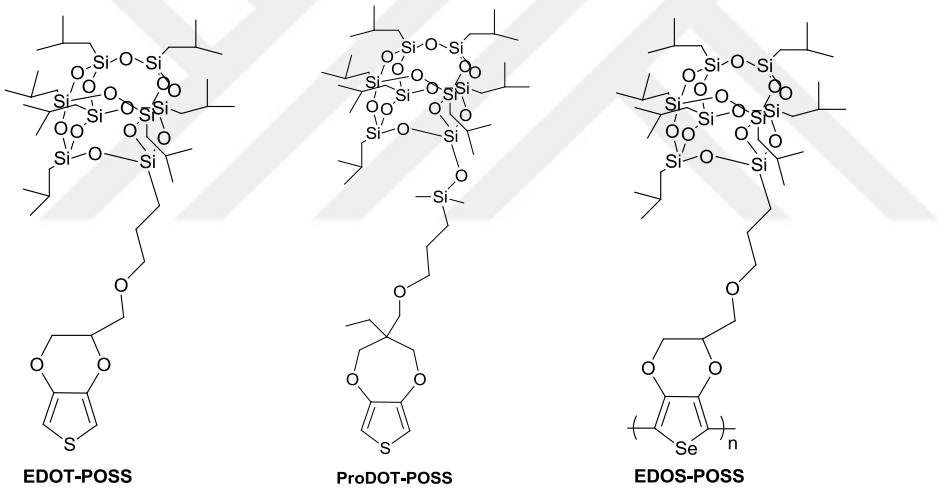

Scheme 1.1. Chemical structures of the target monomers.

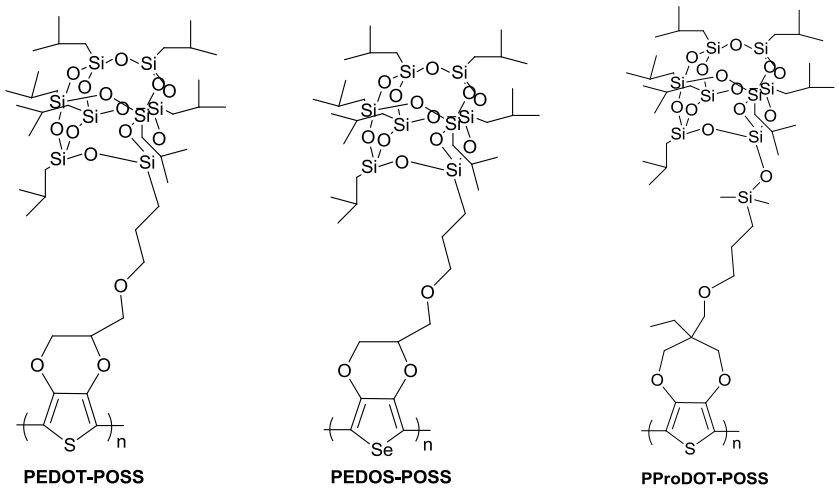

Scheme 1.2. Chemical structures of the target polymers.

CHAPTER 2

EXPERIMENTAL

2.1 Materials

3,4-dimethoxythiophene, 3,4-ethylenedioxythiophene, Se powder, sulfuryl chloride, anhydrous sodium acetate (NaOAc), p-toluenesulfonic acid, tetrabutylammonium hexafluorophosphate (TBAH), Tetraethyl orthosilicate and (3-Aminopropyl)trimethoxysilane and all the solvents were obtained from Sigma Aldrich and used as received. Iron(III)chloride was obtained from Riedel-de Haën and Cobalt(II) chloride 6-hydrate was obtained from Surechem. 1,2-propanediolisobutyl Polyhedral Oligomeric Silsesquioxane (POSS), aminopropylisobutyl POSS and TMP diolisobutyl POSS were bought from Hybrid Plastics and used without further purification. Toluene and dichloromethane were dried over CaH_2 and freshly distilled before they are used in any chemical or electrochemical experiments.

Gel electrolyte used for electrochromic device fabrication was prepared by mixing tetrabutylammonium tetrafluoroborate – poly(methyl methacrylate) (PMMA) – propylene carbonate – acetonitrile in the following ratio 3:7:20:70 by mass, respectively.

2.2 Equipments

Structural characterizations of the synthesized materials were performed by Bruker Spectrospin Avance DPX-400 Spectrometer. The samples were prepared in $CDCl_3$ in order to be used in ^{1}H and ^{13}C NMR analysis and chemical shift interpretations were given relative to tetramethylsilane as the internal standard. The molecular weights of the prepared monomers were obtained by using A Water, Synapt HRMS.

Gamry PCI4/300 and Gamry Reference 600 potentiostat–galvanostat were used to record all the electrochemistry studies at room temperature. Specord S600 Spectrometer was used to carry out spectroelectrochemical studies. The optoelectrochemical spectra of the film were noted *in-situ* under applied different potentials. In order to determine the electrochemical stability and switching behavior of the polymer films square wave potential method by applying constant potential between neutral and oxidized states was utilized and then by using cyclic voltammetry the electroactivity of the polymer films were compared to their initial values. During electrochemistry studies, the electrolyte solutions were prepared with TBAH in two different organic solvents, dichloromethane and acetonitrile. Three-electrode system containing a platinum disc (0.0314 cm^2) as a working electrode, a Ag/AgCl electrode as a reference electrode, and platinum wire as a counter electrode, was utilized during the electrochemical studies. Reference electrode was calibrated by using 10 mM of ferrocene solution before it is used in any electrochemistry studies.

Specord S600 (standard illuminator D65, field of width 10^{o} observer) was also used to record colorimetric measurements and color space was interpreted according to the International Commission of Illumination with luminance (L), hue (a), and intensity (b). Platinum cobalt DIN ISO 621, iodine DIN EN 1557, and Gardner DIN ISO 6430

are the references of colorimetric measurements. Emission measurements were recorded on a Thermo Lumina Fluorescence Spectrometer. FTIR spectroscopy studies were performed with a Bruker Vertex 70 Spectrophotometer. SEM images were recorded by using QUANTA 400F Field Emission High Resolution Scanning Electron Microscope. Molecular weights of the polymers were determined with using Polymer Laboratories PL-GPC 220 Gel Permeation Chromatography device by dissolving in tetrahydrofuran. Thermogravimetric analyses of the polymers were performed by utilizing Perkin Elmer Pyris 1Thermogravimetric analysis instrument.

2.3 Methods and Techniques

2.3.1 Electrochemical Polymerization

All electrochemistry studies were performed by using a Gamry PCI4/300 and Gamry Reference 600 potentiostat–galvanostat. Electrochemical polymerization experiments were carried out electrochemically by applying constant potential electrolysis on both platinum disc electrode and indium-tin oxide (ITO, Delta. Tech. 8–12 Ω, 0.7x5.0 cm^2). The combination of spectrometer and potentiostat-galvanostat was utilized to record switching time and percent transmittance studies in situ by using three-electrode system (an ITO as a working electrode, a platinum wire as a counter electrode and a silver wire as a reference electrode) in a UV cuvette. The reference silver wire was calibrated *vs*. Fc/Fc^+ by dissolving ferrocene in the electrolyte.

2.3.2 Chemical Polymerization

Chemical polymerization of the monomers was carried out by direct oxidation of the monomers using $FeCl_3$ [118,119]. Pre-dissolved four equivalent molar concentration of $FeCl_3$ in chloroform and nitromethane was added dropwise to 0.1 M of monomer dissolved in chloroform at 0 ^oC. The reaction mixture was left to stir at room temperature for 24 h. The resulting mixture was concentrated to 5 mL and poured onto methanol. The solution was refrigerated to get precipitation. The precipitated polymer was filtered and the product was left to wash by using Soxhlet apparatus with methanol and hexane for at least 12 h, respectively. Then, the product was collected by using dichloromethane. Final product was dried at room temperature.

2.3.3 Cyclic Voltammetry

Cyclic voltammetry is the most common electroanalytical method for investigation of the electroactive polymers. Cyclic voltammetry, which can be used to obtain both qualitative and quantitative data, allows measuring the current flow occurring at the working electrode as a function of applied potential [120]. Conjugated polymers can show p- or n-type doping under applied oxidation or reduction potentials. It is easy to determine these oxidation and reduction potentials of the polymers by scanning in the proper potential range. In addition to that, it is used to determine the electrochemical stability of conjugated polymers by repeating cycling.

Cyclic voltammetry is an essential technique to determine important parameters of polymer such as peak current (i_p), diffusion coefficient (D), and scan rate (υ) dependence. Randles & Sevcik equation (Equation 2.1.) [121] summarizes these parameters in way that:

$$i_p = (2.69\times10^5)\, n^{3/2}\, A\, D^{1/2}\, C\, \upsilon^{1/2} \qquad \text{Equation 2.1}$$

Where $2.69x10^5$ is a constant to be able to use at 25 ^oC, n represents the number of electrons transferred, A represents the area of the electrode and C represents the concentration. Equation clearly states that peak current depends on concentration and scan rate. The reversible redox change can be observed in redox behavior of ferrocene where reactant and the product are soluble in electrolyte solution. Reversible redox peaks increase while concentration and the scan rate increase. This proves that there is a diffusion controlled process. However, it is different in electropolymerization process due to the concentration change in the monomer and the polymer formed on electrode surface.

Monomers in the electrolyte solution, which undergo a chemical change, have a tendency to stick on to electroactive surface under applied potential. During repetitive scanning of monomer solution, peak current increases while the monomer concentration decreases. This increase stems from the oligomers, if they are long enough polymers precipitated on to electrode which are insoluble in the electrolytic medium used.

While scanning of the conducting polymer film formed on the electrode in a monomer-free electrolyte solution, the difference in the peak current behavior can be seen when compared to that of diffusion controlled system. The peak current of the conducting polymer film coated on electrode can be calculated by the following equation (Equation 2.2);

$$i_p = n^2 F^2 \gamma \nu / 4RT \qquad \text{Equation 2.2}$$

where, γ represents the amount of electroactive material coated on the electrode surface. By looking at this formula, there is a clear dependency of peak current to scan rate and hence scanning of the polymer film coated on the electrode surface can be called as a non-diffusion controlled process.

2.3.4 Spectroelectrochemistry

Spectroelectrochemistry is another key technique to characterize optical properties of the polymer films. As mentioned above three-electrode cell is used with an ITO working electrode. Optical data obtained from UV-Vis spectrometer is recorded while certain potential is applied. During this process, optical changes upon doping and dedoping occurring on the polymer film coated on the surface of ITO glass can be recorded. The changes represent the formation of polaron and bipolaron upon p-type or n-type doping processes.

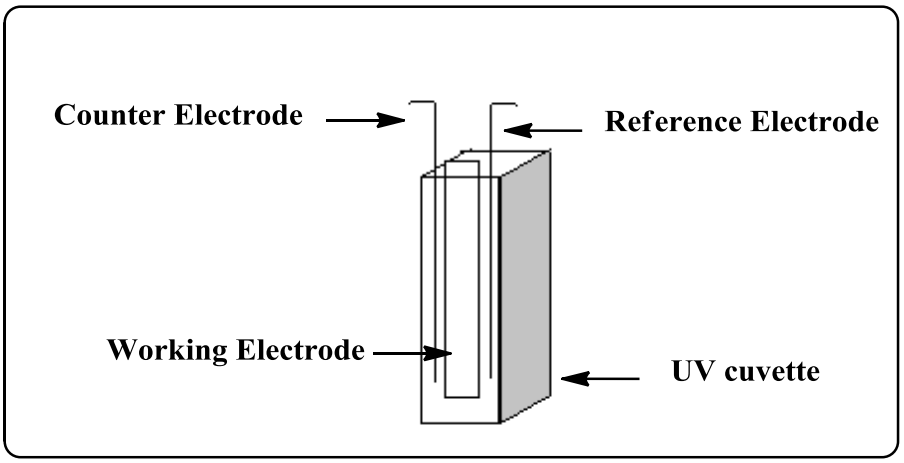

Figure 2.1. Representative set up for potentiostatic technique in optical studies (Counter electrode is Pt wire, reference electrode is a Ag wire and working electrode is an ITO.)

From the UV-VIS spectrum, the maximum absorption wavelength can be determined and the optical band gap (E_g) of the neutral state polymer film can be calculated by using the onset value of the longer wavelength in the absorption spectrum.

2.3.5 Chronoabsorptometry

Similar to spectroelectrochemistry study, chronoabsorptometry is an important technique to investigate the optical properties of the polymer films. Unlike static spectroelectrochemistry, chronoabsorptometry is a dynamic method to record electrochromic shifts occurring during sharp changes in the applied potentials between redox states. While spectroelectrochemistry measures optical changes in the the complete spectrum chronoabsorptometry uses a single wavelength to measure

absorbance/transmittance change regarding the optical behavior of the polymer film. The key parameter measured by chronoabsorptometry is “switching time” required to shift from fully oxidized states to fully reduced state.

During this method, like spectroelectrochemistry, spectrometer and potentiostat work together to record both electrochemical and optical changes during redox shifts. Square-wave method is applied at different potentials from potentiostat and during this spectrometer records the percent transmittance change on film with respect to time. Square-wave method can be fixed to varying time intervals like 10, 5, 3, 2 and 1.

2.3.6 Stability Experiments

Stability studies can be held in two ways by using potentiostat. In one technique, cyclic voltammetry is utilized to scan between the redox potentials of the polymer film by certain amount of cycles. After a certain number of cycles, electrochemical behavior is investigated and compared to initial behavior of the polymer film. In another method, the square-wave method is used to switch between the two redox states of the polymer at the certain number of switch. Like the first method, the electrochemical properties of the polymer are compared to initial behavior of that polymer.

2.3.7 Electrochromic Device Construction

As well as the spectroelectrochemical properties, electrochromic device applicability of the synthesized polymers was investigated. Electrochromic devices having an

ability to change the optical contrast under applied potentials provide a wide application area for conjugated polymers. Electro chromic devices prepared by using polymer films allow scientist to modulate some parameters like emission, transmittance, absorbance and reflectance. By adjusting these parameters electrochromic devices can be used in different fields such as electrochromic displays, windows and mirrors [122, 123].

Device architecture basically contains two electrodes coated with two different polymers. These electrodes are combined with gel electrolyte which allows electron movement in the device. While one polymer is doped oxidatively, the other is in its neutral state (Scheme 2.2).

The gel electrolyte used in the electrochromic devices was prepared by mixing TBAH/ PMMA/ PC/ ACN in a ratio of 3:7:20:70 by weight. Supporting electrolyte TBAH previously dissolved in PC and PMMA were mixed and dissolved in ACN and left to evaporate slowly at around 70 ^{o}C to reach honey-like viscous solution yielding a highly conducting transparent gel [124].

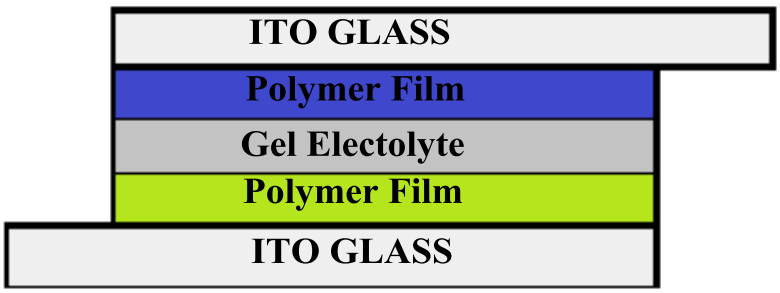

Figure 2.2. Schematic representation of an electrochromic device.

2.3.8 Colorimetry

Electrochromic polymers have a tendency to change their color as a response to change in the applied potential. In order to clarify the change in the color more scientifically, there are some approaches developed by institutions. One of these approaches was stated by The Commission Internationale de l'Eclairge (CIE system). CIE system defines colors in three dimensional coordinates, L*a*b*. L* represents luminescence, the white-black balance, a* represents the red-green balance and b* represents the yellow-blue balance.

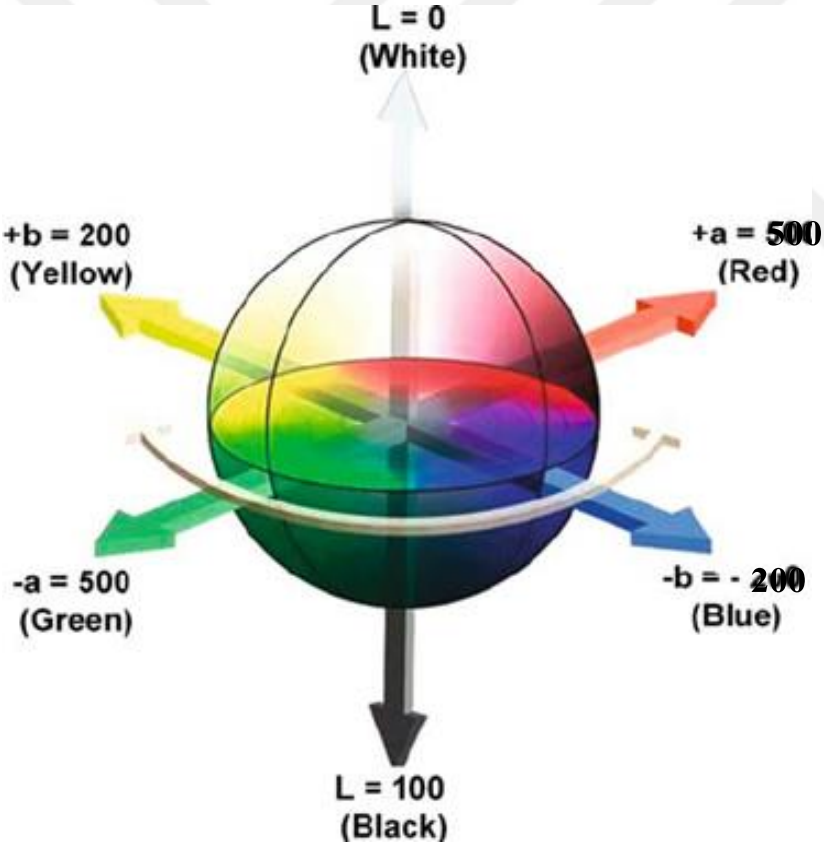

Figure 2.3. Representation of CIE color space coordinates (L*a*b*) (Adopted from [125]).

L*a*b* values are used to calculate the color saturation of the polymer films. Color saturation is a parameter to describe the difference between chromatic color and total color sensation and can be scaled from 0 (grey) to 100 (a pure color) [100]. Color saturation can be calculated by the following equation (Equation 2.3);

$$S_{ab}=\left(\frac{a^{*2}+b^{*2}}{a^{*2}+b^{*2}+L^{*2}}\right)^{1/2} \qquad \text{Equation 2.3}$$

In order to show the difference between the colors of the copolymers, color difference can be calculated quantitatively. It is hard to differentiate the copolymers from each other by naked eye since their colors are close to one another. Color difference can be calculated by using L*a*b* values from the following equation (Equation 2.4);

$$\Delta E^{*}_{ab} = [(\Delta L^{*})^2 + (\Delta a^{*})^2 + (\Delta b^{*})^2]^{1/2} \qquad \text{Equation 2.4}$$

2.3.9 Coloration Efficiency

Coloration efficiency is another important parameter to describe the performance electrochromic polymers. It can be defined as the measure of the change in absorbance behavior of a polymer film at a certain wavelength (Optical density (OD)) with respect to charge injected/ejected. The optical density of the film can be determined for full color switch or in different percentages such as 90% or 95%. It can be calculated by the following equation (Equation 2.5);

$$CE = \Delta OD/Q_d \qquad \Delta OD = \log(T_{bleached}/T_{colored}) \qquad \text{Equation 2.5}$$

where Q_d represents the charge density (injected/ejected charge) during a redox step; $T_{colored}$ and $T_{bleached}$ are the percent transmittance values in the oxidized and neutral states, respectively.

2.4 Monomer Synthesis

2.4.1 Synthesis of EDOT-POSS

In 80 mL freshly distilled dry toluene, 3,4-dimethoxythiophene (0.50 g, 3.47 mmol, 1.0 equiv), 1,2-propanediolisobutyl POSS (4.94 g, 5.2 mmol, 1.5 equiv) and *p*-toluenesulfonic acid (PTSA, 66 mg, 0.35 mmol, 0.1 equiv) were dissolved under argon atmosphere (Scheme 2.1). The reaction mixture was left to reflux for 48 h. After cooling to room temperature, the solvent was removed under reduced pressure. The residue subjected to column chromatography (Hexane-EtAc 12:1) to afford a light brown solid (1.94 g, 54%).

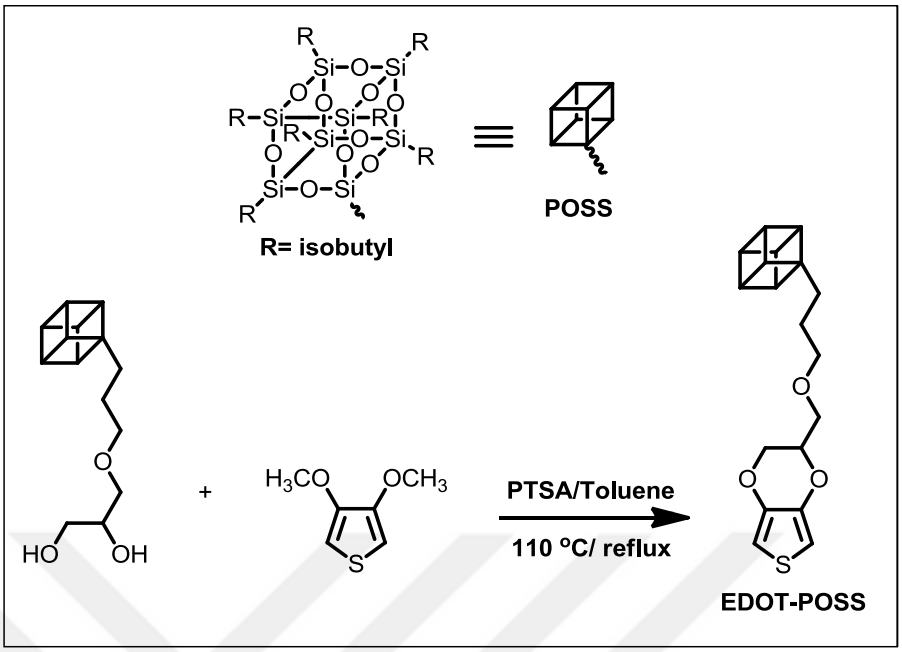

Scheme 2.1. Synthesis of EDOT-POSS monomer.

^{1}H NMR (400 MHz, $CDCl_3$, δ(ppm)): 6.32 (s, 2H; ArH), 4.27 (m, 1H, CH), 4.05 (m, 2H; CH_2), 3.62 (dd, J= 5.54-28.34 Hz, 2H; CH_2), 3.46 (t, , J= 6.80 Hz, 2H; CH_2), 1.80 (m, 7H; CH_2), 1.65 (m, 2H; CH_2), 0.90 (d, J= 6.62 Hz, 42H; CH_2), 0.60 (t, 2H; CH_2), 0.60 (d, J= 7.02 Hz, 14H; CH_2).

^{13}C NMR (100 MHz, $CDCl_3$, δ(ppm)): 141.61, 99.57, 73.95, 72.62, 68.97, 66.27, 29.69, 25.69, 23.88, 22.50, 8.20.

IR (KBr): *v* (cm^{-1}) = 3125 (s; *v*(=C-H in thiophene ring)), 2850-2950 (w; (alkyl units)), 1400-1500 (w; (C=C stretching)), 1230 (s; (Si-C)), 1080 (w; *v*(Si-O-Si and C-O-C), 836 and 680 (s; *v*(C-S in thiophene ring)), 742 (w; (Si-C)).

HRMS (ESI) *m/z*: calcd for $C_{38}H_{76}O_{15}Si_8$, 1029.31; found 1029.32. (Appendix C)

2.4.2 Synthesis of ProDOT-POSS

3,4-dimethoxythiophene (0.50 g, 3.47 mmol, 1.0 equiv), TMP diolisobutyl POSS (5.4 g, 5.2 mmol, 1.5 equiv) and PTSA (66 mg, 0.35 mmol, 0.1 equiv) were dissolved in 80 mL of freshly distilled dry toluene under argon atmosphere (Scheme 2.2). The reaction mixture was left to reflux for 36 hours. After cooling to room temperature, the solvent was removed under reduced pressure. The residue subjected to column chromatography (Hexane-EtAc 10:1) to afford a light brown solid (2.10 g, 52%).

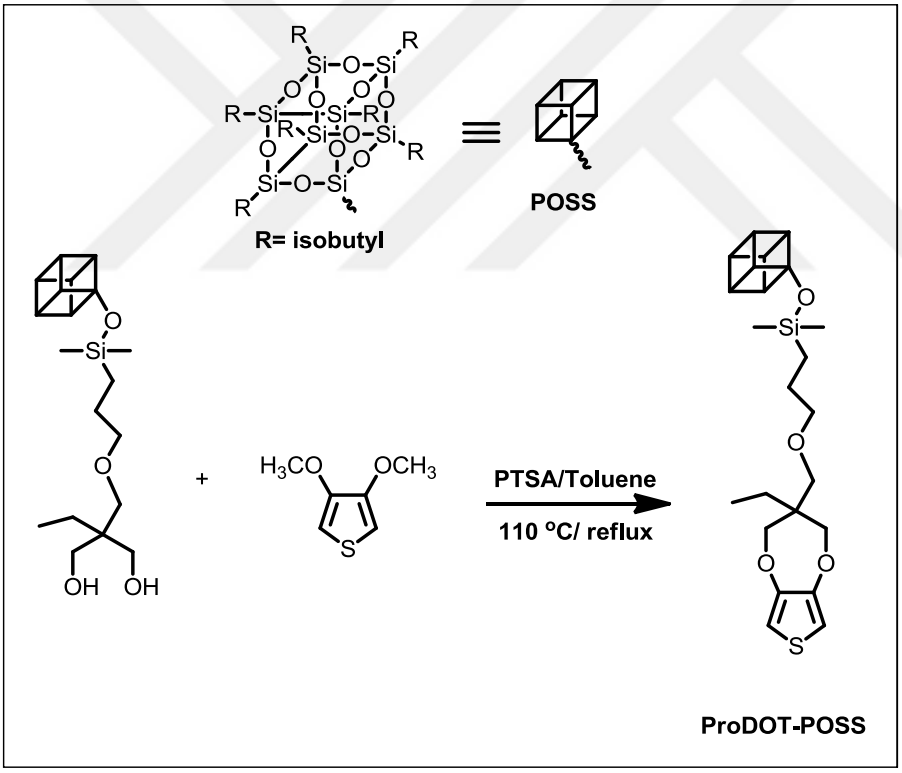

Scheme 2.2. Synthesis of ProDOT-POSS monomer.

^{1}H NMR (400 MHz, $CDCl_3$, δ(ppm)): 6.31 (s, 2H; ArH), 3.79 (dd, J= 18.50-30.05 Hz, 4H, CH_2), 3.29 (s, 2H; CH_2), 3.25 (t, 2H; CH_2), 1.75 (d, 7H; CH_3), 1.46 (m, 2H; CH_2), 1.39 (m, 2H; CH_2), 1.14 (d, 2H; CH_2),0.85 (d, 42H; CH_2), 0.79 (s, 3H, CH_3), 0.51 (t, 14H; CH_2), 0.46 (s, 6H, CH_3)

^{13}C NMR (100 MHz, $CDCl_3$, δ(ppm)): 150.05, 105.09, 75.48, 74.72, 70.76, 46.01, 30.05, 26.17, 24.18, 23.63, 23.43, 22.85, 14.02, 7.86.

IR (KBr): *v*(cm^{-1}) = 3120 (s; *v*(=C-H in thiophene ring)), 2850-2950 (w; (alkyl units)), 1400-1500 (w; (C=C stretching)), 1230 (s; (Si-C)), 1080 (w; *v*(Si-O-Si and C-O-C), 836 and 680 (s; *v*(C-S in thiophene ring)), 742 (w; (Si-C))

HRMS (ESI) *m/z*: calcd for $C_{43}H_{88}O_{16}Si_9$, 1044.37; found 1067.37. It might capture a Na ion from the solvent. (Appendix C)

2.4.3 Synthesis of EDOS-POSS

2.4.3.1 Synthesis of 3,4-dimethoxy selenophene

3,4-dimethoxyselenophene was synthesized according to literature [59]. Selenium powder (3.00 g, 38 mmol) was dissolved in sulfuryl dichloride (SO_2Cl_2) (5.13 g, 38 mmol) at 10 ^{o}C to get selenium dichloride ($SeCl_2$). After stirring 30 minutes, 11 mL of freshly distilled hexane was added to the mixture and the solution was brought to room temperature to stir for 12 hours. Then, formation of $SeCl_2$ was observed in the clear reddish brown solution.

In another flask the solution of 2,3-dimethoxy-1,3-butadiene (3.61 g, 32.0 mmol) and sodium acetate (7.41 g, 90.4 mmol) was prepared in 300 mL of anhydrous hexane at

-78 ^{o}C under argon atmosphere. The solution of $SeCl_2$ was added to this solution and left to stir for 1 hour at -78 ^{o}C. After that, the reaction mixture was removed from cooling bath and left to stir at room temperature. After 4 hours, the final mixture was poured into water and worked up. Organic part was dried over $MgSO_4$ and the solvent was evaporated by vacuum to 30 mL. Column was prepared by using 1% trimethylamine hexane mixture and product (3,4-dimethoxy selenophene, 2,30 g, 38%) was filtered through that column.

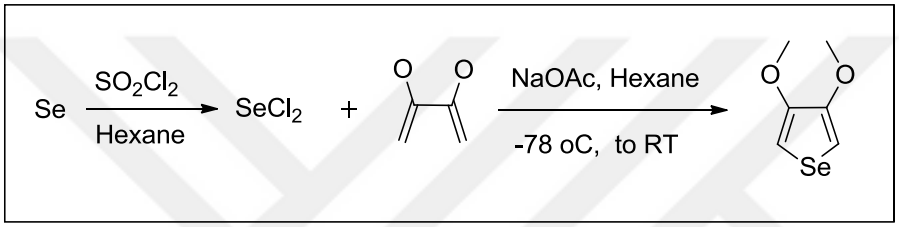

Scheme 2.3. Synthesis of 3,4-dimethoxyselenophene.

2.4.3.2 Synthesis of EDOS-POSS

In 80 mL freshly distilled dry toluene, 3,4-dimethoxyselenophene (0.67 g, 3.47 mmol, 1.0 equiv), 1,2-propanediolisobutyl POSS (4.94 g, 5.2 mmol, 1.5 equiv) and PTSA (66 mg, 0.35 mmol, 0.1 equiv) were dissolved under argon atmosphere (Scheme 2.4). The reaction mixture was left to reflux for 48 h. After cooling to room temperature, the solvent was removed under reduced pressure. The residue subjected to column chromatography (Hexane-EtAc 10:1) to afford a dark yellow solid (2.80 g, 56%).

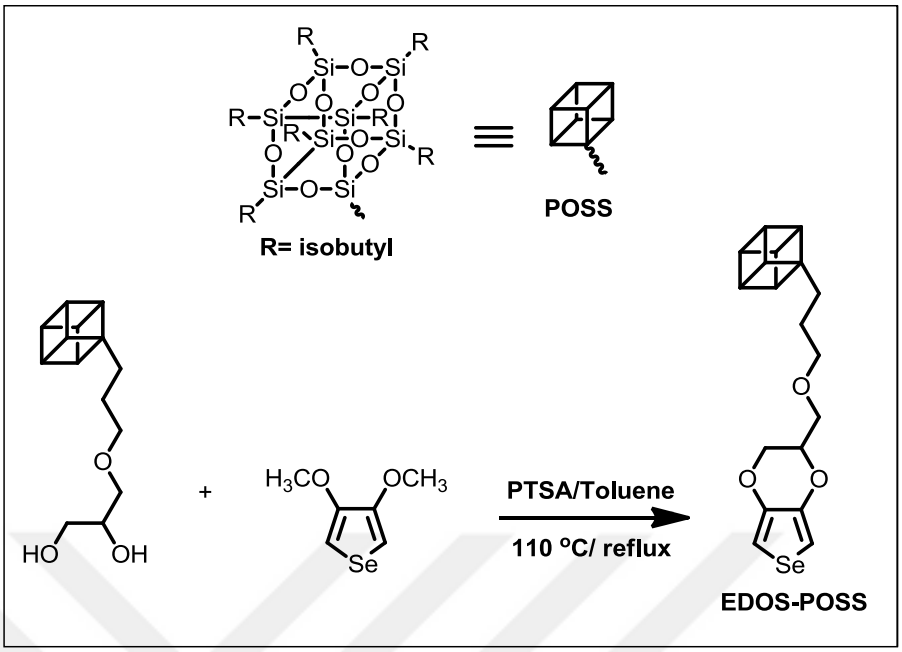

Scheme 2.4. Synthesis of EDOS-POSS monomer.

^{1}H NMR (400 MHz, $CDCl_3$, δ(ppm)): 6.78 (s, 2H; ArH), 4.28 (m, 1H, CH), 4.11 (dd, J=56.9-3.6 Hz, 2H; CH_2), 3.62 (dd, J= 5.50-28.1 Hz, 2H; CH_2), 3.47 (t, J= 6.4 Hz, 2H; CH_2), 1.85 (m, 7H; CH), 1.66 (m, 2H; CH_2), 0.95 (d, J= 6.6 Hz, 42H; CH_3), 0.61 (t, 2H; CH_2), 0.61 (d, J= 5.3, 14H; CH_2).

^{13}C NMR (100 MHz, $CDCl_3$, δ(ppm)): 142.65, 101.68, 73.97, 99, 65.98, 31.41, 25.68, 23.47, 22.51, 8.19.

IR (KBr): ν(cm^{-1}) = 3120 (s; ν(=C-H in thiophene ring)), 2850-2950 (w; (alkyl units)), 1460 (w; (N-H stretching)), 1400-1500 (w; (C=C stretching)), 1230 (s; (Si-C)), 1202 (s, (C-N stretching)), 1080 (w; ν(Si-O-Si)),836 and 680 (s; ν(C-S in thiophene ring)), 742 (w; (Si-C)).

2.4.4 Synthesis of Magnetic Nanoparticle Loaded PEDOT-POSS

2.4.4.1 Preparation of Magnetic Nanoparticle

(i) Cobalt Ferrite Magnetic Nanoparticles

1.08 g $FeCl_3.6H_2O$, 0.476 g $CoCl_2.6H_2O$ and 20 mL of deionized water were vortexed in a tube and then placed in a beaker. After 20 mL 3 M NaOH and 10 mL of 1.5 M NaCl added dropwise under constant stirring. When the solution turned orange color the solution was left to stir at 80 ^oC for 1 h. When the solution was cooled to room temperature, the black precipitates were collected with a magnet. In order to remove the supernatant, particles were washed three times with deionized water.

(ii) Silica Coating on Cobalt Ferrite Magnetic Nanoparticles

Sol-gel method was utilized to coat the cobalt ferrite magnetic nanoparticles with silica shell. First of all 160 mL ethanol, 338 μL Tetraethyl orthosilicate and 28.8 μL (3-Aminopropyl)trimethoxysilane were mixed in a beaker. 20 mL cobalt ferrite colloid was added to that solution and stirred for 3 hours at room temperature. After the formation of core shell particles, these particles were collected with the magnet and washed three times with deionized water.

2.4.4.2 Preparation of MNP loaded PEDOT-POSS

EDOT-POSS (100 mg, 0.097 mmol, 1 equiv.), MNP (100 mg) and $FeCl_3$ (0.079 g, 0.486 mmol, 5 equiv.) were dissolved in CH_2Cl_2 at room temperature. Solution was left to stir at room temperature for 24 hours. The mixture was concentrated under vacuum and poured into methanol to get precipitate. The precipitate of the resulting

polymer was filtrated and washed with methanol and hexane in Soxhlet apparatus. After drying MNP loaded PEDOT-POSS was collected to give 160 mg blackish solid.

CHAPTER 3

RESULTS AND DISCUSSION

3.1 Electrochemical and Electro-optical Characterization of EDOT-POSS and Its Polymer PEDOT-POSS

3.1.1 Electrochemistry of EDOT-POSS

In order to understand the effect of incorporation of POSS unit on EDOT monomer cyclic voltammetry results were compared. Cyclic voltammetry studies showed that EDOT-POSS monomer has a similar electrochemical behavior when compared to the parent EDOT. Figure 3.1 shows the comparison of electrochemical behaviors of EDOT-POSS and EDOT monomers. Both monomers exhibited one irreversible oxidation peak at 1.45 V vs. Ag/AgCl which is responsible from the electrochemical polymerization. It can be concluded that the presence of POSS unit substituted onto the ethylenedioxy bridge of EDOT did not result in a shift in the oxidation potential of EDOT unit.

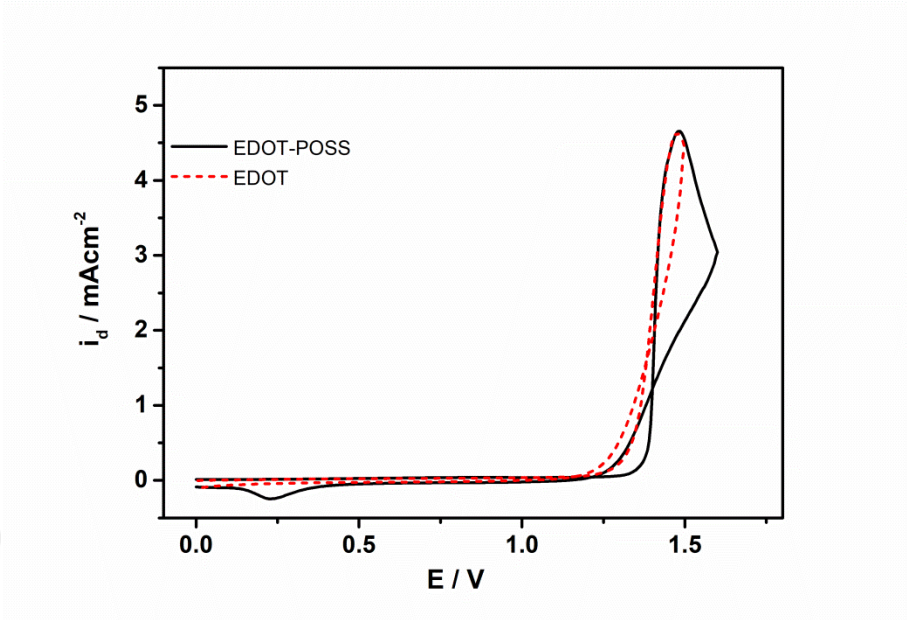

Figure 3.1. Electrochemical behaviors of EDOT and EDOT-POSS monomers in 0.1 M TBAH dissolved in dichloromethane at a scan rate of 100 mV/s on a Pt electrode.

3.1.2 Electropolymerization of EDOT-POSS

Figure 3.2 looks like a fingerprint of the formation of an electroactive polymer film on the electrode surface, which is confirmed by the appearance of a new redox couple between -0.2 V and 0.6 V during scanning and also by an increase in its current density after each successive cycle.

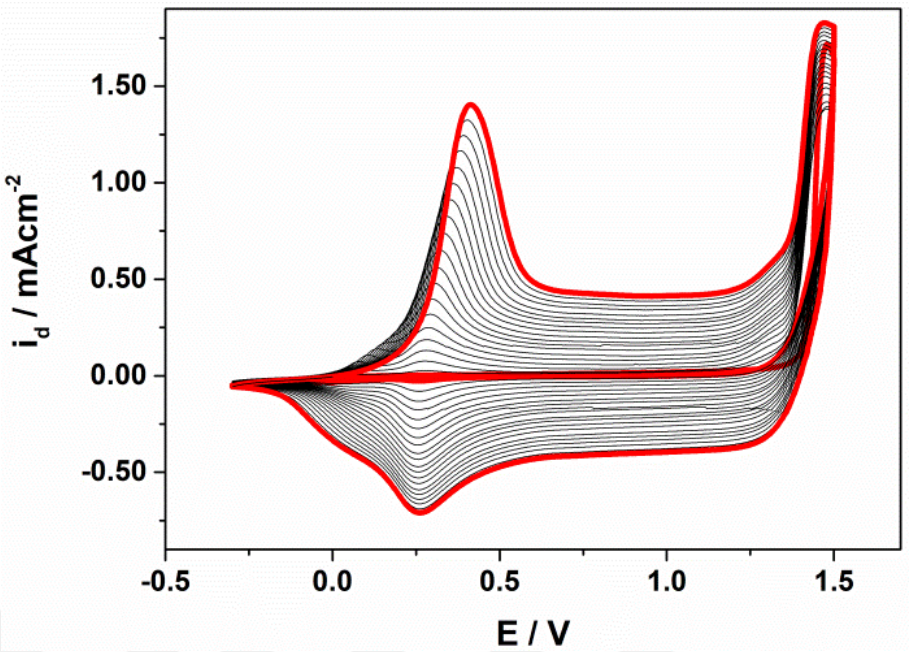

Figure 3.2. Potentiodynamic polymerization of EDOT-POSS ($5.0x10^{-3}$ M) to get PEDOT-POSS in 0.1 M TBAH dissolved in a mixture of dichloromethane and acetonitrile (1/2.5 by v/v) between -0.30 V and 1.55 V at a scan rate of 100 mV/s on a Pt electrode vs. Ag/AgCl reference electrode.

As shown in Figure 3.2, the monomer EDOT-POSS can easily be polymerized via potentiodynamic polymerization between -0.30 V and 1.55 V to get the corresponding polymer called as PEDOT-POSS (Scheme 3.1).

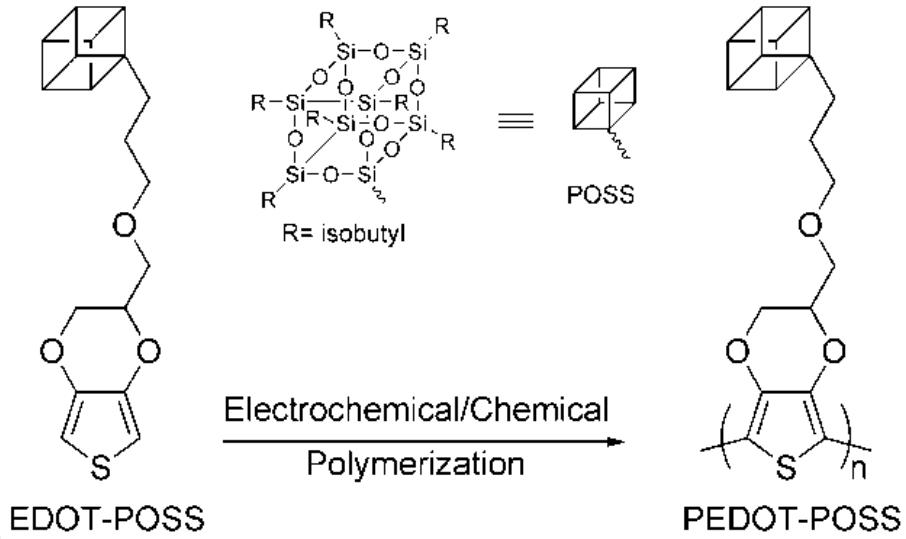

Scheme 3.1. Chemical structures of the EDOT-POSS and its corresponding polymer PEDOT-POSS.

3.1.3 Characterization of PEDOT-POSS

The presence of POSS unit in PEDOT-POSS polymer was verified by using FTIR spectroscopy and it is found that PEDOT-POSS spectra in Figure 3.3 show the specific peaks at around 2900 cm^{-1} and 1100 cm^{-1} belonged to aliphatic groups and Si-O-Si bonds, respectively. Moreover, the peak around 3100 cm^{-1} responsible for C-H vibrations of thiophene ring was not observed due to the polymerization through α-hydrogens of thiophene ring (Appendix B). In addition to that, ^{1}H NMR spectrum of PEDOT-POSS was compared to understand better that if the aromatic hydrogens in the thiophene ring can still be observed. The results showed that the signals belonged to these hydrogens are disappeared (Figure 3.4 and Appendix A).

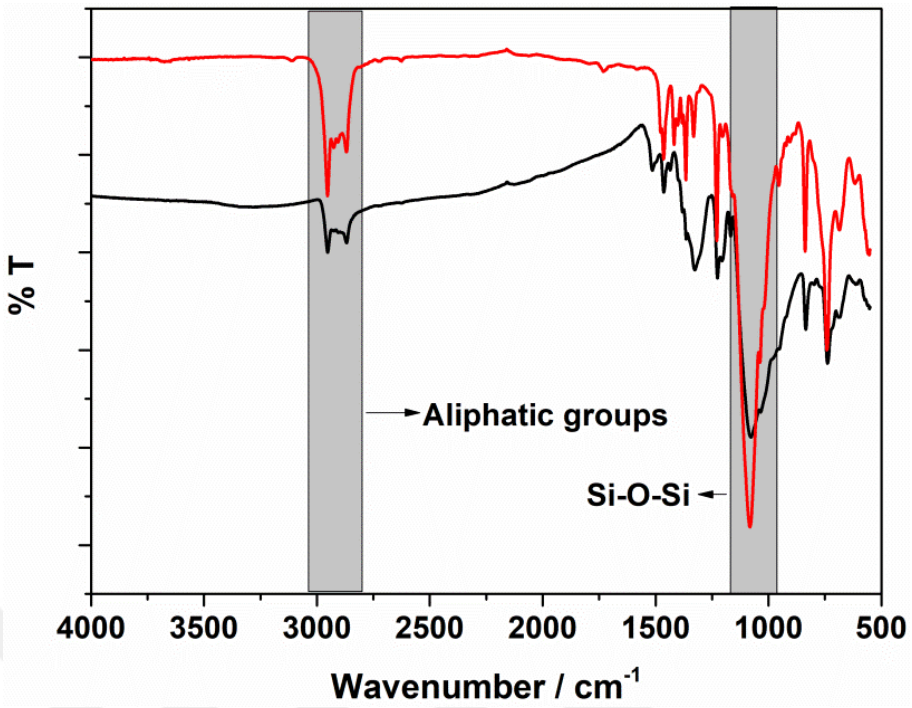

Figure 3.3. FTIR spectra of EDOT-POSS monomer and chemically obtained PEDOT-POSS.

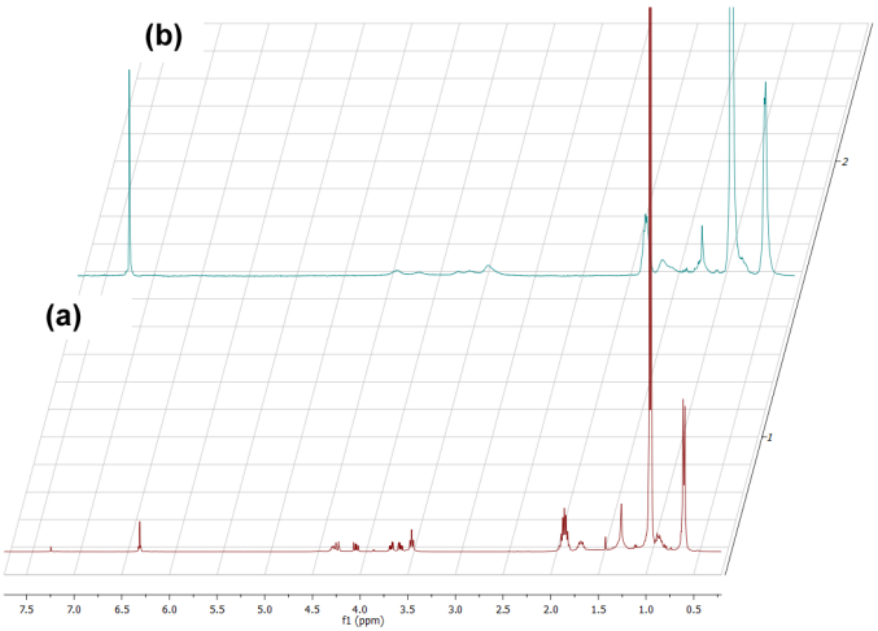

Figure 3.4 ^{1}H NMR spectra of (a) EDOT-POSS and (b) chemically obtained PEDOT-POSS in d-$CHCl_3$.

3.1.4 Electrochemistry of PEDOT-POSS

As shown in Figure 3.5, PEDOT has a very broad redox couple between -0.8 V and 1.0 V, which can be attributed to the slow doping process due to the well-packed polymer backbone. On the other hand, as expected, PEDOT-POSS has a well-defined and sharp redox couple with a half-wave potential of 0.30 V, which showed that the movement of counter ions inside/outside of polymer backbone will be easier since the presence of POSS units will lead to gaps among the polymer chains (Scheme 3.1).

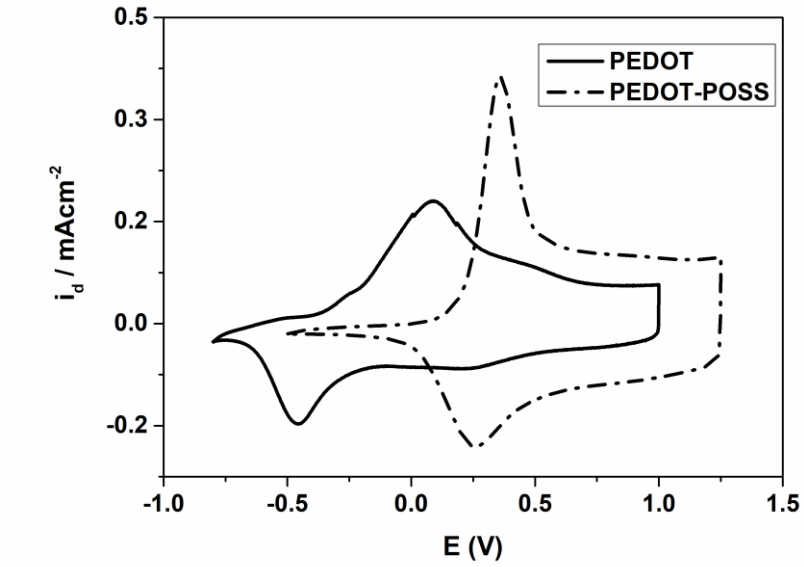

Figure 3.5 Comparison of the redox behaviors of the PEDOT (solid line, 160 mC/cm^2) and the PEDOT-POSS (dash dot line, 160 mC/cm^2) polymers coated on the Pt electrode in 0.1 M TBAH dissolved in acetonitrile at a scan rate of 50 mV/s vs. Ag/AgCl reference electrode.

Also, the scan rate dependence of PEDOT-POSS polymer film was investigated. The linear increase in the redox currents of the polymer film with increasing scan rate is

an indication of a well-adhered polymer film on the working electrode. PEDOT-POSS polymer film coated both on Pt electrode and ITO glass electrode and the scan rate dependence of the films was investigated for each polymer. It is found that the linear dependence of peak currents and scan rate indicated a non-diffusional redox process of a well-adhered polymer film on the electrode surface.

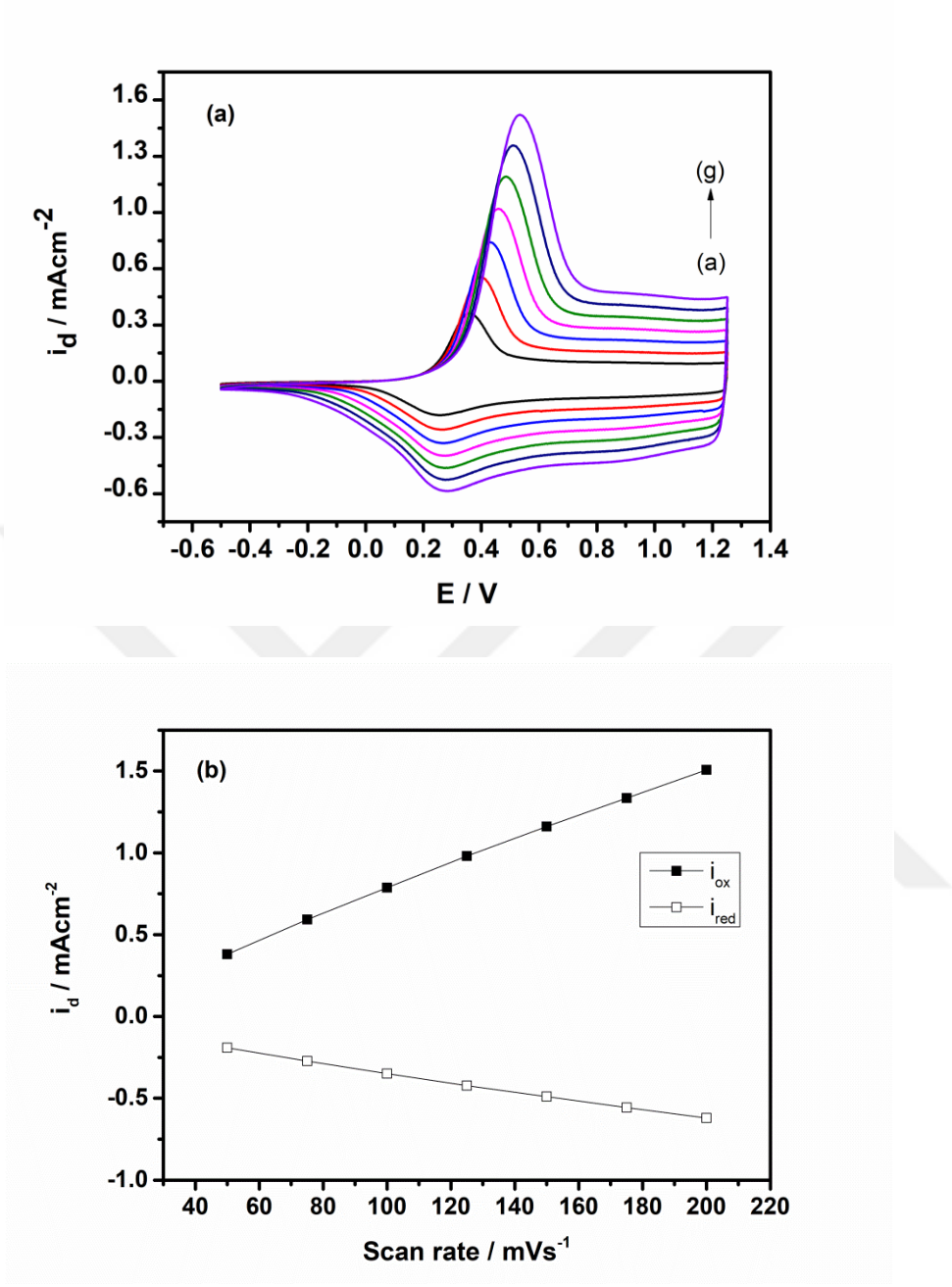

Figure 3.6. (a) Scan rate dependence of PEDOT-POSS film on Pt disc electrode in 0.1 M TBAH dissolved in acetonitrile at a scan rate of (a) 50, (b) 75, (c) 100, (d) 125, (e) 150, (f) 175, (g) 200 mV/s between -0.5 V and 1.25 V (b) The current vs. scan rate plot of the polymer film with increasing scan rate.

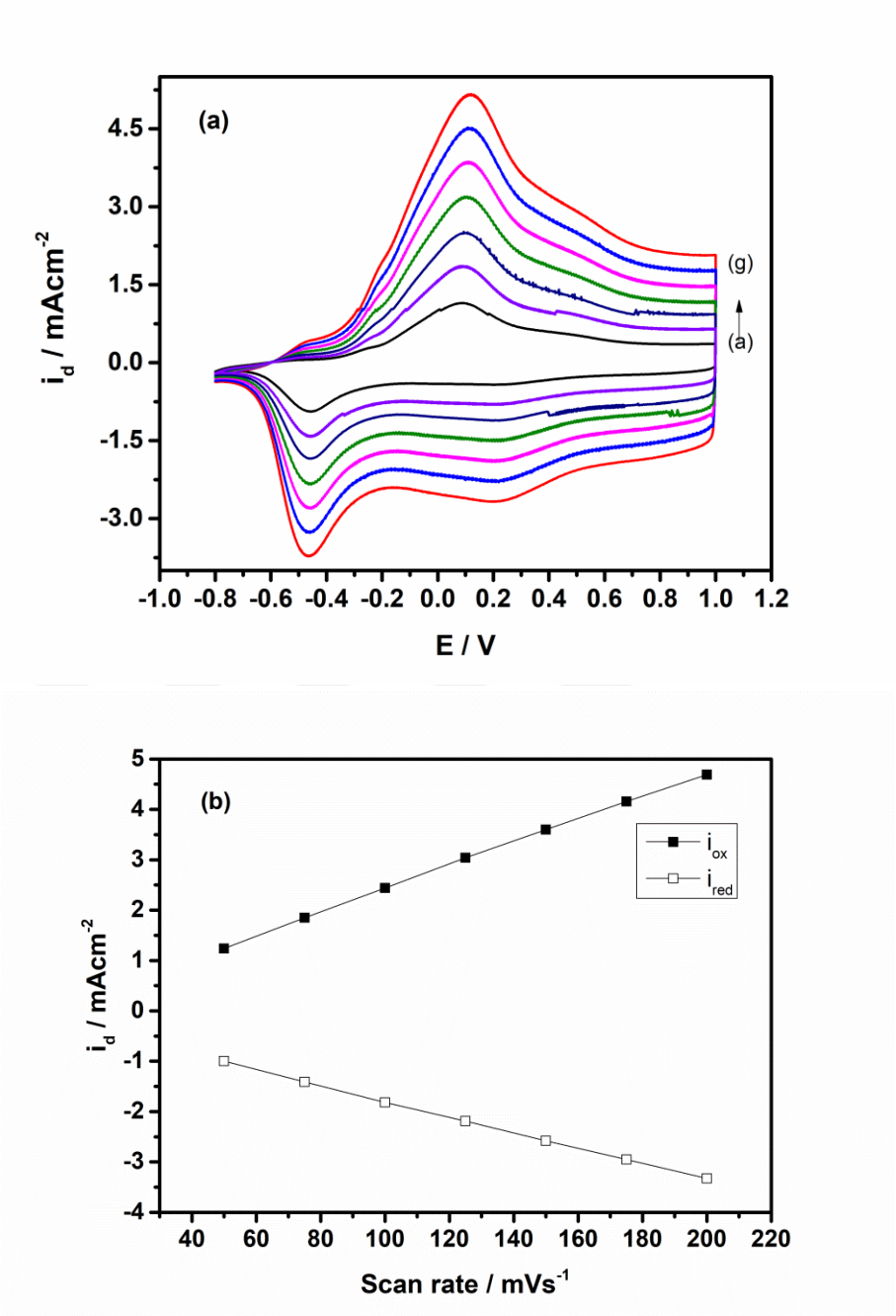

Figure 3.7. (a) Scan rate dependence of PEDOT-POSS film on ITO electrode in 0.1 M TBAH dissolved in acetonitrile at a scan rate (a) 50, (b) 75, (c) 100, (d) 125, (e) 150, (f) 175, (g) 200 mV/s between -0.5 V and 1.25 V (b) The current vs. scan rate plot of the polymer film with increasing scan rate.

The stability test under ambient conditions in the presence of oxygen is crucially important for the materials since they can be amenable to use in industrial applications when passed this test. The test showed that PEDOT-POSS is more robust and stable than PEDOT since no appreciable change was observed in the redox behavior of PEDOT-POSS even after thousands of cycles (Figure 3.8). For example, after 5.000 cycles, whereas the PEDOT lost its all electroactivity, PEDOT-POSS lost only 7% of its electroactivity.

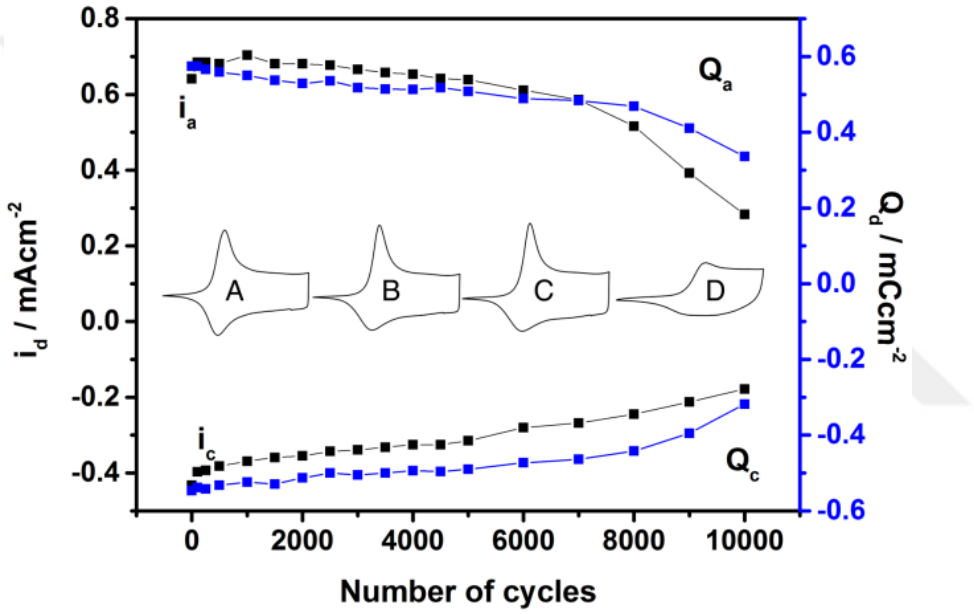

Figure 3.8. Stability test for electrochemically obtained PEDOT-POSS film in 0.1 M TBAH/CH_3CN at a scan rate of 50 mV/s under ambient conditions by cyclic voltammetry as a function of the number of cycles: A: 1, B: 3000, C: 5000, D: 10000 cycles; Q_a (anodic charge stored), Q_c (cathodic discharge), (b) i_a (anodic peak current), (c) i_c (cathodic peak current).

Besides electrochemical stability, PEDOT-POSS, as expected, represented somewhat better thermal stability. While PEDOT has a maximum decompose temperature at

373 ^{o}C, this temperature is 394 ^{o}C for PEDOT-POSS. (Appendix D) Also, the molecular weight of PEDOT-POSS was determined by GPC using polystyrene as a standard. As the average molecular weight, the measurement of chemically and electrochemically obtained PEDOT-POSS samples yielded 60100 (PDI=2.75) and 8223 (PDI= 2.46), respectively (Appendix E).

3.1.5 Optical and Electrochromic Behavior of PEDOT-POSS

When compared to PEDOT (1.60 eV with a maximum wavelength of 627 nm), PEDOT-POSS coated on ITO electrode has somewhat a higher band gap of 1.71 eV with a maximum wavelength of 618 nm. The neutral state PEDOT-POSS exhibited a narrower absorption band than PEDOT (Figure 3.9 and Figure 3.10 (a)). Due to this narrow absorption band, the absorbance between 400 and 500 nm become lower and the PEDOT-POSS film exhibited nearly a pure blue color [65,67,128,129], which is one of the legs in RGB color pallet. This promising property combined with its solubility in common organic solvent (chloroform, dichloromethane, tetrahydrofuran, etc.) makes it a strong competitor against the PEDOT and a promising candidate for opto-electronic applications. The presence of POSS unit in the polymer backbone overcame the insolubility problem of the PEDOT which is one of the most important materials in chemistry and material science.

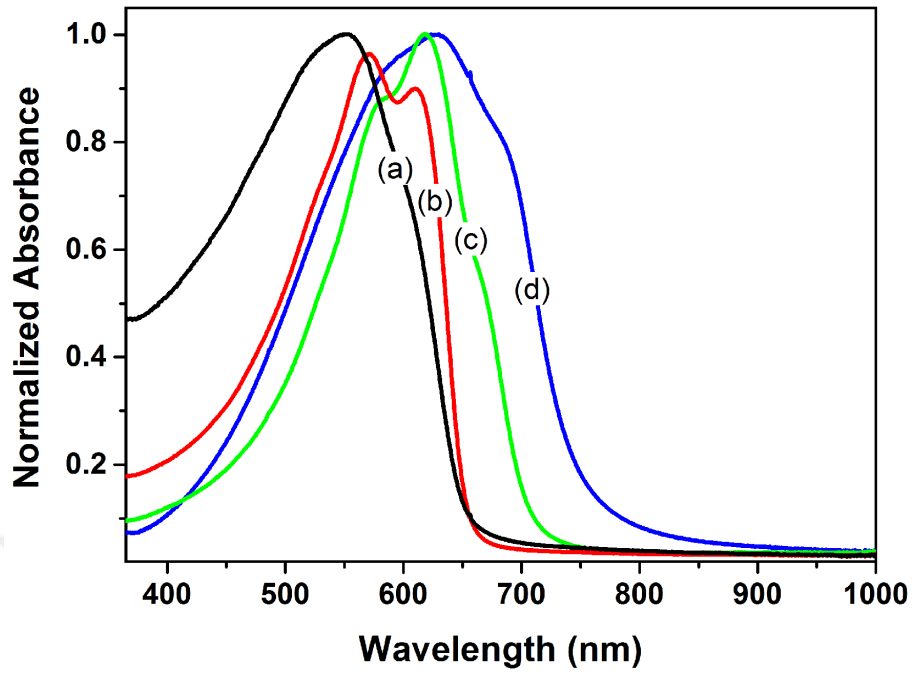

Figure 3.9. Absorption spectra of (a) chemically and (b) electrochemically obtained PEDOT-POSS polymer in CH_2Cl_2, electrochemically obtained (c) PEDOT-POSS film and (d) PEDOT film on ITO electrode.

The electro-optical properties of PEDOT-POSS film were investigated by monitoring the changes in electronic absorption spectra under applied external potentials. As shown in Figure 3.10 (b), the intensity of the absorption band at 618 nm attributed to the π-π* transition band started to decrease simultaneously upon oxidation and a new absorption band beyond 700 nm started to intensify and received a maximum value due to the formation of polaron charge carriers. Upon further oxidation, the π-π* transition band reached the minimum intensity and due to the formation of bipolaron charge carriers, the polaron absorption band diminished. All these changes in the optical absorption spectrum can be followed by color changes of the films: blue (L= 53.4; a=-0.6; b= -48.0;) at neutral state and highly transparent (L= 92.6; a=-2.6; b= -2.0;) at oxidized state (see inset of Figure 3.10 (b)).

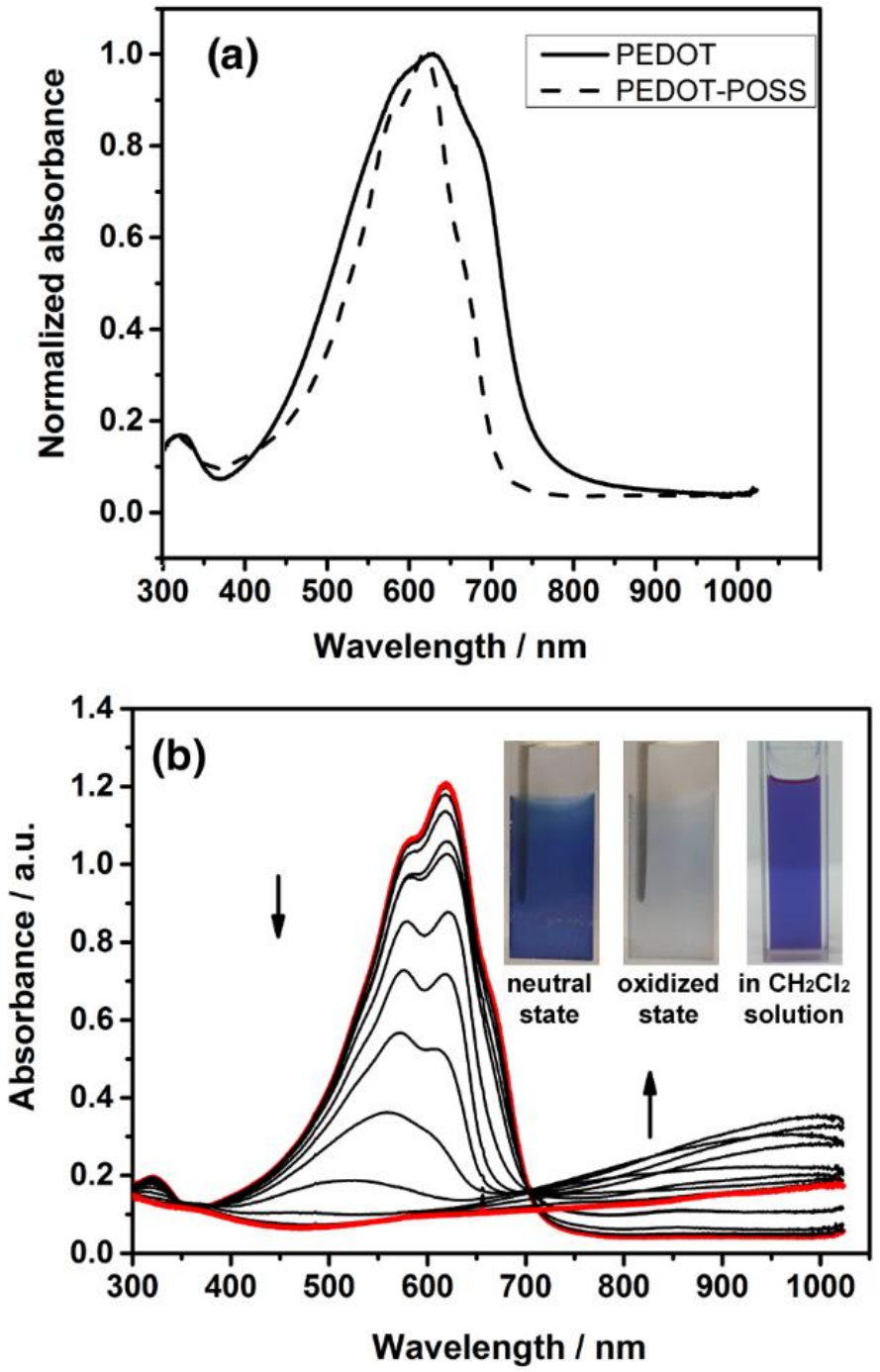

Figure 3.10. (a) Absorption spectra of the neutral state PEDOT and PEDOT-POSS films on ITO and (b) Electronic absorption spectra of the PEDOT-POSS film on ITO in 0.1 M TBAH/CH_3CN at various applied potentials between -1.0 V and 1.0 V. Inset: The colors of PEDOT-POSS at neutral and oxidized states and the polymer dissolved in dichloromethane.

The percentage transmittance change (optical contrast ratio, Δ%T) of PEDOT-POSS was calculated as 74% at 618 nm, which is higher than that of PEDOT (61% at 627 nm) (Figure 3.11). This difference can be attributed to the presence of POSS units due to easier ion injection into the polymer structure during doping process. As shown in Table 3.1, PEDOT-POSS demonstrated higher coloration efficiency (582 cm^2/C at 95% of the full contrast) and faster switching time (0.9 s) when compared to its parent PEDOT analogue.

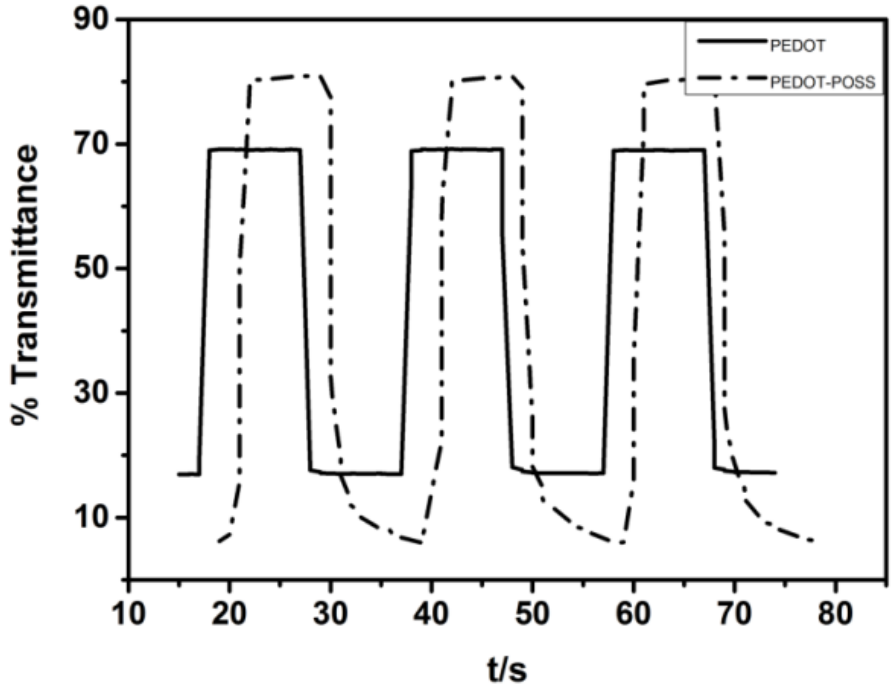

Figure 3.11. Chronoabsorptometry experiments for PEDOT (at 627 nm, 17 mC/cm^2) and PEDOT-POSS (at 618 nm, 17 mC/cm^2) films on ITO in 0.1 M TBAH/CH_3CN while the polymer films were switched with an interval time of 10 s between -0.5 and 0.9 V.

On the other hand, as expected from a soluble and conjugated polymer, the corresponding PEDOT-POSS polymer has a fluorescence property. As shown in Figure 3.12, both chemically and electrochemically obtained polymers exhibited similar emission band. For example, chemically obtained PEDOT-POSS polymer showed broad emission bands centered at 651 nm and 698 nm, which corresponds to reddish orange emission. Under the light of this finding, it can be safely concluded that unlike PEDOT, the soluble and fluorescent PEDOT-POSS polymer can find a number of applications like organic lasers or an active emitter in light emitting diodes. Also, the reddish orange emission can make it amenable to use in bio-applications like imaging the cancer cells.

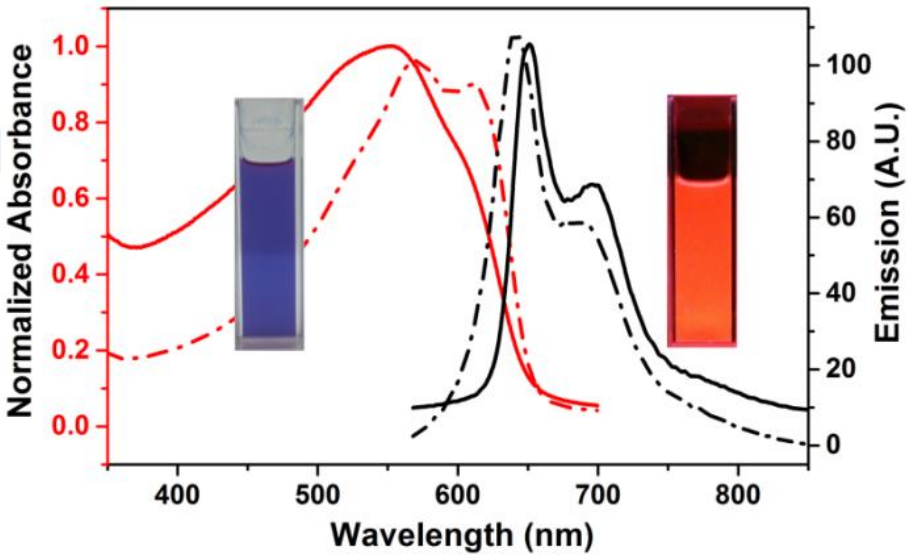

Figure 3.12. Absorbance (red) and emission (black) spectra of chemically (line) and electrochemically (dash line) obtained PEDOT-POSS in CH_2Cl_2. Inset: Colors of the PEDOT-POSS polymer in CH_2Cl_2 under ambient light (left) and handheld UV lamp (right) at 365 nm.

Table 3.1. Optical properties of electrochemically obtained PEDOT (17 mC/cm^2) and PEDOT-POSS (17 mC/cm^2) films.

Polymers	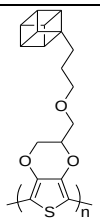 **PEDOT-POSS**	 **PEDOT**
λ_{max} (nm)	618	627
E_g (eV)*	1.71	1.60
HOMO (eV)*	-4.64	-4.17
LUMO (eV)*	-2.93	-2.57
Δ%T	74 %	61 %
t_{ox} (s)	0.9	1.2
CE (cm^2/C)	582	350

The optical E_g values were calculated from the onset of the low energy end of π-π transition band of the polymer films at their neutral states E_g= 1240 nm/λ_{onset}. HOMO values were calculated from the cyclic voltammetry according to the following equation [130,131]: E_{HOMO} = -($E_{[onset,ox\ vs\ Fc+/Fc]}$ + 4.80)(eV). Finally, by using the E_g= E_{HOMO} - E_{LUMO} formula, E_{LUMO} values were calculated. 2.50 mM solution of ferrocene/ferrocenium (Fc/Fc+) couple in CH_2Cl_2 has a reversible redox couple at a half wave of 0.48 mV with an onset oxidation value at 0.40 V vs Ag/AgCl.

3.1.6 Electrochromic Device Application of PEDOT-POSS Polymer

Based on the foregoing results, a representative application of PEDOT-POSS polymer will be more meaningful in order to think this polymer as a promising candidate for opto-electronic applications instead of PEDOT. Therefore, a dual type PEDOT-POSS/poly(4,7-bis(2,3-dihydrothieno[3,4-b][1,4]dioxin-5-yl)benzo[c] [1,2,5]selenadiazole) (PESeE) [39] (Figure 1.13) based electrochromic device was constructed and its optical behavior was investigated under applied external potential. Figure 3.14 showed the change in optical absorbance spectra of the device at different applied potentials from -2.2 V to 1.85 V. While the color of the device at -2.2 V was dark blue (L: 55.2, a: -0.55, b: -36.0), it was changed to light green (L: 80.5, a: -17.9, c: 7.39) at 1.85 V with a switching time of 1.1 s. Upon moving from -2.2 V to 1.85 V, the broad band bearing two maximum wavelengths at 580 nm and 624 nm between 400 nm and 700 nm, which is attributed to the neutral state of PEDOT-POSS film (Figure 3.18.(b)), starts to lose its intensity and new peaks start to appear and intensify at 430 nm and 783 nm due to the neutral state of PESeE film (Figure 3.14) [39]. On the other hand, the electrochromic device showed a reversible and robust behavior when switched between its redox states. The device retained its electroactivity without significant loss in its performance even after hundreds of cycles. For instance, 57% of its electroactivity remained after 750 cycles (Figure 3.15).

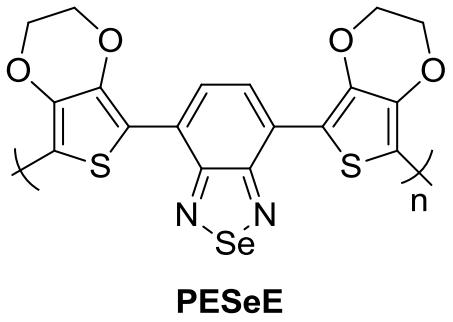

PESeE

Figure 3.13. Chemical structure of the polymer PESeE.

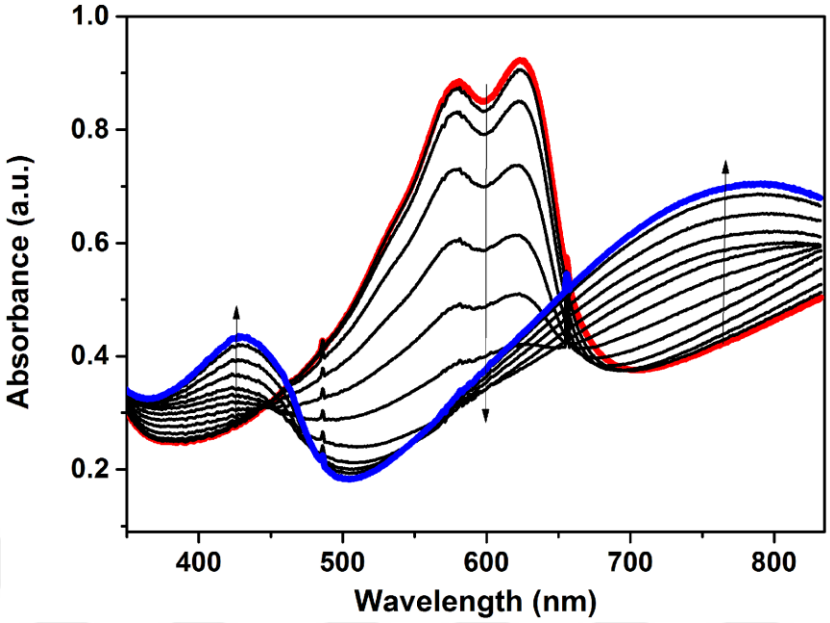

Figure 3.14. Electronic absorption spectra of PEDOT-POSS/PESeE based electrochromic device at various applied potentials between -2.2 V and 1.85 V.

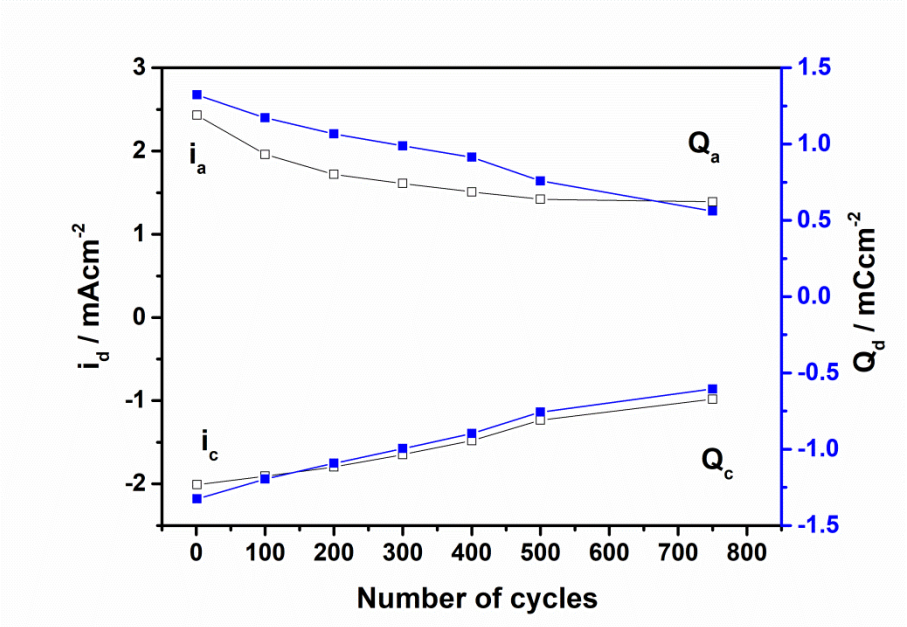

Figure 3.15. Stability test for PEDOT-POSS/PESeE based electrochromic device after a certain number of switching under an applied square voltage signal with an interval of 3 s between -2.2 V and 1.85 V film under ambient conditions: Q_a (anodic charge stored), Q_c (cathodic discharge), (b) i_a (anodic peak current), (c) i_c (cathodic peak current).

3.1.7 Photocatalytic Application of PEDOT-POSS Polymer

The photocatalytic activities of PEDOT [132] and PEDOT-POSS were investigated for decolorization of methylene blue (MB) dye under UV light. For this purpose 15 mg of the polymer was added to 10 mL of MB aqueous solution and stirred in the dark until the concentration of MB solution became constant. Then, the mixture was exposured with a UV light at constant magnetic stirring to obtain good mixing of photocatalyst and MB solution.

In order to find the catalytic activity of the polymers under UV exposure, decoloration of MB was checked at every 10 min by taking 2 mL of sample with a syringe. Removal of the MB dye was revealed by using a UV-Vis spectrophotometer. To calculate the amount of MB removed, the absorbance maximum at 660 nm was followed. The results revealed that PEDOT-POSS polymer is a promising candidate for dye removal. PEDOT-POSS itself removed 65.6% of the dye in 10 minutes and in one hour it removed nearly all of the dye (Figure 3.16, Figure 3.17, Table 3.2 and Table 3.3).

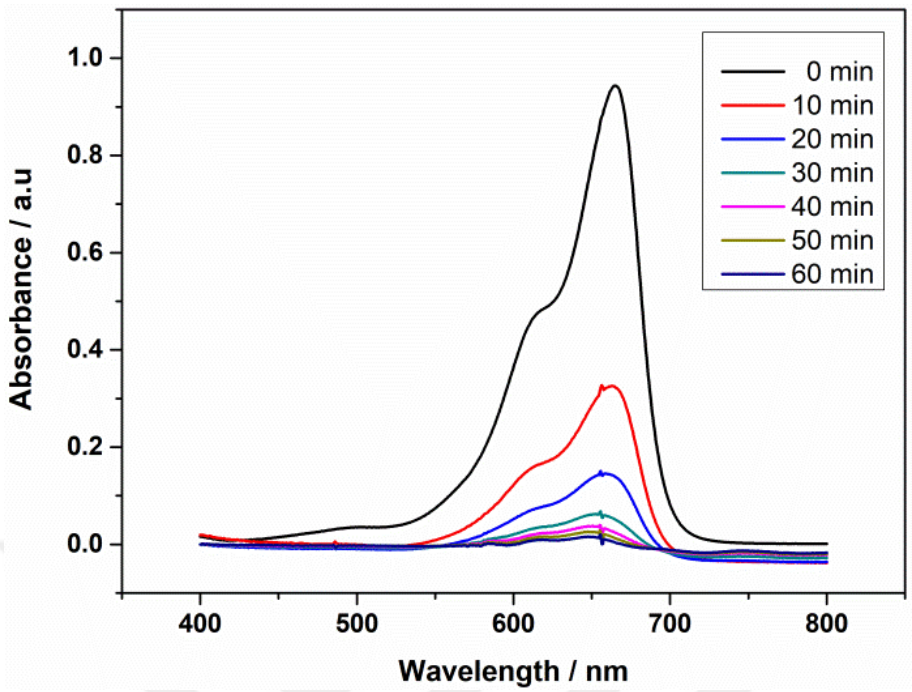

Figure 3.16. UV-Vis spectra of MB solution processed with 15 mg of PEDOT-POSS under UV light illumination.

Table 3.2. Percent MB removal results of PEDOT-POSS under UV light exposure for different durations.

Time (min)	**% Removal (PEDOT-POSS)**
0	
10	65.6
20	85.1
30	94.5
40	97.4
50	98.6
60	99.5

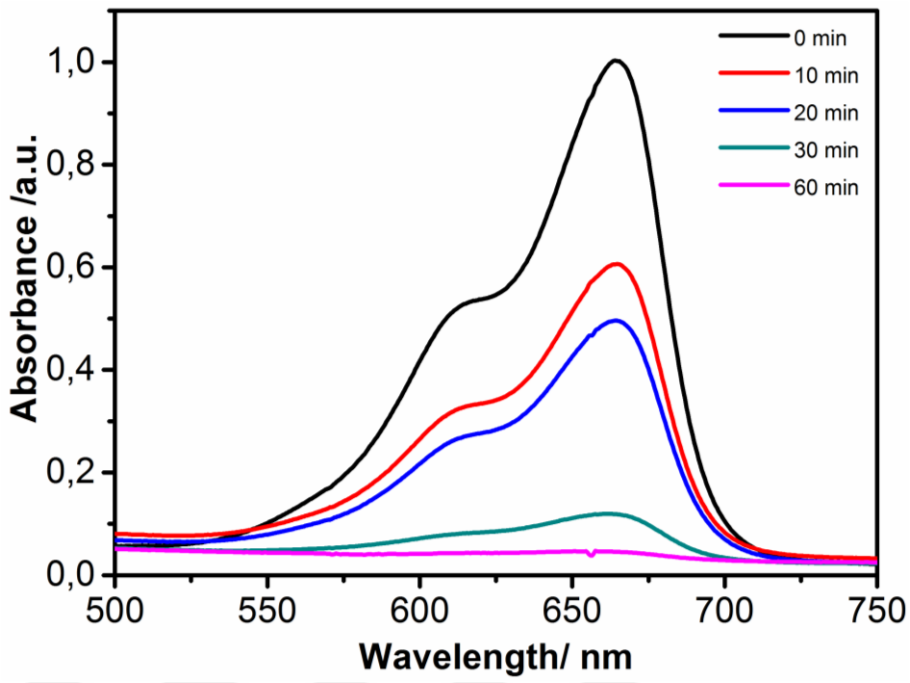

Figure 3.17. UV-Vis spectra of MB solution processed with 15 mg of PEDOT under UV light illumination.

Table 3.3. Percent MB removal results of PEDOT under UV light exposure for different durations.

Time (min)	**% Removal (PEDOT)**
10	39.4
20	50.4
30	88.1
60	95.0

Reusability is one of the most important parameters in heterogenous catalysis. In order to make it easier, magnetic nanoparticles have been utilized to recover the catalyst easily. PEDOT-POSS polymer was mixed with MNPs for easy recovery and the result showed that MNP loaded polymer responded faster than neat polymer (Figure 3.18 and Table 3.4)).

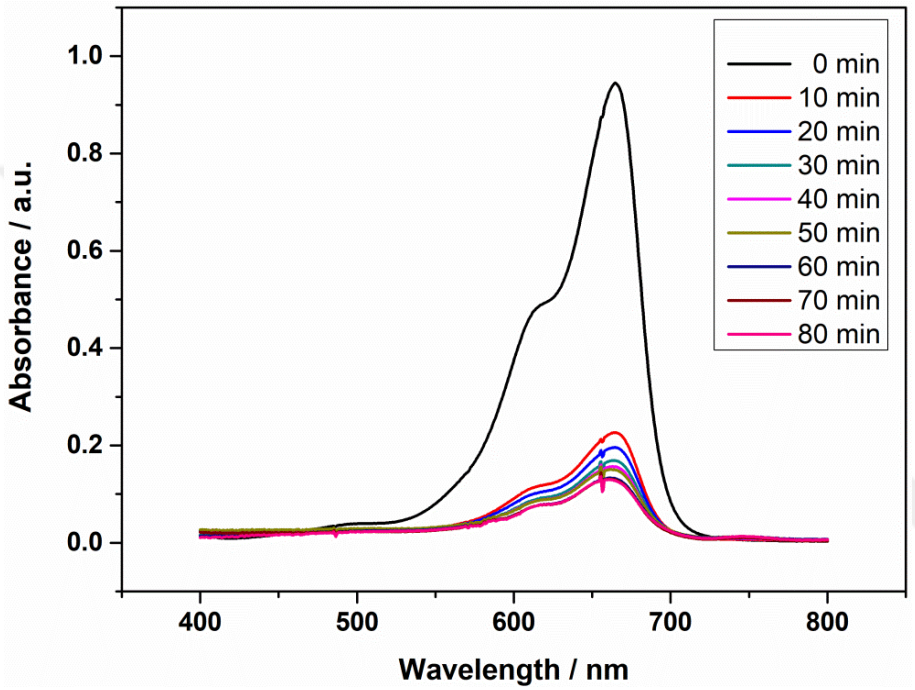

Figure 3.18. UV-Vis spectra of the MB solution processed with 10 mg of MNP loaded PEDOT-POSS under UV light illumination.

Table 3.4. Percent MB removal results of MNP loaded PEDOT-POSS under UV light exposure for different durations.

Time (min)	% Removal (MNP-PEDOT-POSS)
0	
10	76.0
20	79.2
30	82.1
40	83.4
50	84.1
60	86.0
70	86.3
80	86.4

The results mentioned above showed that conjugated polymers are good candidates for photocatalytic applications. When we compare the results it can easily be seen that PEDOT-POSS exhibited better performance on removal of MB dye and it can be attributed to the presence of the POSS unit on the polymer backbone because POSS unit does not let polymer chains to get closer to each other and this allows better contact with the dye molecules.

3.2 Synthesis and Electrochemical and Electro-optical Characterization of Poly(EDOT-co-EDOT-POSS)

3.2.1 Comparison of the Electrochemistry of EDOT and EDOT-POSS Monomers and Their Copolymerization

The redox behaviors of EDOT and EDOT-POSS monomers were investigated by using a cyclic voltammetry technique since the oxidation values of the co-monomers must be appropriate to each other in order to get reasonable copolymers via constant potential or potentiodynamic electrolysis. As shown in Figure 3.19(a), both monomers exhibited an irreversible oxidation peak at 1.46 V vs Ag/AgCl, which indicates that the electrochemical copolymerization of EDOT and EDOT-POSS was feasible.

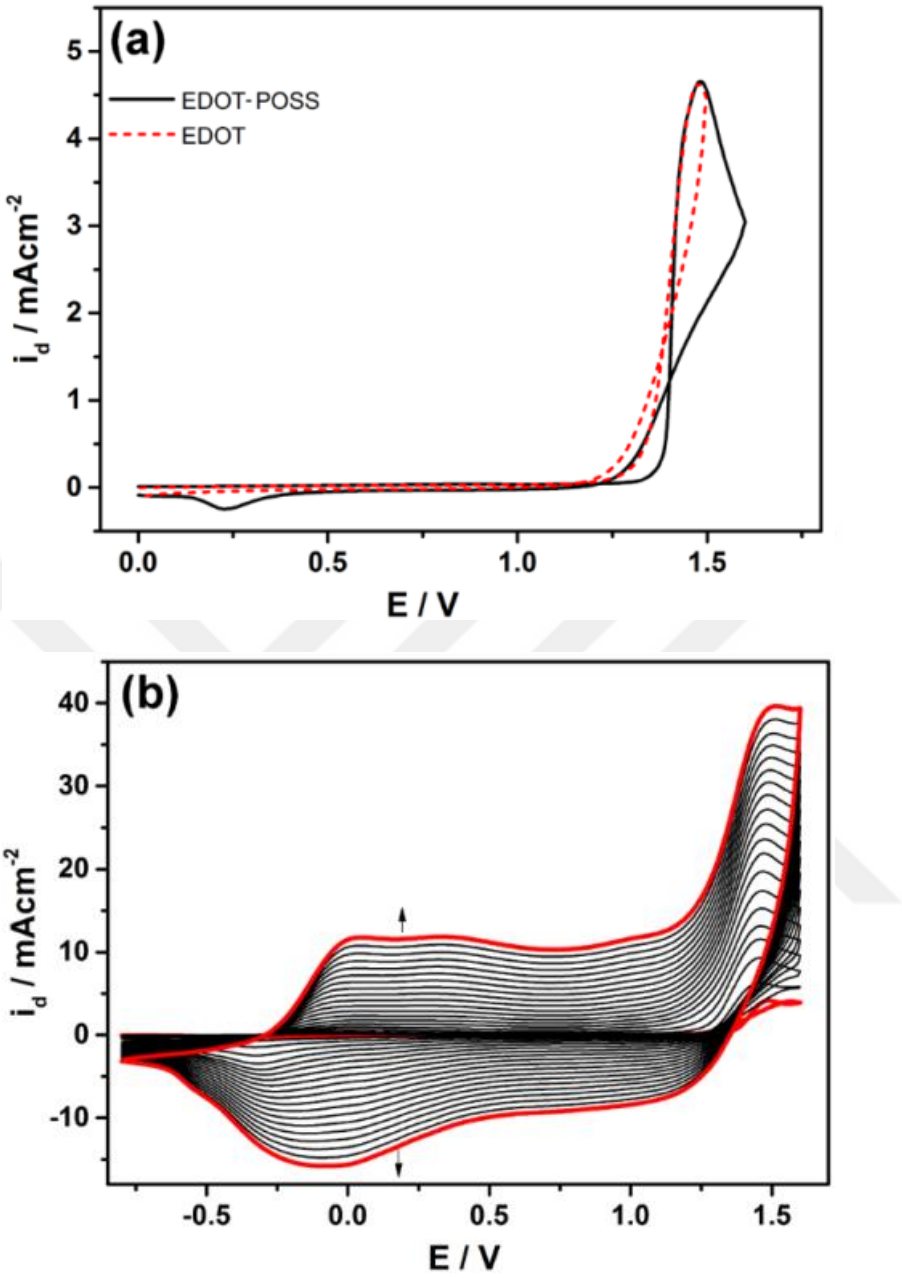

Figure 3.19. (a) Cyclic voltammograms of EDOT (6.67 mM) and EDOT-POSS (6.67 mM) and (b) cyclic voltammogram of the repeated scan electropolymerization of a mixture of EDOT (6.67 mM) and EDOT-POSS (0.67 mM) with 10:1 monomer feed ratio to give poly(EDOT-co-EDOT-POSS) in an electrolyte solution of 0.1 M TBAH dissolved in a mixture of dichloromethane and acetonitrile (1/3, v/v) on Pt disk working electrode at a scan rate of 100 mV/s vs. Ag/AgCl.

The monomer EDOT-POSS and its corresponding polymer were soluble in dichloromethane and insoluble in acetonitrile, which hinders the electropolymerization on the electrode surface. Therefore, the copolymerization was carried out by using the solvent mixture in order to hinder the solubility of the polymer film formed on the electrode surface by cosolvent effects.

As seen in Figure 3.19(b), the cyclic voltammogram obtained after a certain number of potentiodynamic scans looks like a fingerprint of the formation of a conjugated polymer film. The repetitive scans between -0.8 V and 1.6 V resulted in a formation of an insoluble copolymer film called poly(EDOT-co-EDOT-POSS) (CP-n, where n= 1, 5, 10, 15 defines the percentage of EDOT-POSS in co-monomer mixture) (Table 3.5 and Scheme 3.2) on the electrode surface since upon successive scan a new redox couple appeared between -0.1 V and 1.5 V and intensified as a function of scan numbers.

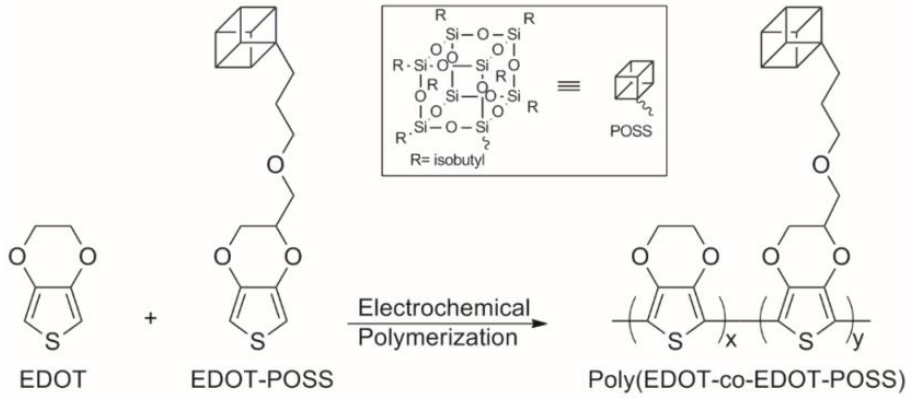

Scheme 3.2. Chemical structures of EDOT, EDOT-POSS and their corresponding copolymer poly(EDOT-co-EDOT-POSS).

Table 3.5. Optical properties of PEDOT, PEDOT-POSS and their corresponding copolymers on ITO in 0.1 M TBAH/CH_3CN.

Polymers	Feed ratio (EDOT:EDOT-POSS)	EDOT-POSS content (%)	λ_{max} (nm)	Eg^a (eV)	Δ%T	CE (cm^2/C)	$t_{switching}$ [b] (s)
PEDOT	1:0	0	621	1.61	54	352	1.2
CP-1	100:1	1	620	1.62	58	323	1.1
CP-5	100:5	5	620	1.62	60	354	1.1
CP-10	100:10	9	621	1.62	65	463	1.0
CP-15	100:15	13	621	1.63	65	493	1.0
PEDOT-POSS	0:1	100	619	1.71	74	582	0.9

[a]optical band gap, [b]100% of full switch from colored to bleached states.

FTIR spectroscopy can be a useful method to clarify the presence of POSS cages in the copolymer structure by proving the presence of Si-O-Si stretching band. As shown in Figure 3.20, the comparison of the FTIR spectra of PEDOT-POSS and the copolymer CP-10 is given and like PEDOT-POSS spectrum, Si-O-Si stretching band was observed at around 1073 cm^{-1} as well as CH stretching of aliphatic groups appearing at 2850 and 2929 cm^{-1}. These findings clearly prove the presence of POSS cages in the copolymer structure.

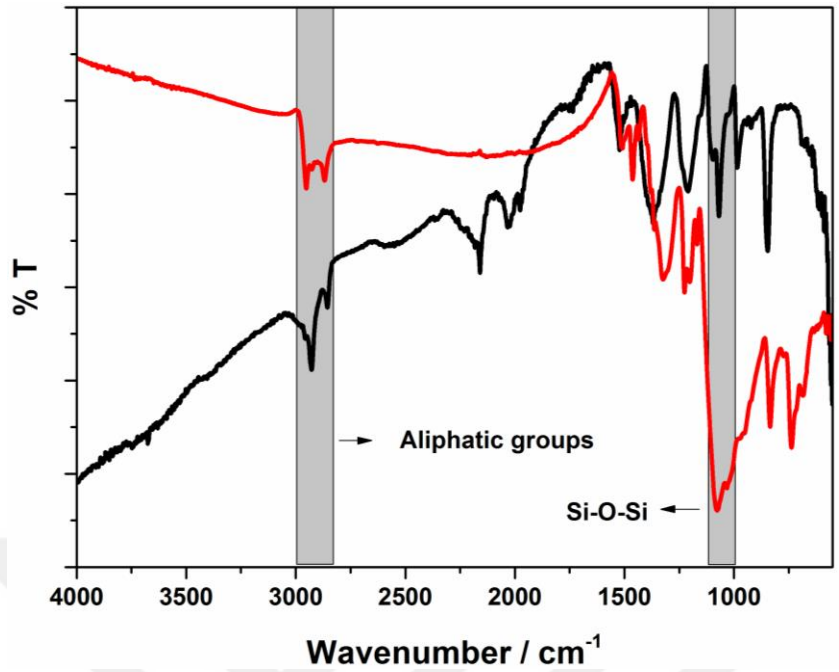

Figure 3.20. FTIR spectra of chemically obtained PEDOT-POSS and Poly(EDOT-co-EDOT-POSS) obtained via constant potential electrolysis at 1.5 V in an electrolyte solution of 0.1 M TBAH dissolved in the mixture of dichloromethane and acetonitrile (1/3: v/v) on ITO electrode.

Also, the insertion of EDOT-POSS monomers into PEDOT polymer backbone can easily be seen in comparison of the cyclic voltammograms of the copolymers with the parent PEDOT and PEDOT-POSS polymers. As seen in Figure 3.21(a), the presence of EDOT-POSS units was confirmed by the appearance of a new oxidation peak at nearly -0.10 V, which intensified as a function of increasing ratio of EDOT-POSS in a co-monomer mixture. Also, whereas the copolymers and PEDOT exhibited their redox behavior in the range of -0.8 V to 1.1 V, PEDOT-POSS polymer represented its redox behavior at higher positive potential. It was also shown that the peak current intensities of the copolymers' redox couples changed linearly as a function of scan rates during p-doping (Figure 3.21(b)), which confirmed that the redox process of the copolymer firmly coated on Pt electrode is not-diffusion controlled.

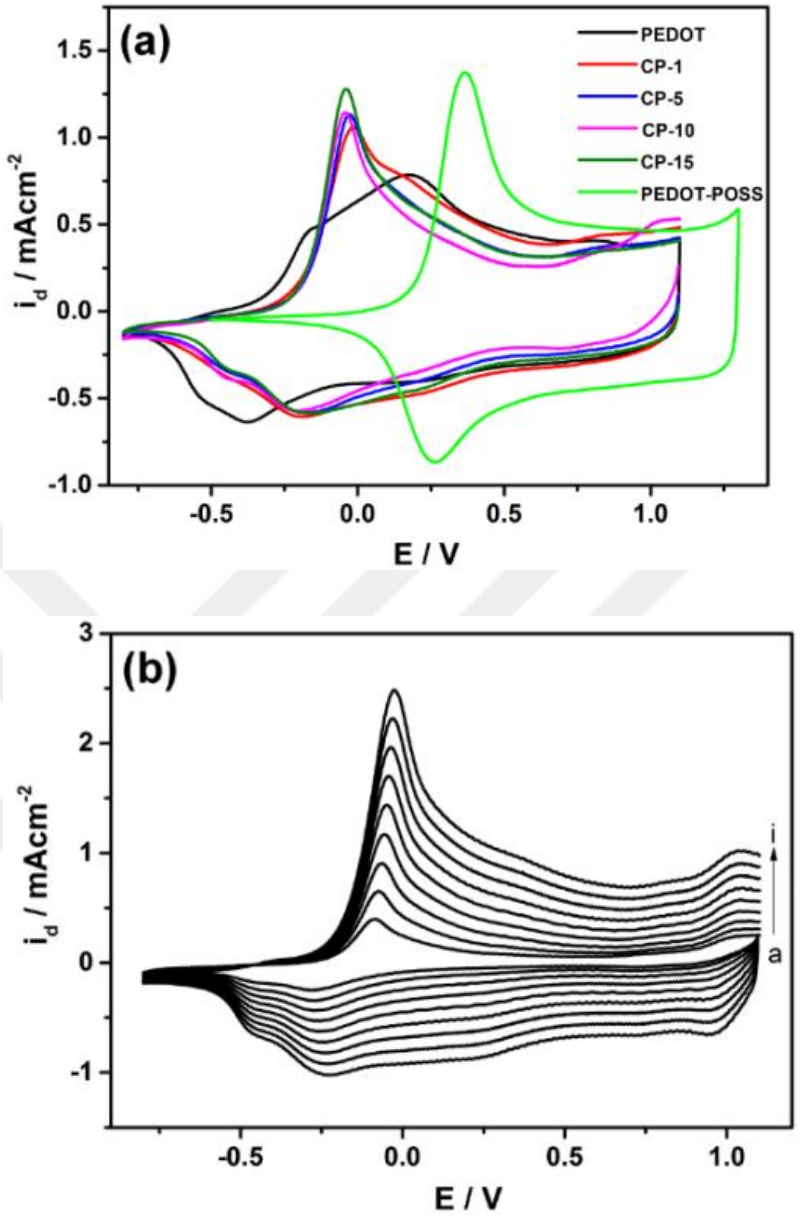

Figure 3.21. Cyclic voltammograms of the polymers coated on Pt electrode with a charge of 3.0 mC/cm^2 via constant potential electrolysis at 1.55 V vs. Ag/AgCl: PEDOT, PEDOT-POSS and their copolymers obtained from a co-monomer feed ratio of 100:1, 100:5, 100:10 and 100:15 in an electrolyte solution of 0.1 M TBAH dissolved in the mixture of dichloromethane (1/3, v/v) acetonitrile at a scan rate of 100 mV/s, and (b) scan rate dependence of the copolymer CP-10 film in 0.1 M TBAH/CH_3CN at different scan rates (mV/s): (a) 40, (b) 60, (c) 80, (d) 100), (e) 120, (f) 140, (g) 160, (h) 180 and (i) 200.

The stability test was performed by switching the polymer film between its neutral and oxidized states by using a square wave potential method. The tests showed that while the copolymer CP-10 retained 86 % of its electroactivity (Figure 3.22(a)) after 1750 switching, PEDOT is completely lost its electroactivity (Figure 3.22(b)). As a result, it can be safely concluded that EDOT-POSS units in PEDOT backbone improved the electrochemical stability of the copolymer film and these units gave more stability and environmental robustness under ambient conditions. Also it can be conjectured that this higher electroactivity can be due to the presence of POSS units which makes the ion exchange easier by increasing the distance between chains. [107, 108, 133-136]

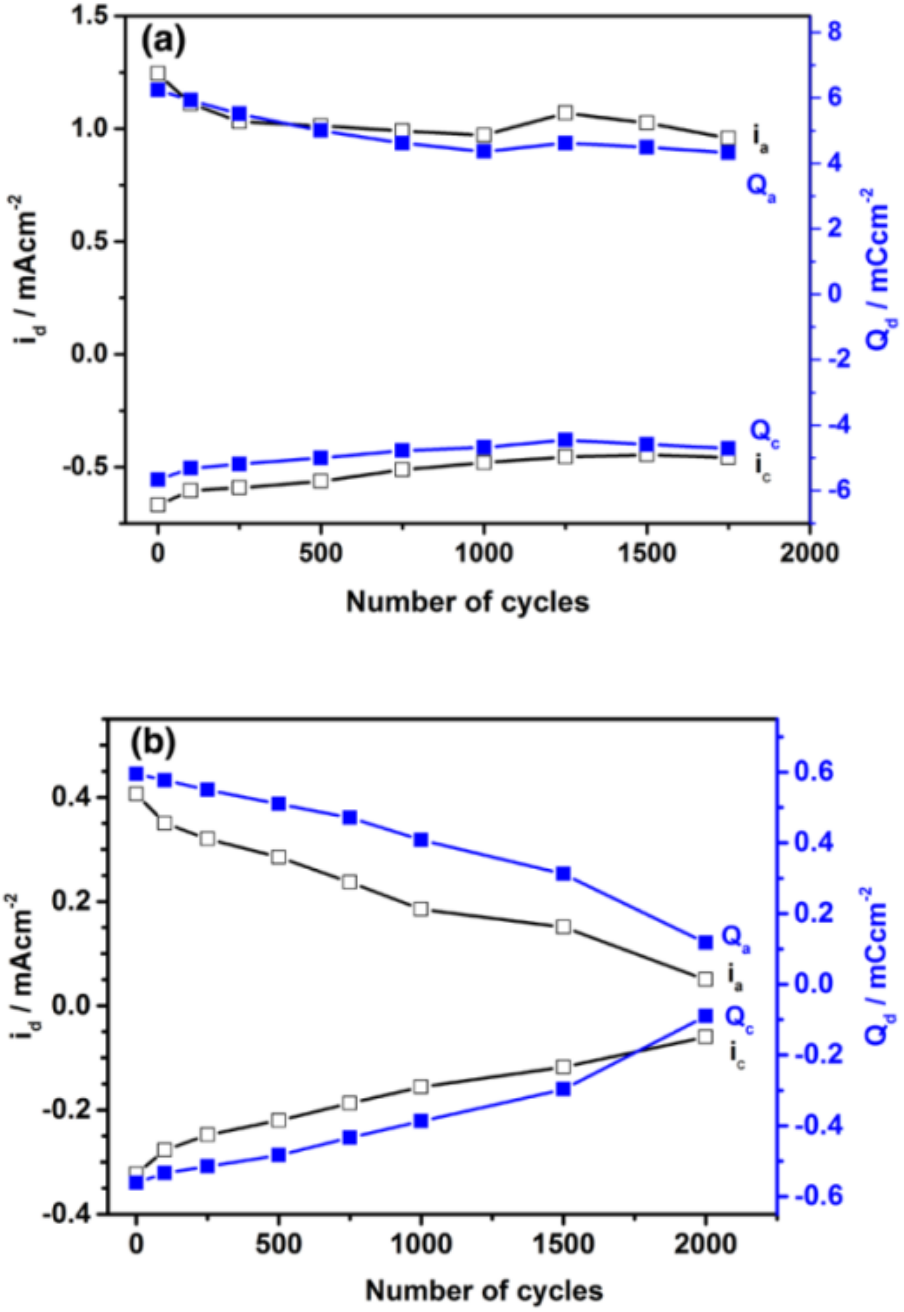

Figure 3.22. Stability tests for (a) the copolymer CP-10 and (b) PEDOT films (3 mC/cm^2) in 0.1 M TBAH/CH_3CN by using a square wave potential method at -0.8 V and at 0.6 V with an increment of 3 s under ambient conditions at a scan rate of 100 mV/s; (a) Q_a (anodic charge stored), (b) I_{pa} (anodic peak current), (c) I_{pc} (cathodic peak current).

3.2.2 Optical and Electrochromic Behaviors of Poly(EDOT-co-EDOT-POSS)

The main purpose of this study is to improve the optical properties (percent transmittance change, switching time, coloration efficiency, etc.) of PEDOT polymer without changing its redox and electrochromic behaviors, so the neutral state absorption spectra of the copolymers were compared with those of PEDOT and PEDOT-POSS. As shown in Figure 3.23(a), the presence of EDOT-POSS units in the PEDOT polymer backbone does not cause any appreciable change in the PEDOT's absorption bands since the neutral state copolymer films represented nearly the same absorption bands of PEDOT.

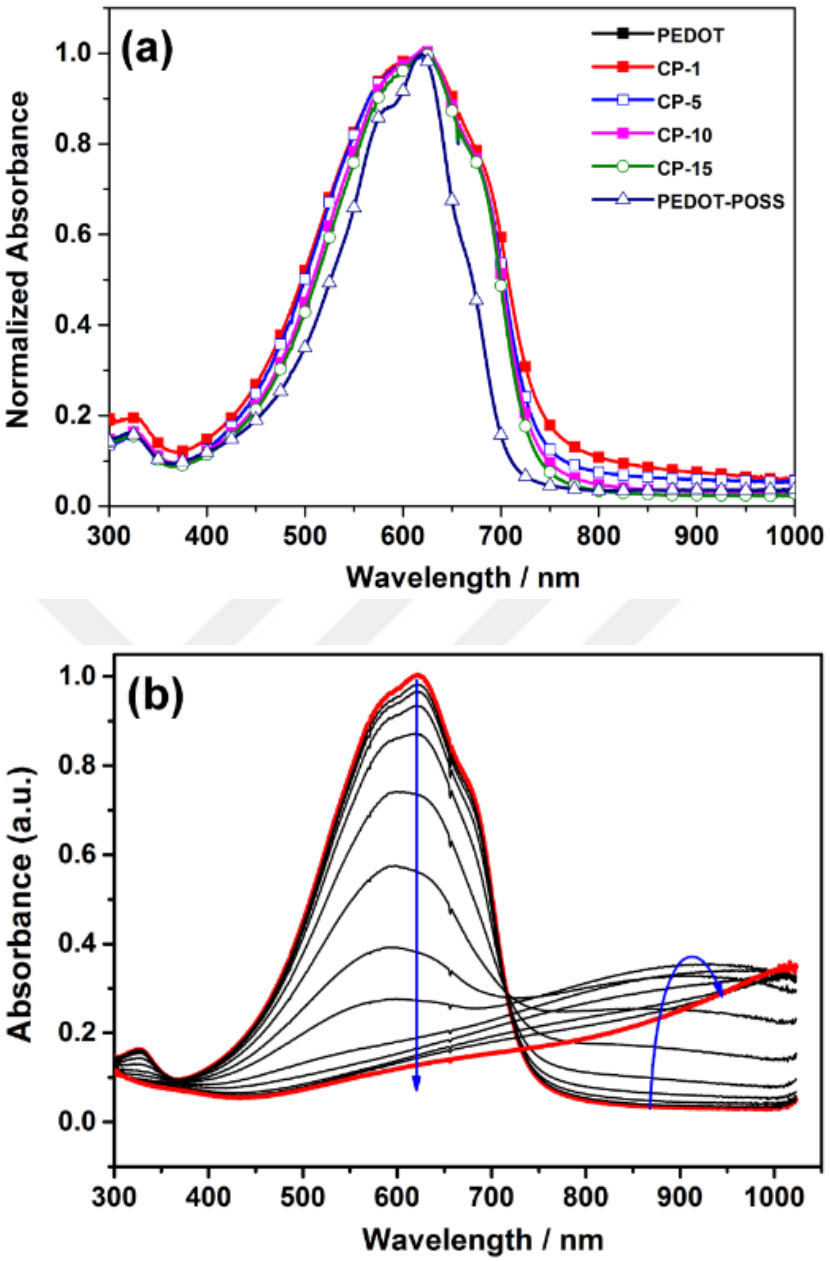

Figure 3.23. (a) Neutral state absorption spectra of PEDOT, PEDOT-POSS and the copolymers CP-1, CP-5, CP-10, CP-15 obtained via constant potential electrolysis at 1.5 V in an electrolyte solution of 0.1 M TBAH dissolved in the mixture of dichloromethane and acetonitrile (1/3: v/v) on ITO electrode with a charge of 12 mC/cm^2. (b) Electronic absorption spectra of the copolymer CP-10 film coated on ITO electrode at various applied potentials between -0.8 V and +1.1 V in 0.1 M TBAH/CH_3CN.

The copolymer CP-10 obtained electrochemically from a monomer feed ratio of 10:1 exhibited a broad absorption band centered at 620 nm with two shoulders at 580 nm and 671 nm attributed to the π-π* transition band. From the commencement of the low energy end of the π-π* transition band, the optical band gaps of the copolymers were calculated as 1.62 eV with a maximum wavelength of 620 nm similar to that of PEDOT (1.61 eV with a maximum wavelength of 621 nm) (Table 3.5). Upon moving from –0.8 V to +1.1 V, the intensity of the π-π* transition band started to decrease simultaneously as expected from a homogenous conjugated polymer rather than a heterogeneous/bilayer one (Figure 3.23 (b)). During the decrease in the intensity of the band, a concomitant absorption band was appeared at 900 nm and intensified during oxidation due to the formation of charge carriers called polarons. Further oxidation converted polaron charge carriers into bipolaron charge carriers and this conversion can be monitored by decreasing intensity of the polaron band and by appearing and intensifying a new band beyond 1000 nm. During this observation, the π-π* transition band diminished completely. These observed changes in absorption spectra of the copolymers can directly be followed by a color change: while the neutral state copolymers just as PEDOT film are dark blue/violet, their oxidized forms are more transparent than PEDOT film. Therefore, the copolymer films represented higher percent transmittance change (from 58 % to 65 %) than PEDOT (54%) on account of the presence of EDOT-POSS units in the copolymer structure (Figure 3.24 and Table 3.5).

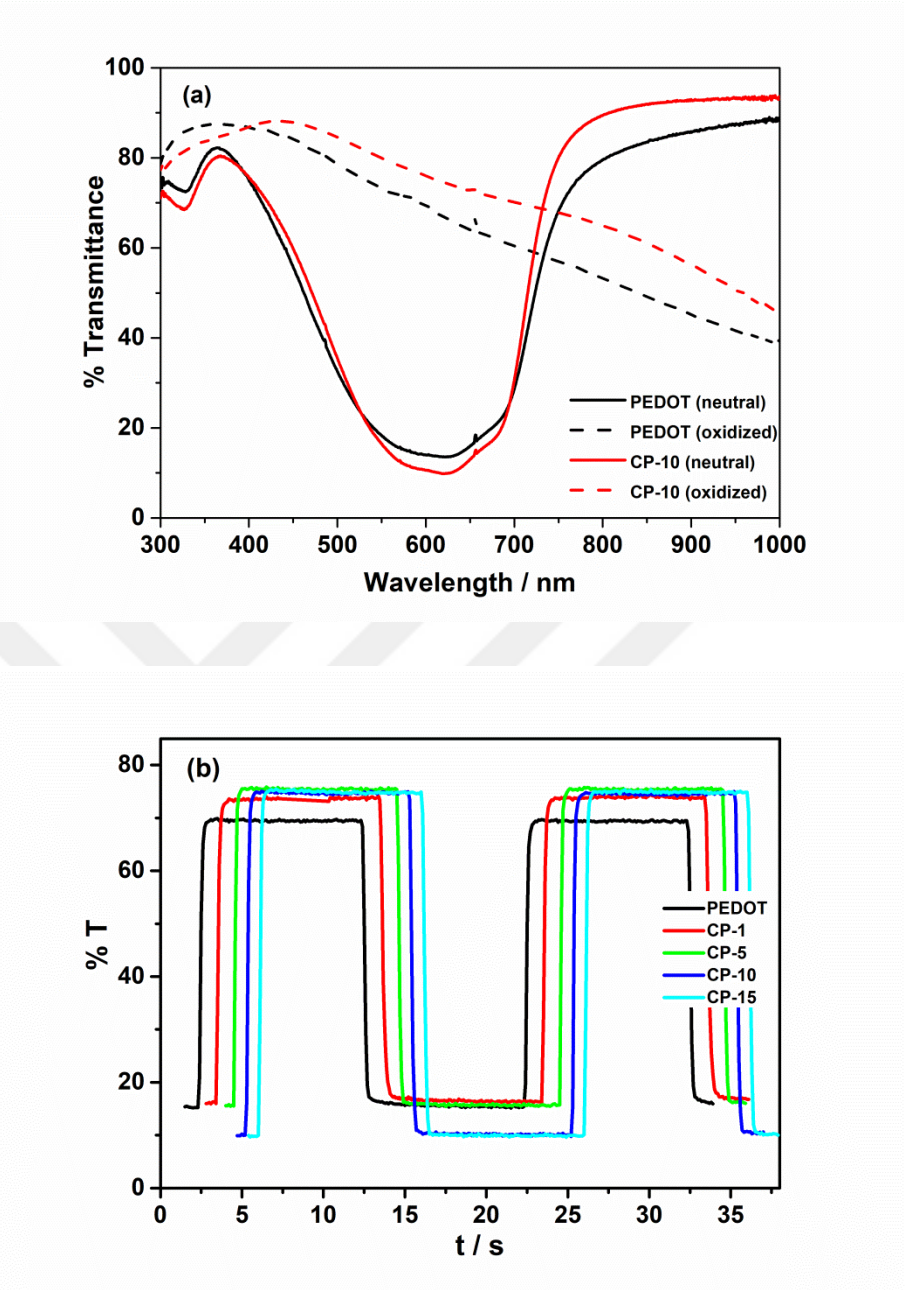

Figure 3.24. (a) Transmittance spectra of PEDOT and CP-10 on ITO in their neutral and oxidized states in 0.1 M TBAH/CH_3CN. (b) chronoabsoptometry experiments for the PEDOT and the copolymers when the polymers were switched for 10 s intervals between redox states in 0.1 M TBAH/CH_3CN. The polymers were obtained via constant potential electrolysis at 1.5 V in an electrolyte solution of 0.1 M TBAH dissolved in the mixture of dichloromethane and acetonitrile (1/3: v/v) on ITO electrode with a charge of 12 mC/cm^2.

Color changes can also be defined more scientifically by using L*a*b* coordinates, where L* is the luminescence (the white-black balance), a* and b* are the red-green balance and yellow-blue balance of the corresponding color, respectively. As shown in Figure 3.26, PEDOT and the corresponding copolymer represent the similar behaviors when switched between their redox states.

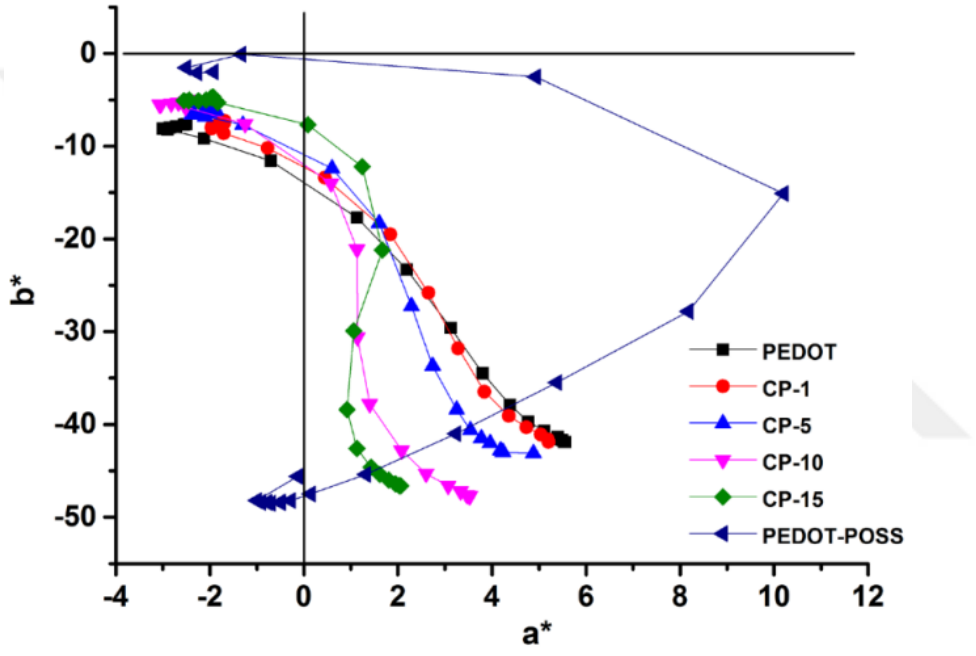

Figure 3.25. a*b* coordinate of the color change of the polymers upon moving from -0.8 V to 1.1 V with 0.1 V increments.

Also, L*a*b* coordinates can be used to determine the degree of color saturation, S_{ab}, defined as the ratio of chromatic color. Its value has a range from 0 to 100, where 0 is gray and 100 is a pure color. It can be calculated according to Equation 2.3 [137]. All polymer films represented color saturation between 60 and 67 (Table 3.6). The copolymer films showed very similar color purity with PEDOT (60). These findings can also be confirmed by comparing the color difference ΔE^*_{ab} given in Equation 2.4 [137].

$$S_{ab}=\left(\frac{a^{*2}+b^{*2}}{a^{*2}+b^{*2}+L^{*2}}\right)^{1/2} \qquad \text{Equation 2.3}$$

$$\Delta E^*_{ab} = [(\Delta L^*)^2 + (\Delta a^*)^2 + (\Delta b^*)^2]^{1/2} \qquad \text{Equation 2.4}$$

The ΔE^*_{ab} values vary from 2.3 to 6.8 versus PEDOT and the colors of the polymers are nearly indistinguishable by naked eye since the ΔE^*_{ab} values are lower than 2.3.

Table 3.6. Colorimetry and optical comparisons of PEDOT, PEDOT-POSS and the copolymers.

Polymers	**L*, a*, b* (neutral)**	**L*, a*, b* (oxidized)**	**Color saturation**	**ΔE^*_{ab} of the copolymers vs PEDOT (neutral)**	**ΔE^*_{ab} of the copolymers vs PEDOT-POSS (neutral)**	**Color at neutral state**	**Color at oxidized state**
PEDOT	L: 56 a: 6 b: -42	L: 90.2 a: -2.5 b: -7.6	60	0	9.0		
CP-1	L: 53.2 a: 5.2 b: -41.6	L: 86.1 a: -1.7 b: -7.2	62	2.7	8.7		
CP-5	L: 57.5 a: 4.2 b: -42.9	L: 91.4 a: -1.9 b: -6.1	60	2.3	8.1		
CP-10	L: 53.3 a: 3.5 b: -47.7	L: 91.9 a: -2.4 b: -5.0	67	6.8	4.1		
CP-15	L: 55.5 a: 2.0 b: -46.6	L: 92.7 a: -1.9 b: -4.7	64	5.8	3.7		
PEDOT-POSS	L: 53.4 a: -0.6 b: -48	L: 92.6 a: -2.6 b: -2.0	67	9.0	0		

The presence of bulky POSS units prevents the interactions and increases the distance between chains; therefore, the entrance of counter ions in the polymer structure will be easier [109,138]. As a result, while the percent transmittance change (optical contrast ratio) increases, the switching time will be shorter. In order to prove this suggestion, the effect of switching time on the percent transmittance changes was monitored via a square-wave potential method between -0.8 V and +1.1 V with switching times of 10, 5, 3, 2 and 1 s. As seen in Figure 3.26, the copolymer CP-10 film has a very short switching time since it preserved its percent transmittance change even when switched in 1 s. The optical contrast value for CP-10 decreased 3.1% (dropping from 65% to 63%) when switching time was decreased from 10 s to 1 s and this value is 7.5% for PEDOT polymer (dropping from 54% to 50%).

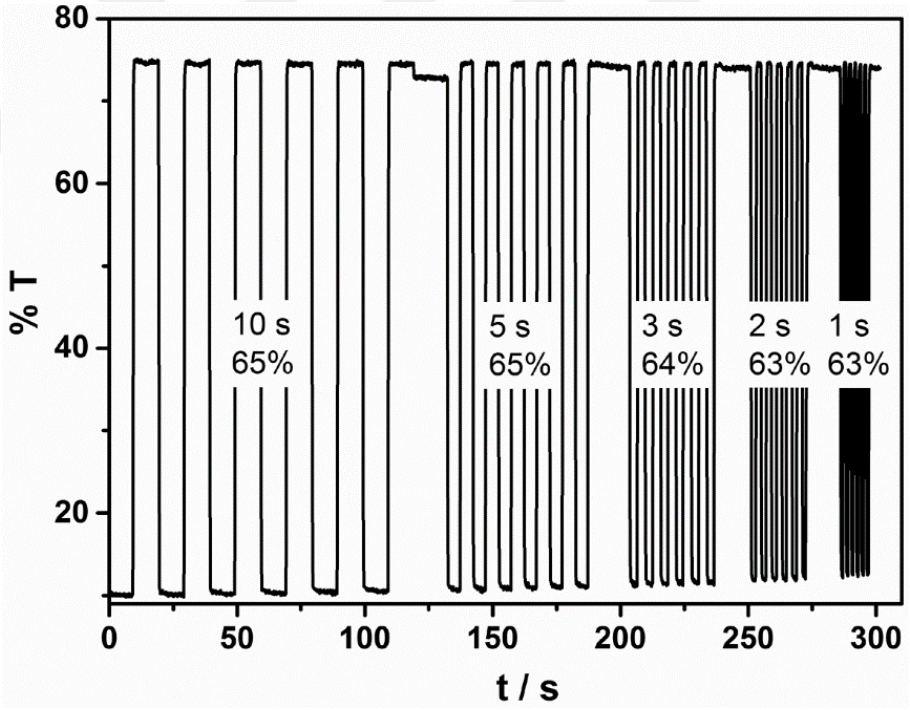

Figure 3.26. Chronoabsoptometry experiments for the copolymer CP-10 film on ITO in 0.1 M TBAH/CH_3CN while the polymer were switched between its redox states in different time intervals (10, 5, 3, 2, and 1 s).

One of the optical properties of the electrochromic materials is the coloration efficiency (CE), which is defined as the power efficiency of the material to change its color from neutral state to oxidized state or vice versa. By using Equation2.5, the CE of the copolymer CP-10 was calculated as 463 cm^2/C, which is greater than PEDOT (352 cm^2/C) (Table 3.5).

3.3 Electrochemical and Electro-optical Characterization of ProDOT-POSS and Its Polymer

3.3.1 Electrochemical Behaviour of ProDOT-POSS

Redox behavior of ProDOT-POSS was investigated by using cyclic voltammetry in an electrolyte solution of 0.1 M TBAH dissolved in dichloromethane. The monomer has one irreversible oxidation peak, which is responsible from its electropolymerization at 1.65 V vs Ag/AgCl reference electrode. When compared to aromatic and alkyl substituted ProDOT derivatives [61,62], the oxidation peak is somewhat higher. It can be conjectured that there is an insignificant effect of POSS cage on the oxidation value of ProDOT unit [133].

Electropolymerization was performed in a mixture of dichloromethane and acetonitrile since the corresponding product is soluble in dichloromethane and the monomer is insoluble in acetonitrile. Based on this information, the solvent ratios were adjusted as 1:3 by v:v for dichloromethane and acetonitrile, respectively. As shown in Figure 3.27, ProDOT monomer represented an irreversible oxidation peak at 1.65 V in this electrolyte medium containing 0.1 M TBAH. During reverse scan, a nucleation loop was observed, which confirms the formation of electroactive species like oligomers on the electrode surface [141]. Also, during second scan, a new redox couple with a half wave of 0.32 V was appeared and its intensity increases after each successive scan. After a certain number of scans, the redox couple responsible from

the formation of an electroactive polymer called as PProDOT-POSS (Scheme 3.3) on the electrode surface starts to shift higher potential values. This shift can be due to a decrease in the electroactivity of the polymer film on the electrode surface or an increase in the polymer thickness which makes the insertion of ions into the polymer backbone difficult [142].

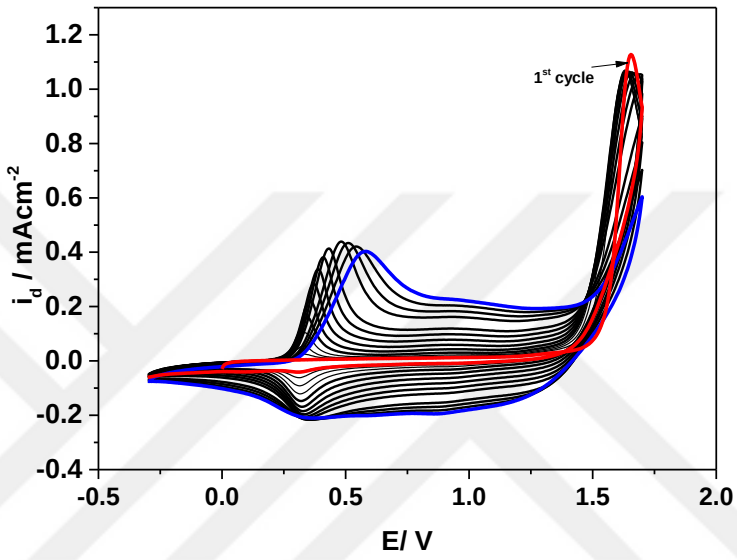

Figure 3.27. Potentiodynamic polymerization of ProDOT-POSS ($5.0x10^{-3}$ M) to get PProDOT-POSS in 0.1 M TBAH dissolved in a mixture of dichloromethane and acetonitrile (1/2.5 by v/v) between -0.30 V and 1.70 V at a scan rate of 100 mV/s on a Pt electrode vs. Ag/AgCl reference electrode.

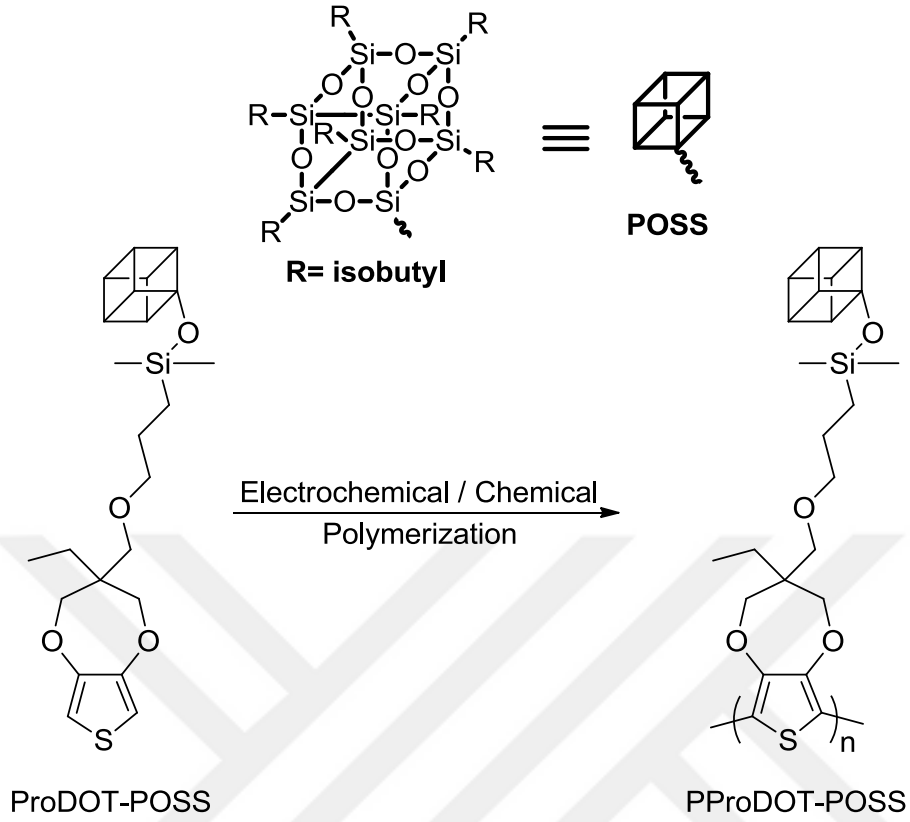

Scheme 3.3. Chemical structures of ProDOT-POSS and its corresponding polymer PProDOT-POSS.

3.3.2 Characterization of PProDOT-POSS Polymer

One of the useful ways to clarify the presence of POSS cages in the polymer backbone is to confirm the presence of Si-O-Si stretching band by using FTIR spectroscopy. As shown in Figure 3.28, Si-O-Si stretching band at around 1073 cm^{-1} as well as CH stretching of aliphatic groups at 2850 and 2929 cm^{-1} in the monomer spectrum was remained unaltered upon polymerization and was observed in the polymer spectrum, which unambiguously indicates the presence of POSS cages in the structure. In addition, the disappearance of the band at 3098 cm^{-1} (for alpha-hydrogens of thiophene ring) confirms the coupling at 2,5-position of the thiophene

ring, which confirms that the corresponding polymer has linear chains due to the proceeding polymerization via 2,5 linkages.

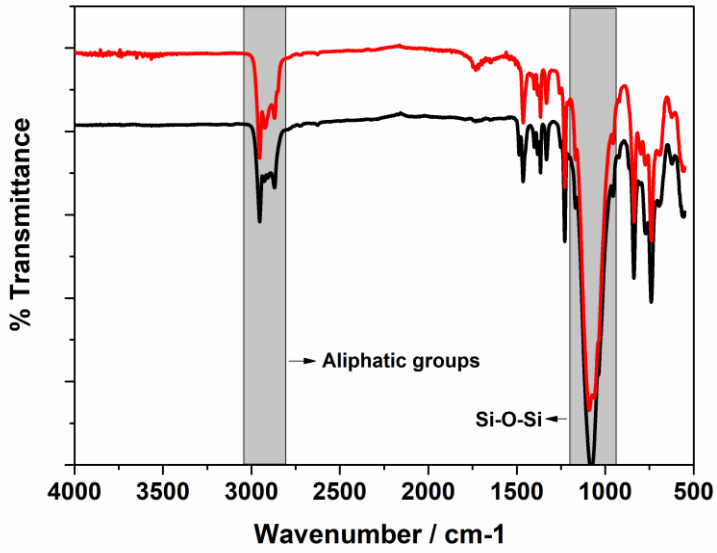

Figure 3.28. FTIR spectra of ProDOT-POSS monomer and chemically obtained PProDOT-POSS.

NMR spectroscopy is also a useful method to prove the existence of POSS cages in the polymer structure. The alkyl groups on POSS cages clearly confirmed by the peaks appeared at around 0.60, 0.90 and 1.80 ppm in both the spectra of the monomer and its polymer (Figure 3.29). Also, the peak at 6.32 ppm responsible from H atoms of 2,5 position in the monomer disappears in the polymer spectrum, which confirmed the formation of a linear polymer backbone via 2,5-coupling (Appendix A).

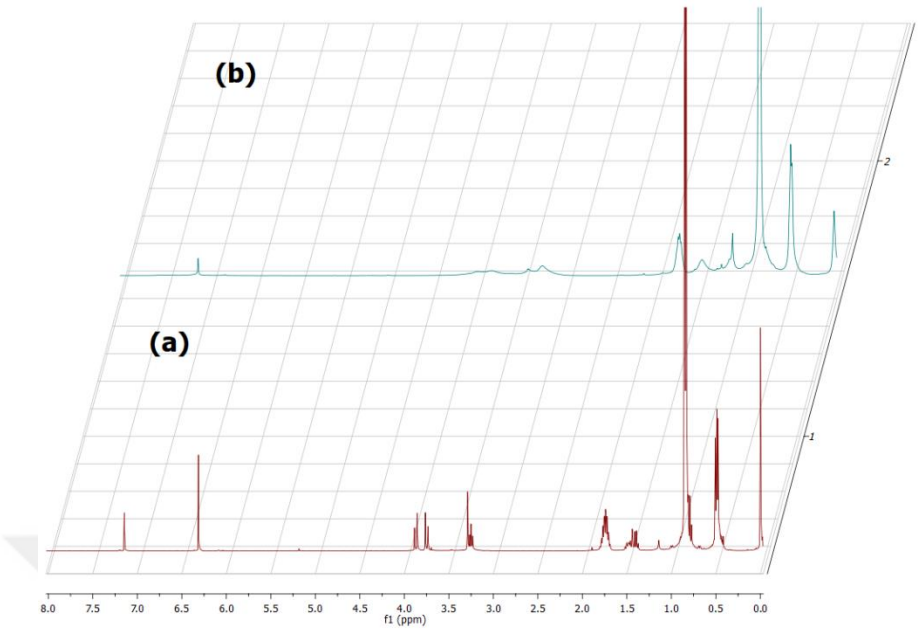

Figure 3.29. ^{1}H NMR spectra of (a) ProDOT-POSS and (b) chemically obtained PProDOT-POSS in d-$CHCl_3$.

3.3.3 Electrochemical Behaviour of PProDOT-POSS Polymer

Eelectrochemical behavior of PProDOT-POSS film was performed in a monomer free electrolyte solution of 0.1 TBAH dissolved in acetonitrile. The polymer film has a quasi-reversible redox couple with a half wave of 0.21 V (see Figure 3.30(a)) and the current intensity of this redox couple changes linearly as a function of scan rate, confirming a non-diffusional redox process and the presence of a well adhered polymer film on the electrode surface.

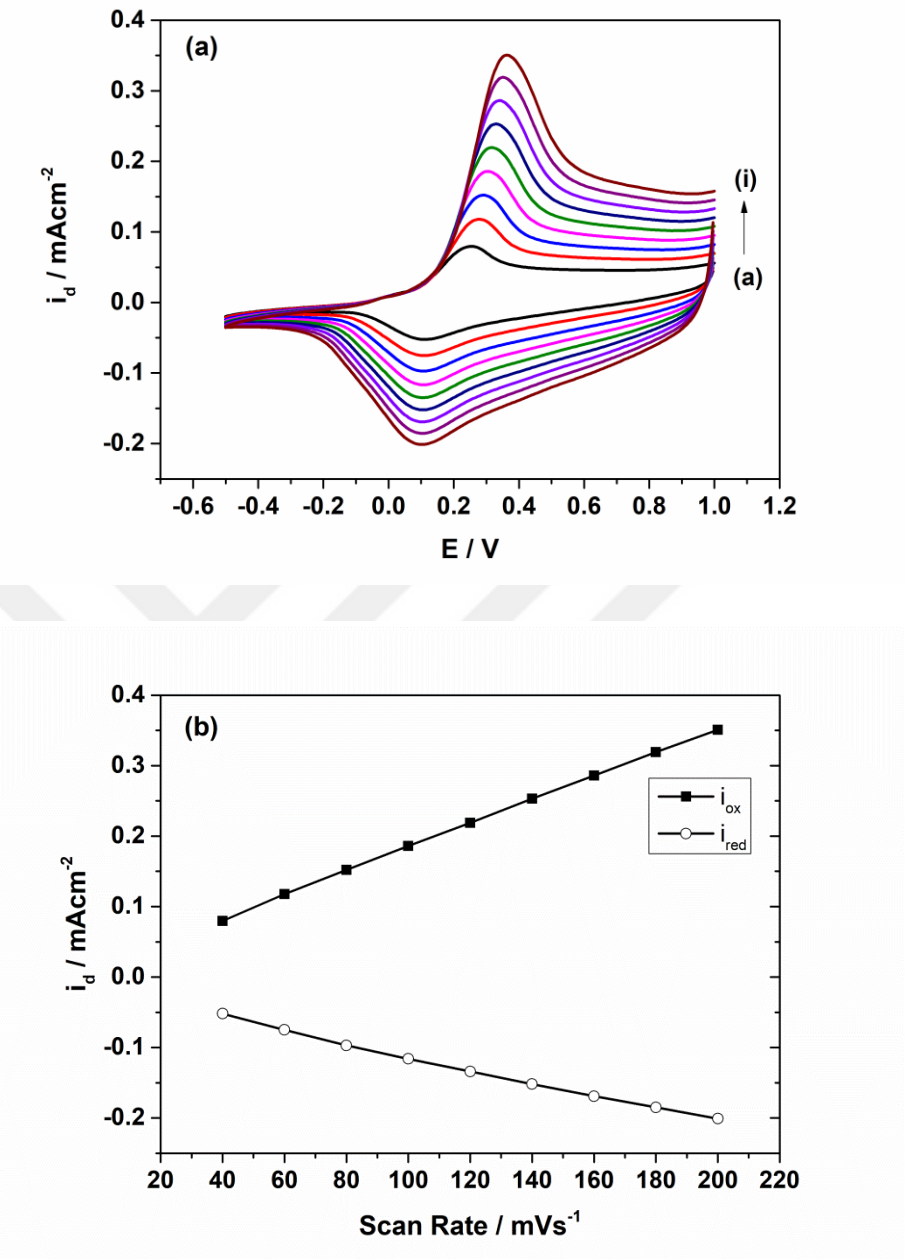

Figure 3.30. (a) Scan rate dependence of PProDOT-POSS film on a Pt electrode in 0.1 M TBAH dissolved in acetonitrile at different scan rates between a:40,b:60, c:80, d:100, e:120, f:140, g:160, h:180 and i:200 mV/s. (b) The current vs. scan rate plot of the polymer film with increasing scan rate.

3.3.4 Optical and Electrochromic Behavior of PProDOT-POSS polymer

In order to find the optical band gap of PProDOT-POSS, the polymer film was coated on the electrode surface electrochemically and then the film was neutralized in a monomer free electrolyte solution at -1.0 V vs Ag wire. The spectrum of the neutral state polymer represented a very well developed vibronic coupling as a fingerprint of a linear polymer backbone [141,142]. For example, PProDOT-POSS film has a broad π-π* transition band containing two well-resolved absorption bands at 555 nm (2.23 eV) and 598 nm (2.07 eV) with a shoulder at 517 nm (2.40 eV) (Figure 3.31). From the commencement on the low energy end of the π-π* transition band, the band gap of the polymer was calculated as 1.95 eV, which is comparable with those of aromatic and alkyl substituted PProDOT derivatives [61,62] (Table 3.7). When compared to the parent PProDOT, substituted PProDOT derivatives have higher E_g values due to the presence of substituents, the kind of which does not have significant effect on the E_g values of the corresponding polymers.

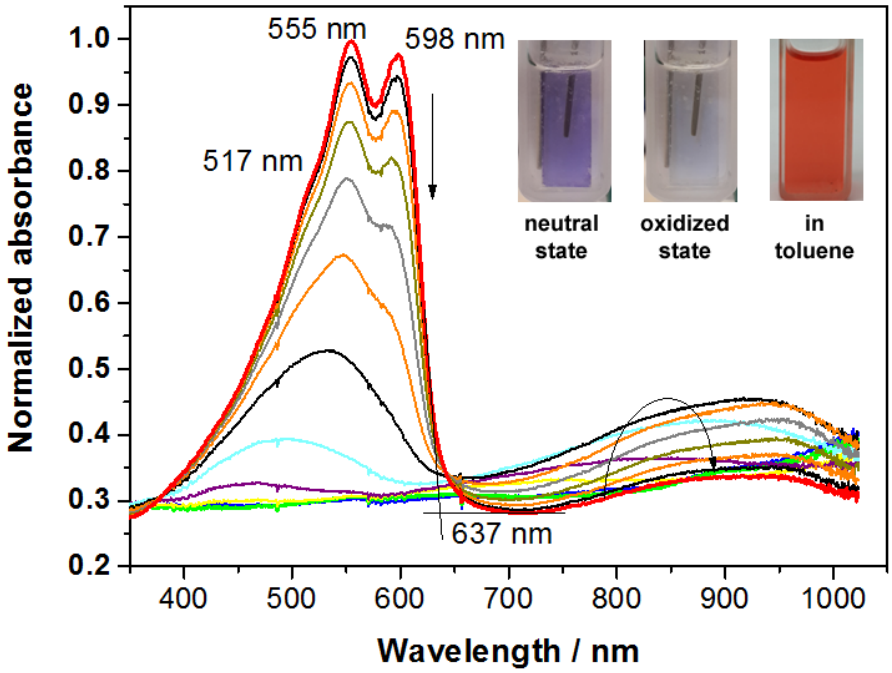

Figure 3.31. Electronic absorption spectra of the PProDOT-POSS film on ITO in 0.1 M TBAH/CH_3CN at various applied potentials between -1.0 V and 1.0 V. Inset: The colors of the PProDOT-POSS at neutral and oxidized states and the polymer dissolved in toluene solution.

The changes in electro-optical properties of PProDOT-POSS film were investigated under applied external potentials. As shown in Figure 3.31, upon moving from -1.0 V to 1.0 V, the π-π* transition band started to lose its intensity and the absorption band centered at 900 nm started to intensify and received a maximum value due to an increase in the density of polaron charge carriers during p-doping. Upon further oxidation, the π-π* transition band diminished completely and due to the combination of polaron charge carriers and the formation of bipolaron charge carriers the intensity of the broad absorption band beyond 650 nm began to decrease and reach a minimum level.

Table 3.7. Optoelectronic properties of some alykyl and aromatic PProDOT derivatives. (See Appendix F for the chemical structures)

Polymers	λ_{max} (nm)	E_g [a] (eV)	Δ%T	CE (cm^2/C)	$t_{switching}$ [b] (s)	Ref
PProDOT-Me_2	578	Not reported	78	200	0.3-0.8	[143]
PProDOT-Et_2	580	1.75	75	505	<0.5	[144]
PProDOT-Bu_2	632, 573, 517	1.86	76	1365	0.45	[145]
	582	1.83	68.1	850	1.2	[62]
PProDOT-Hex_2	634, 584	1.80	71	1270	0.43	[145]
	572	1.88	64.7	514	1.0	[62]
	627	Not reported	74	Not reported	1.0	[146]
PProDOT-$EtHex_2$	623, 567, 517	1.96	53	1204	0.5	[4]
PProDOT-Dec_2	571, 622	1.82	73	306	0.6	[61]
PProDOT-$Dodec_2$	604	Not reported	77	Not reported	1.0	[146]
PProDOT-Bz_2	632	Not reported	89	550-600	0.4-0.6	[7]
PProDOT-POSS	555, 598	1.95	55	504	1.0	This Study

Also, PProDOT-POSS film has an electrochromic property; therefore, all these changes in the optical absorption spectrum occuring during doping (or vice versa) can be followed by color changes: violet (L= 53.21, a= 23.29, b= -35.61) when neutralized and highly transparent (L= 87.45, a= -0,29, b= -2,13) when oxidized (see the inset of Figure 3.31).

On the other hand, keep in mind that due to the presence of POSS cages the polymer is completely soluble in common organic solvents such as toluene, chloroform, dichloromethane, tetrahydrofuran, etc (see the inset of Figure 3.31). Without doubt, this property makes it a good candidate for bio- and opto-electronic applications. By the help of this property, chromic properties of PProDOT-POSS polymer can also be controlled chemically. For this aim, $SbCl_5$ and N_2H_5OH solutions can be used as oxidizing and reducing agents, respectively; therefore, chemically obtained polymer can be doped and dedoped reversibly. As shown in Figure 3.32, different redox states of the polymer as well as the changes in absorption spectra can be monitored after the addition of various amounts of $SbCl_5$. Like electrochemically p-doping, the π-π^* transition band at 595 nm started to lose its intensity with a concomitant absorption band appeared and intensified at 900 nm by the addition of $SbCl_5$ solution. Increasing doping ratio by further addition of $SbCl_5$ resulted in the disappearence of the π-π^* transition band and a bathocromic shift for the polaron carriers from 900 nm to 750 nm. Also, the appearence of the band responsible from the formation of bipolaron charge carriers beyond 850 nm was observed.

In addition, the polymer exhibited chemochromic properties during this process and the color changes could be nicely observed upon chemical switching (the inset of Figure 3.32): reddish orange (L= 60.71, a= 44.73, b= 31.73) at neutral state and transparent sky blue (L= 71.28, a= -8.30, b= -1.66) at oxidized state.

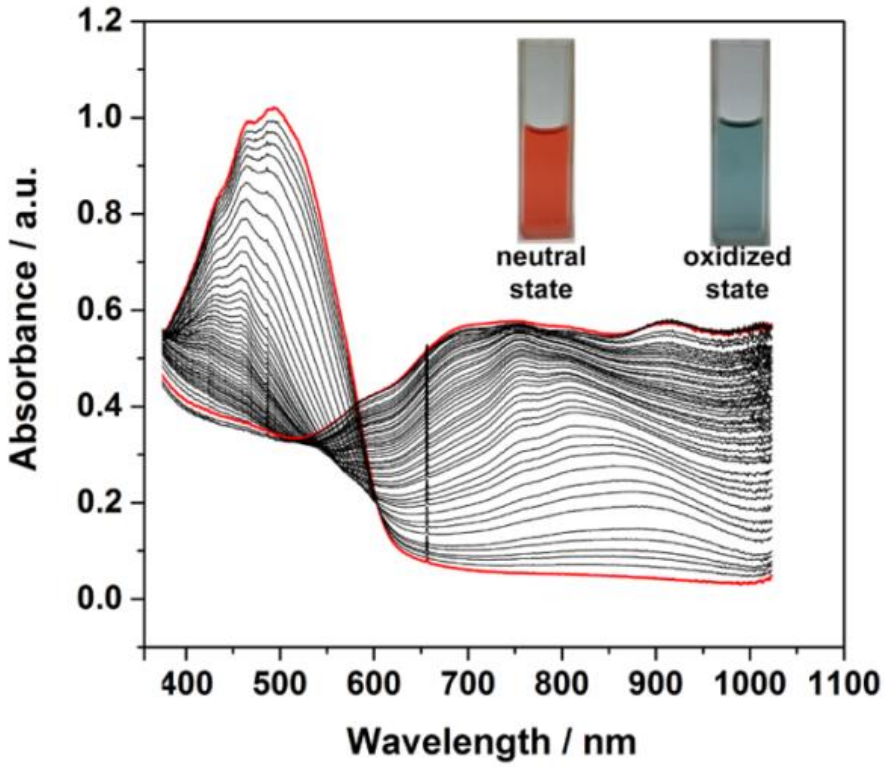

Figure 3.32. Changes in the absorption spectra of chemically obtained PProDOT-POSS dissolved in toluene during chemical oxidation by using 10^{-4} M $SbCl_5$ oxidant. Inset: Colors of PProDOT-POSS dissolved in toluene at neutral and oxidized states.

Electrochemically obtained PProDOT-POSS film on ITO has a percentage transmittance change (Δ%T) of 55 at 555 nm, which is lower than that of the parent PProDOT (71.5% at 571 nm) [62]. Also, PProDOT-POSS has a coloration efficiency of 502 cm^2/C at 95% of the full contrast with a switching time of 1.0 s. Switching time is one of the most important parameters for electrochromic materials to be a candidate for electro-optical applications. The color change of the polymer film was tested by recording the percent transmittance changes as a function of applied switching time at a constant potential via a square-wave potential method. The polymer film was switched between -1.0 V and 1.0 V with switching times of 10, 5, and 3 s (Figure 3.33). The polymer film has a very short response time and it

preserved the percent transmittance change without any appreciable changes upon moving from 10 s to 3 s. For example, only about 7% optical contrast change (from 55.0 to 50.9) was observed when the switching time was decreased to 3 s.

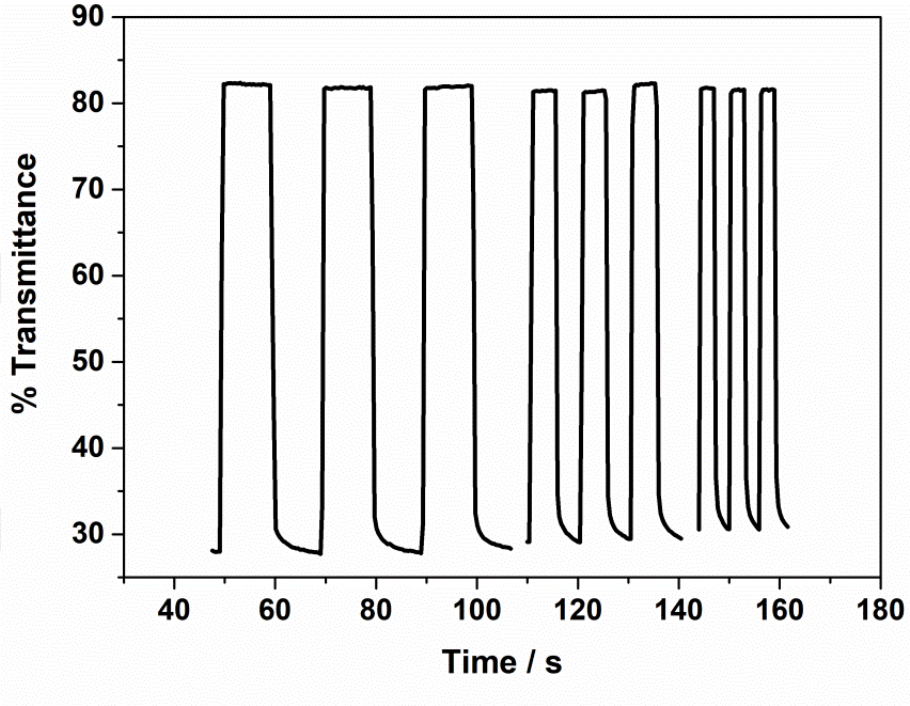

Figure 3.33. Chronoabsorptometry experiment for PProDOT-POSS (at 618 nm, 17 mC/cm^2) films on ITO in 0.1 M TBAH/CH_3CN while the polymer film was switched with an interval time of 10 s, 5 s and 3 s between -0.5 and 0.9 V.

On the other hand, chemically and electrochemically obtained soluble and conjugated PProDOT-POSS polymer samples, as expexted, exhibited a reddish orange emission centered about at 605 nm when excited at 500 nm (Figure 3.34). Both chemically and electrochemically obtained polymers exhibited similar emission band between 500 nm and 800 nm. To the best of our knowledge, unlike aromatic

and alkyl substituted PProDOT derivatives [61,62], PProDOT-POSS polymers are the first fluorescent examples of PProDOT derivatives. Under the light of this finding, it can be safely concluded that PProDOT-POSS can certainly find some various applications in opto-electronics like an active emitter in light emitting diodes or organic lasers and also can be used in bio-applications like imaging the cancer cells.

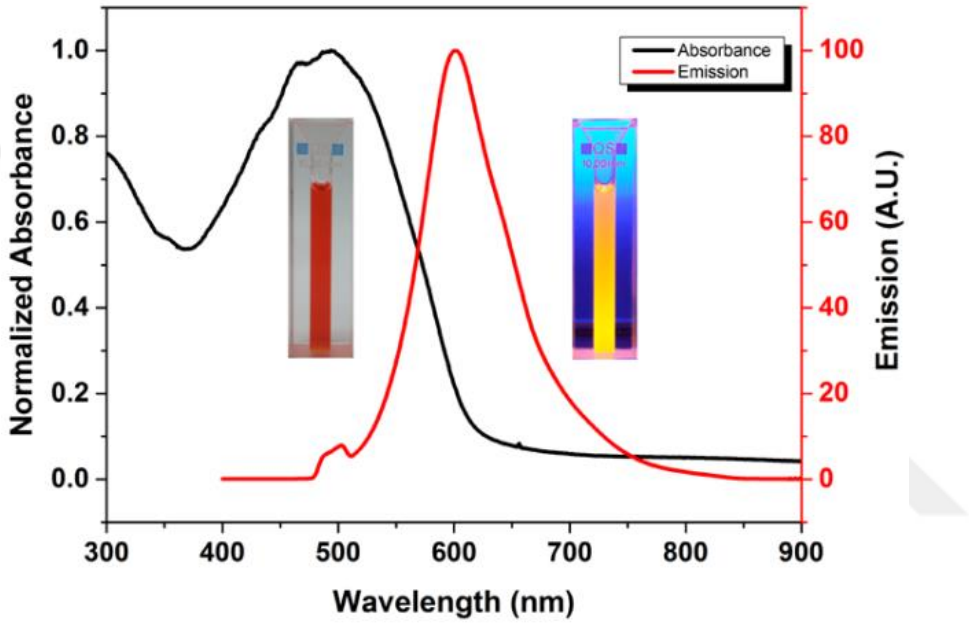

Figure 3.34. Absorbance (black) and emission (red) spectra of chemically (line) and electrochemically (dash line) obtained PProDOT-POSS in toluene. Inset: Colors of the PProDOT-POSS polymer in toluene under ambient light (left) and handheld UV lamp (right) at 365 nm

Table 3.8. Optical properties of some polyalkylenedioxythiophene derivatives.

	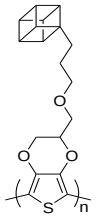		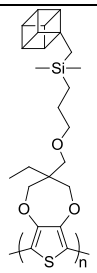	
Polymers	PEDOT-POSS	PEDOT	PProDOT-POSS	PProDOT
λ_{max} (nm)	618	627	555	590
E_g (eV)	1.71	1.60	1.95	1.70
HOMO (eV)	4.64	4.17	4.55	-
LUMO (eV)	2.93	2.57	2.60	-
Δ%T	74 %	61 %	55 %	54 %
t_{ox} (s)	0.9	1.2	1.0	2.2
CE (cm^2/C)	582	350	504	-

3.4 Electrochemical and Electro-optical Characterization of EDOS-POSS and Its Polymer

3.4.1 Electrochemical Behaviour of EDOS-POSS

First of all, the redox behavior of EDOS-POSS monomer was investigated by using cyclic voltammetry in an electrolyte solution of 0.1 M tetrabutylammonium perchlorate/propylene carbonate solution. Upon moving from 0.0 V to 1.5 V, the monomer exhibited a well-defined irreversible oxidation peak at 0.90 V vs. Fc/Fc^+, which is somewhat higher than its parent EDOS monomer (0.88 V vs. Fc/Fc^+ in tetrabutylamminum perchlorate/propylene carbonate electrolyte/solvent couple) [59]. This result showed that the presence of POSS bulky group on the ethylenedioxy

bridge of EDOS does not affect the electron donating abilities of the oxygen atoms and therefore it is possible to get almost the same oxidation potential values for the monomers.

On the other hand, while the product obtained during polymerization was soluble in dichloromethane, it is insoluble in acetonitrile. Due to this reason, the electropolymerization of EDOS-POSS monomer was performed potentiodynamically in a mixture of dichloromethane and acetonitrile (1/3, v/v) containing 0.1 M TBAH. As shown in Figure 3.35(a), after first cycle, a new redox couple responsible from the electrolpolymerization started to appear between -0.2 V and 0.3 V, and the current intensity of this redox couple increased as a function of repetitive anodic scan. Figure 3.35(a) represented the fingerprint of the formation of an electroactive polymer film called PEDOS-POSS on the electrode surface (Scheme 3.4).

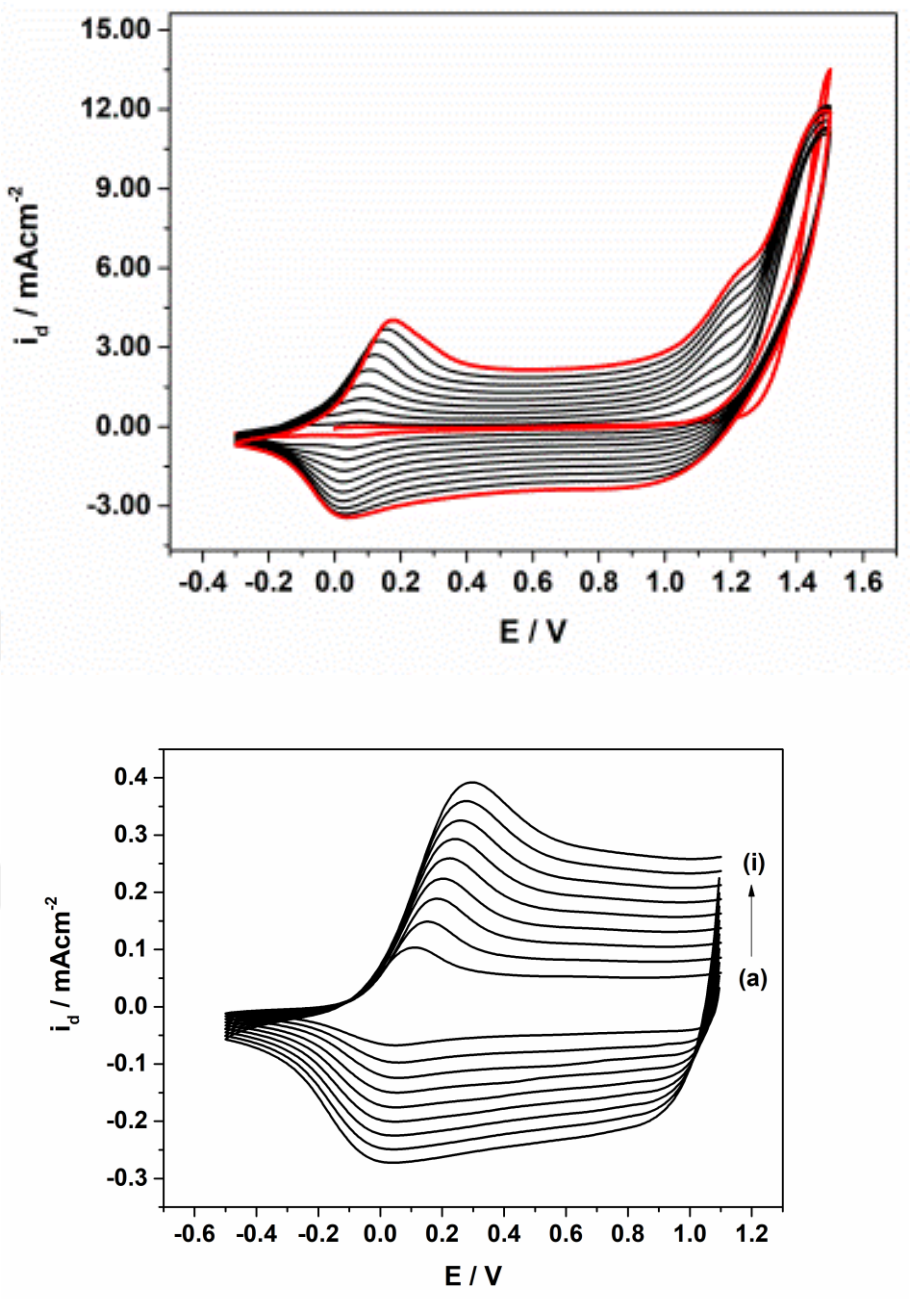

Figure 3.35. (a) Potentiodynamic polymerization of EDOS-POSS ($5.0x10^{-3}$ M) to get PEDOS-POSS in 0.1 M TBAH dissolved in a mixture of dichloromethane and acetonitrile (1/2.5 by v/v) between 0.30 V and 1.55 V at a scan rate of 100 mV/s on a Pt electrode vs. Ag/AgCl reference electrode. (b) Scan rate dependence of PEDOS-POSS film on a Pt disk electrode in 0.1 M TBAH/acetonitrile at different scan rates, a: 40 mV/s, b: 60 mV/s, c: 80 mV/s, d: 100 mV/s, e: 120 mV/s, f: 140 mV/s, g: 160 mV/s, h: 180 mV/s, and i: 200 mV/s.

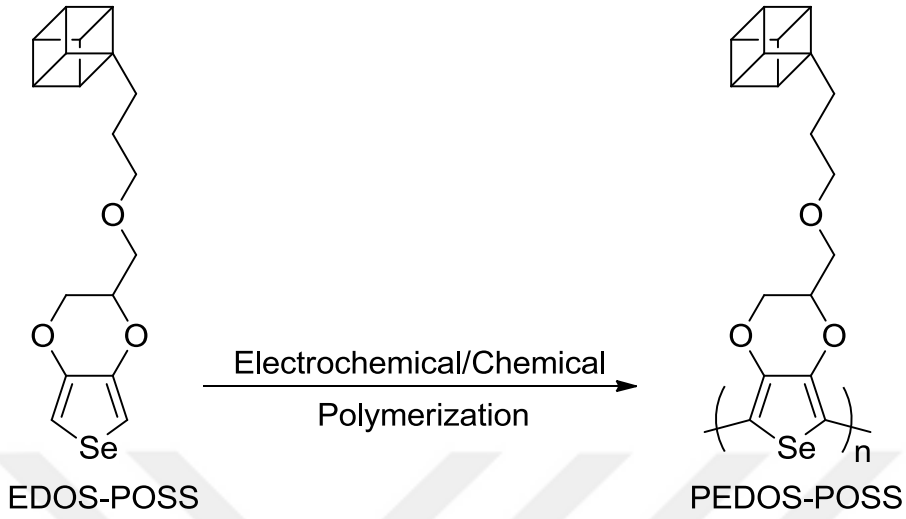

Scheme 3.4. Electrochemical and Chemical polymerization of EDOS-POSS to get PEDOS-POSS polymer.

3.4.2 Characterization of PEDOS-POSS

FTIR spectroscopy can be used as one of the efficient ways to verify the presence of POSS cages in the polymer backbone. As shown in Figure 3.36, Si-O-Si stretching band at around 1073 cm^{-1} as well as CH stretching of aliphatic groups at 2850 and 2929 cm^{-1} in the monomer spectrum was remained unaltered in the polymer spectrum, which absolutely confirming the presence of POSS cages in the polymer backbone. Also, the disappearance of the band at 3098 cm^{-1}, which is responsible from alpha-hydrogens of thiophene ring at 2,5-positions, clarifies the formation of a linear polymer chain due to the proceeding polymerization via 2,5 linkages.

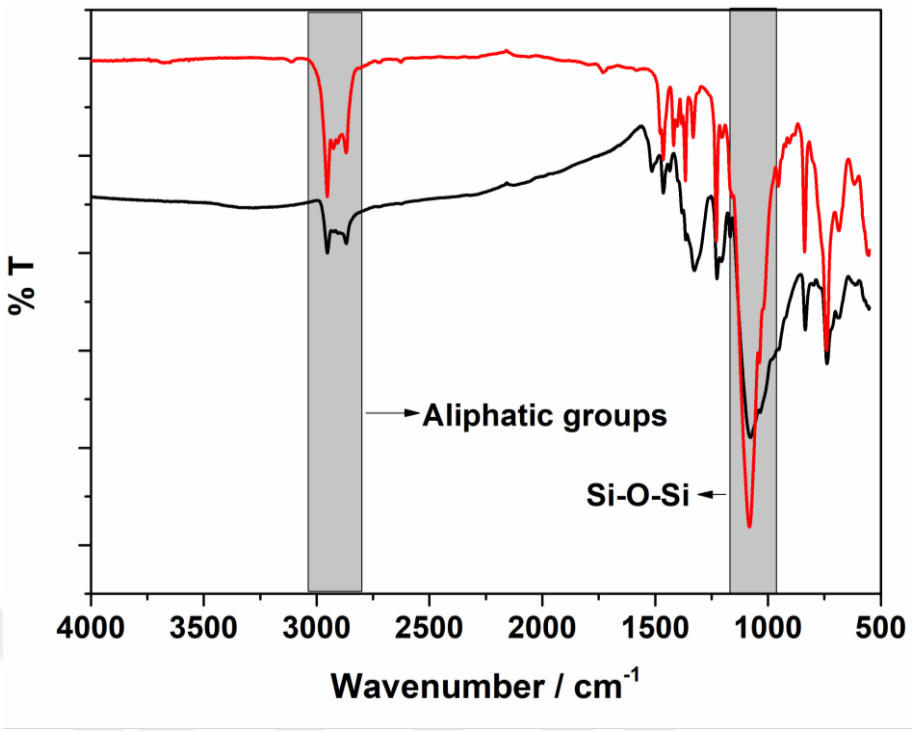

Figure 3.36. FTIR spectra of (a) EDOS-POSS and (b) chemically obtained PEDOS-POSS.

Like FTIR spectroscopy, NMR spectroscopy can also confirm the existence of POSS cages in the polymer structure. The alkyl groups on POSS cages in polymer structure showed themselves clearly at around 0.61, 0.95 and 1.85 ppm (Figure 3.37 (b)). Also, the peak at 6.78 ppm responsible from H atoms of 2,5 position in the monomer spectrum (Figure 3.37(a)), responsible from the formation of a linear polymer chain via 2,5-coupling, disappears after polymerization.

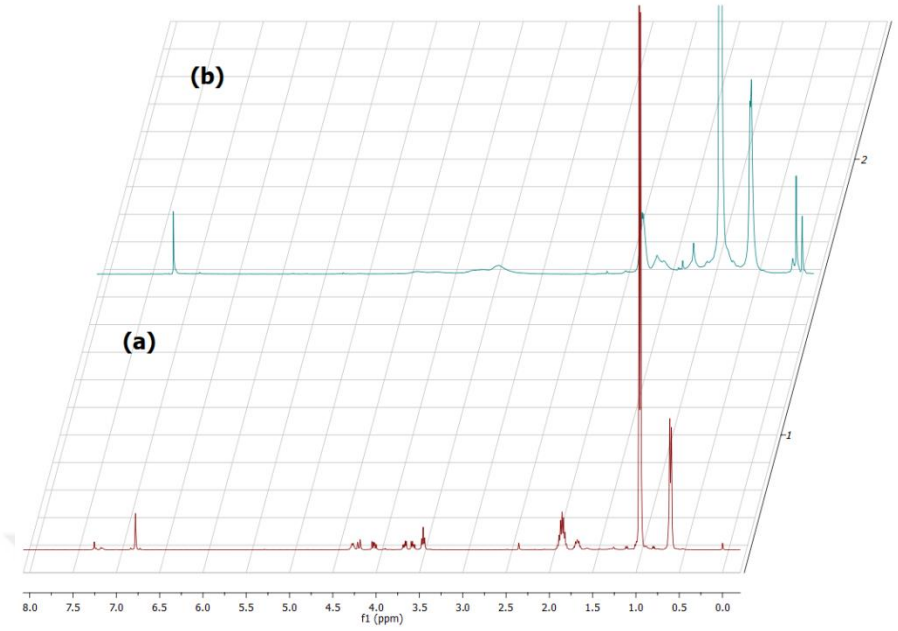

Figure 3.37 ^{1}H NMR spectrum of (a) EDOS-POSS and (b) chemically obtained PEDOS-POSS in d-$CHCl_3$.

3.4.3 Electrochemical Behaviour of PEDOS-POSS

The cyclic voltammogram of electroactive PEDOS-POSS film showed a well-defined and reversible redox couple with a half wave of 0.10 V vs. Ag/AgCl (Figure 3.35(b)). The current intensity of redox couple as a function of scan rate increases linearly and as expected from a conjugated electroactive film, the polymer film represents a non-diffusional redox process.

It is noteworthy to mention that PEDOS-POSS film exhibited a characteristic feature of electrochemical capacitors in the shape of cyclic voltammogram since the voltammogram looks like nearly a rectangle with a wide potential window between 0.15 V and 1.1 V (Figure 3.38(a)). The rectangle shape has remained unchanged

even at high scan rates. As shown in Figure 3.38(b), the intensity and charge/discharge of the flat current response increased linearly as a function of scan rates, which indicates a fast charge (doping)/discharge (dedoping) process even at high scan rates (Figure 3.39). It can be easily concluded that this capacitive behavior makes the polymer PEDOS-POSS a promising candidate for battery and supercapacitor.

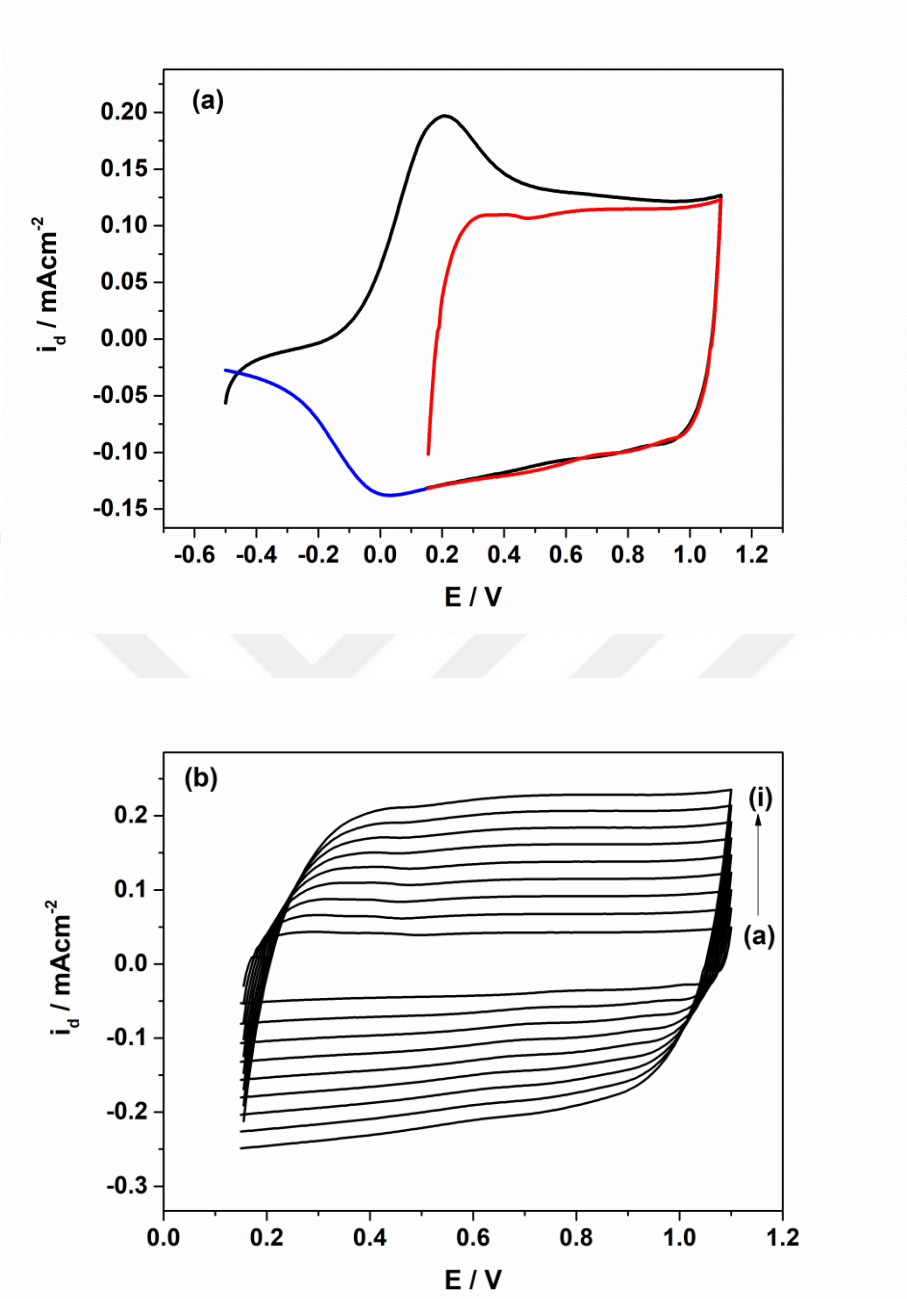

Figure 3.38 Cyclic voltammograms of PEDOS-POSS film coated on Pt electrode in 0.1 M TBAH/acetonitrile solution between -0.5 V and 1.1 V, and between 0.15 V and 1.1 V at a scan rate of 100 mV/s. (b) Capacitance effect of PEDOS-POSS film by cyclic voltammetry at scan rates of a) 40, b) 60, c) 80, d) 100, e) 120, f) 140, g) 160, h) 180, and i) 200 mV/s.

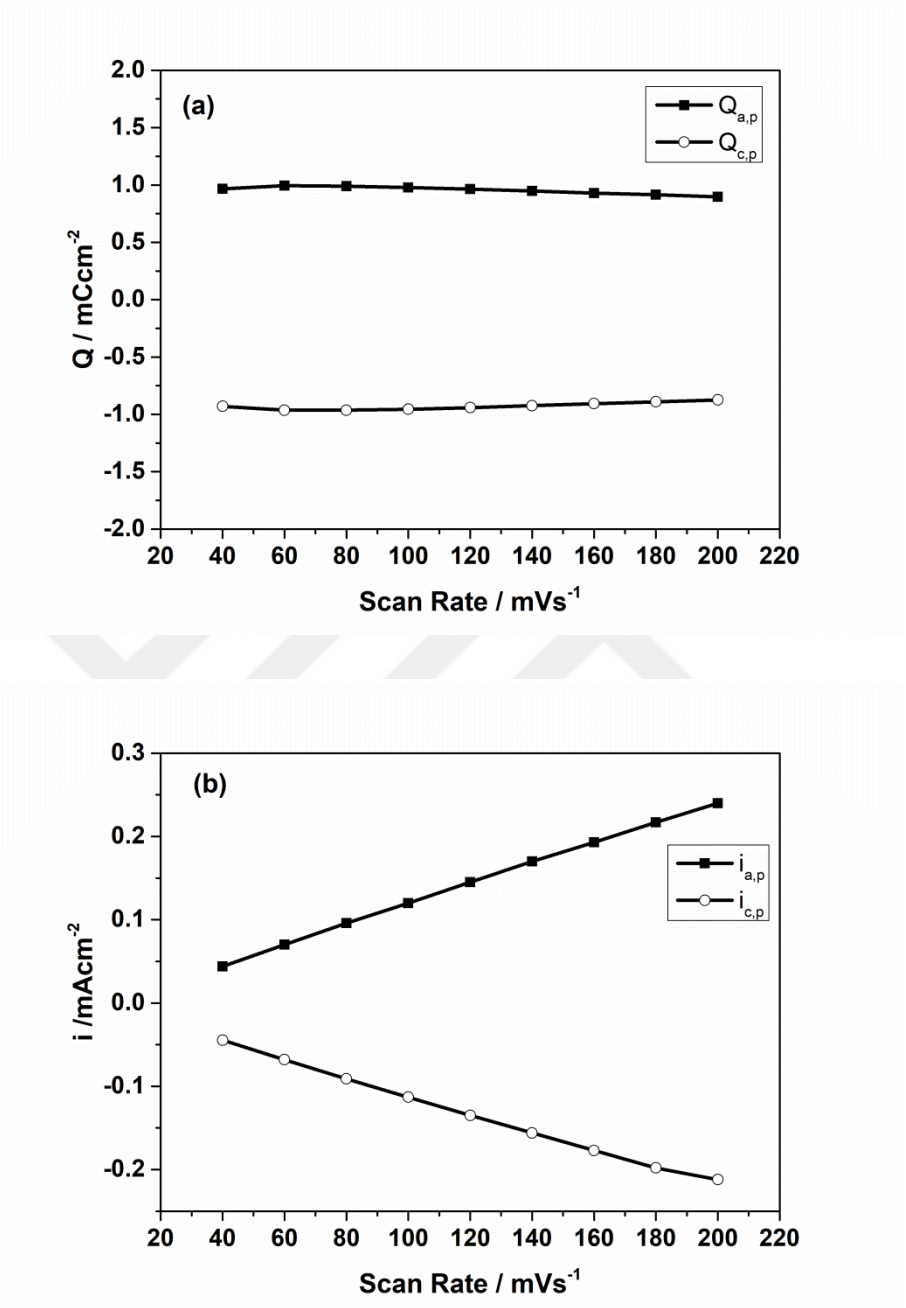

Figure 3.39. (a) Relationship of charge/discharge values of the redox couple of PEDOS-POSS as a function of scan rate in 0.1 M TBAH/acetonitrile solution between -0.3 V and 1.1 V, (b) Relationship of anodic/cathodic current values of the redox couple of PEDOS-POSS as a function of scan rate in 0.1 M TBAH/acetonitrile solution between -0.3 V and 1.1 V.

The stability test under ambient conditions in the presence of oxygen is crucially important for the materials since they can be amenable to use in industrial applications when passed this test. The test showed that PEDOS-POSS polymer exhibited a stability performance (retaining 76% of its electroactivity after 5000 cycles) close to PEDOS analogue (retaining 83% of its elecroactivity after 5000 cycles) (Figure 3.40). PEDOS also managed to retain 68% of its electroactivity even after 9000 cycles.

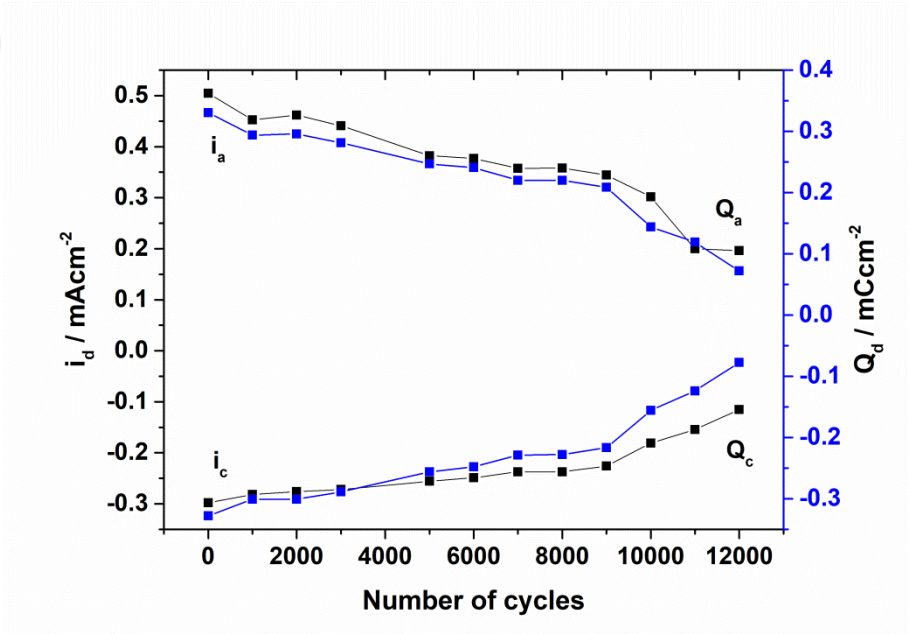

Figure 3.40 Stability test for electrochemically obtained PEDOT-POSS film in 0.1 M TBAH/CH_3CN at a scan rate of 100 mV/s under ambient conditions by cyclic voltammetry as a function of the number of cycles: Q_a (anodic charge stored), Q_c (cathodic discharge), (b) i_a (anodic peak current), (c) i_c (cathodic peak current).

3.4.4 Optical and Electrochromic Behavior of PEDOS-POSS polymer

The neutral state PEDOS-POSS polymer film coated on ITO has two maximum wavelengths of 668 nm and 724 nm attributed to the π-π* transition band (see Figure 3.41). Also, when compared to the parent PEDOS (1.40 eV with λ_{max}= 666 nm), it has a narrow band gap of 1.50 eV calculated from the onset of the low energy end of the π-π* transition. Moreover, the polymer film has a pure blue color (L= 64.82, a= -10.0, b= -13,05) at its neutral state due to nearly the absence of absorbance between 400 nm and 500 nm. This property makes the polymer a good candidate for electrochromic windows and monitors since blue is one of the legs in RGB color pallet [61,62,133].

From the viewpoint of opto-electronic applications, the electro-optical properties of the polymer film were studied under applied external potentials during p-doping moving from -0.5 V to 1.1 V. Upon oxidation, due to the formation of charge carriers on the polymer backbone the π-π* transition band started to lost its intensity simultaneously. Upon further oxidation, the polymer film exhibited no absorption band in the visible region and these changes were accompanied with color changes from pure blue (L= 64.82, a= -10.0, b= -13,05) to highly transparent state (L= 81.25, a= -3.23, b= 6.35) (see inset of Figure 3.41). Based on the foregoing findings, it can be concluded that PEDOS-POSS can be a promising material for optical devices and displays by the help of its switchable visible window under applied external voltages.

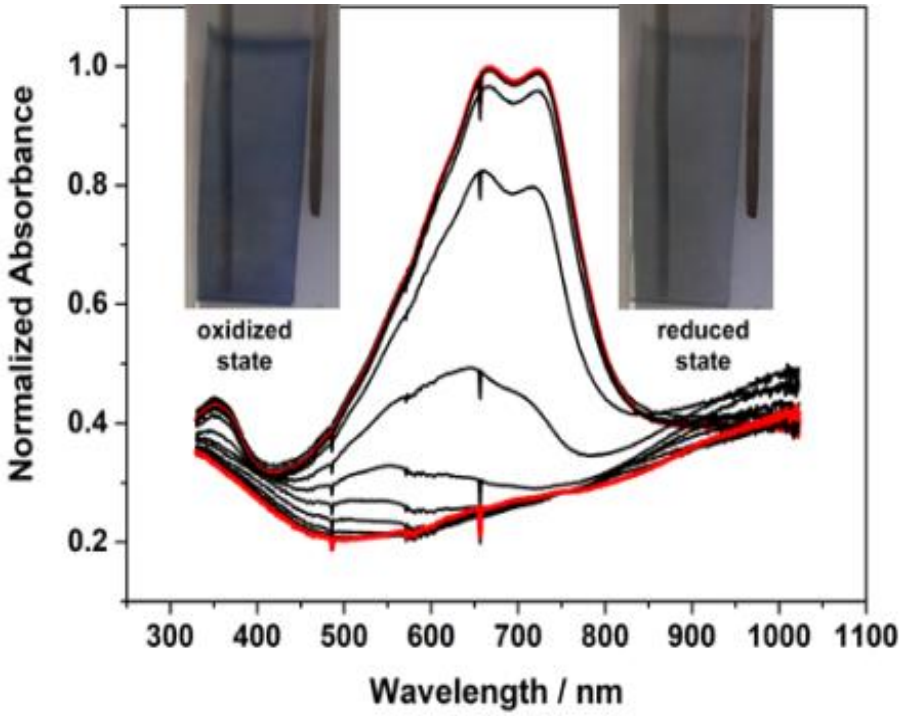

Figure 3.41 Optical absorption spectra of the PEDOS-POSS film (17 mC/cm^2) coated on ITO in 0.1 M TBAH/acetonitrile at various applied potentials between -1.0 V and 1.0 V. Inset: Colors of the polymer at neutral and oxidized states.

In order to find any application in industrial area, the solubility is also one of the most important properties since it will be possible to coat the polymer on any surface. Chemically and electrochemically synthesized PEDOS-POSS polymer samples are completely soluble in common organic solvents like toluene, tetraheydrofuran, dichloromethane and chloroform. To the best of our knowledge, PEDOS-POSS is the first soluble example of PEDOS analogues [67,129]. This property makes it a promising candidate for industrial applications since it is possible to coat polymer samples on any surface via spray coating method (Figure 3.42(a)). Therefore, chromic properties PEDOT-POSS polymer samples can also be controlled chemically in both solution and film forms. For example, chemically obtained

polymer can be doped and dedoped by using $SbCl_5$ and N_2H_5OH as oxidizing and reducing agents, respectively. Different redox states of the polymer samples in solution and film forms can be followed by monitoring the changes in the absorption spectra during the addition of various amounts of $SbCl_5$. (see Figure 3.42(b) and (c)). During chemical oxidation, the π-π^* transition bands started to lose their intensities and as a result of doping process the charge carriers are formed and they can be monitored by the appearance of a new band beyond 600 nm by the addition of $SbCl_5$ solution. Doping and dedoping processes can be performed reversibly and the corresponding polymer showed a chemochromic properties during this reversible process: reddish orange (L= 44.30, a= 24.63, b= -32.40) at neutral state and transparent sky blue (L= 82.52, a= -1.13, b=4.10) at oxidized state for solution form and pinkish orange (L= 78.02, a= 1.78, b= -15.92) when neutralized and transparent sky blue (L= 90.92, b= 0.67, b= -1.09) when oxidized for film form.

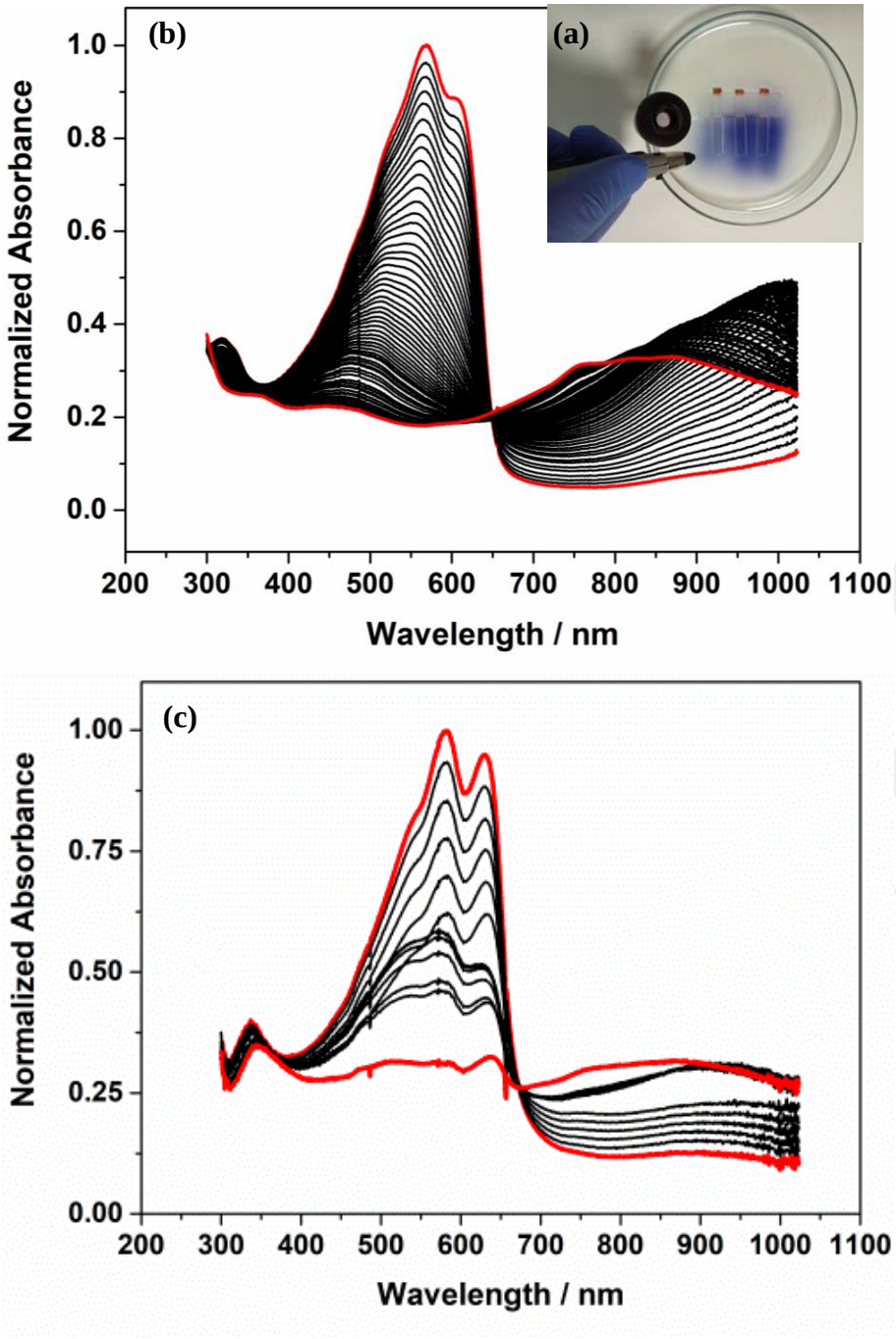

Figure 3.42. (a) Spray coating of PEDOS-POSS dissolved in toluene on ITO electrodes, (b) Changes in the absorption spectra of chemically obtained PProDOT-POSS dissolved in toluene during chemical oxidation by using 10^{-4} M $SbCl_5$ oxidant and (c) Changes in the absorption spectra of chemically obtained PProDOT-POSS coated on ITO electrode under applied external potentials between -0.5 V and 2.0 V in 0.1 M TBAH/CH_3CN.

The percentage transmittance change (Δ%T) of PEDOS-POSS was calculated higher than that of PEDOS (55% at 666 nm). Upon moving from – 0.5 V to 1.1 V, the Δ%T of the PEDOS-POSS was found as 59% at 668 nm. Also, the presence of POSS cages was improved some electro-optical properties. For example, when compared to PEDOS (212 cm^2/C at 95% of the full contrast), electrochemically obtained PEDOT-POSS has higher coloration efficiency (593 cm^2/C at 95% of the full contrast) and nearly same switching time (0.7 s) (Table 3.9).

On the other hand, to the best of our knowledge, chemically and electrochemically obtained soluble and conjugated PEDOS-POSS polymer samples are the first fluorescent example of polyalkylenedioxyselenophene derivatives [67,129]. When PEDOS-POSS dissolved in toluene excited at 500 nm, it exhibited a reddish orange emission centered about at 620 nm (Figure 3.43). Both chemically and electrochemically obtained polymers exhibited similar behavior. Based on the foregoing results like solubility and fluorescence property, PEDOS-POSS can be a promising material for opto-electronic applications. Also, the reddish orange emission can make it amenable to use in bio-applications like imaging the cancer cells.

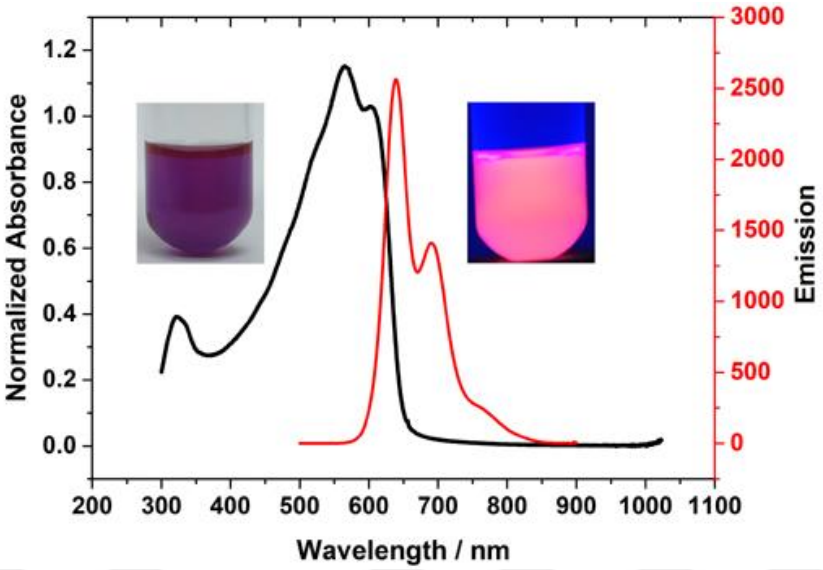

Figure 3.43 Absorbance (black) and emission (red) spectra of chemically (line) and electrochemically (dash line) obtained PProDOT-POSS in toluene. Inset: Colors of PEDOS-POSS dissolved in toluene under ambient light (left) and handheld UV lamp (right) at 365 nm.

Table 3.9 Optical properties of some polyalkylenedioxythiophene and polyalkylenedioxyselenophene derivatives.

	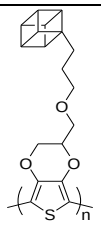		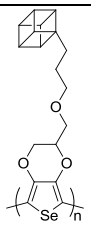	
Polymers	PEDOT-POSS	PEDOT	PEDOS-POSS	PEDOS
λ_{max} (nm)	618	627	668	666
E_g (eV)	1.71	1.60	1.50	1.42
Δ%T	74 %	61 %	59 %	55 %
t_{ox} (s)	0.9	1.2	0.7	0.6
CE (cm^2/C)	582	350	593	212

CHAPTER 4

CONCLUSION

A highly soluble PEDOT analogue was synthesized without using any surfactants and dispersants. The PEDOT analogue bearing alkyl substituted POSS cages showed much better electrochemical and optical properties than PEDOT. Soluble PEDOT-POSS exhibited electrochromic behavior: blue at neutral state and highly transparent when oxidized.

On the other hand, the bridge center on ProDOT unit was functionalized with alkyl substituted POSS cage and the hybrid monomer was polymerized successfully via both chemical and electrochemical polymerization techniques. The findings showed that the soluble corresponding polymers exhibited both electrochromic (violet when neutralized and transparent sky blue when oxidized) and fluorescent (a reddish orange emission centered about at 605 nm) properties.

Also, a highly solution processable and fluorescent neutral state pure blue PEDOS analogue called PEDOS-POSS was synthesized firstly. The presence of alkyl substituted POSS cages improved the electrochemical and optical properties when compared to the parent PEDOS. Also, PEDOT-POSS samples can be doped chemically in both solution and film and electrochemically in film. In addition, soluble PEDOT-POSS also exhibited electrochromic behavior such as pure blue when neutralized and highly transparent when oxidized.

All these properties (Table 4.10) make these polymers (PEDOT-POSS, PProDOT-POSS, and PEDOS-POSS) promising materials to be use in various applications like electrochromic devices and displays, solar cells, transistors, capacitors, etc. In addition, these properties make them promising candidates for bio-applications like

imaging the cancer cells as well as electro-optic and photocatalytic applications. Further work in the application line is currently underway in our laboratories and the results will be reported in due time.

Table 4.10. Optical properties of some polyalkylenedioxythiophene and polyalkylenedioxyselenophene derivatives with and without POSS units.

Polymers	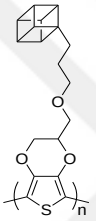 PEDOT-POSS	 PEDOT	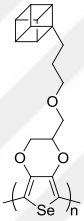 PEDOS-POSS	 PEDOS	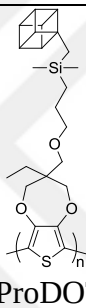 PProDOT-POSS	 PProDOT
λ_{max} (nm)	618	627	668	666	555	590
E_g (eV)	1.71	1.60	1.50	1.42	1.95	1.70
Δ%T	74 %	61 %	59 %	55 %	55 %	54 %
t_{ox} (s)	0.9	1.2	0.7	0.6	1.00	2.2
CE (cm^2/C)	582	350	593	212	504	-

REFERENCES

1. Skotheim T.A., Reynolds J.R., *Handbook of Conducting Polymers*, 3rd ed.; CRC Press, Boca Raton, FL, 2007.

2. Perepichke I.F., Perepichake D.F., *Handbook of Thiophene-based Materials*, John Wiley & Sons, Hoboken, NJ, 2009.

3. Rasmussen S.C. and Strom E.T., *In 100+ Years of Plastics. Leo Baekeland and Beyond*, ACS Symposium Series, Washington DC, 2011.

4. Inzelt G., Conducting Polymers*; A New Era In Electrochemistry*, 2nd Ed., Springer-Verlag Berlin, Heidelberg, 2013.

5. MacDiarmid A.G., *Angew. Chem. Int. Ed.*, 2001, 40, 2581.

6. Rasmussen S.C., Ogawa K., Rothstein S.D., *Handbook of Organic Electronics and Photonics*, American Scientific Publishers, Stevenson Ranch, CA, 2008.

7. Neo W.T., Ye Q., Chua S.J., Xu J., *J. Mater. Chem. C*, 2016, 4, 7364.

8. Anguera G., Sanchez-Garcia D., *Afinidad*, 2014, 71, 251.

9. Zhang W., Yu G., *Organic Semiconductors for Field-Effect Transistors in Organic Electronic Materials; Lecture Notes in Chemistry*, 91, Ed.; Yongfang Li, Springer Int. Pub., Switzerland, 2015.

10. Long Y. and Hou J., *Conjugated Polymer Photovoltaic Materials in Organic Electronic Materials; Lecture Notes in Chemistry 91*, Ed.; Yongfang Li, Springer Int. Pub., Switzerland, 2015.

11. Guan X., Liu S., Huang F., *Conjugated Polymer Electroluminescent Materials in Organic Electronic Materials; Lecture Notes in Chemistry, 91*, Ed.; Yongfang Li, Springer Int. Pub., Switzerland, 2015.

12. Jensen J., Hösel M., Dyer A. L., Krebs F. C., *Adv. Func. Mater.*, 2015, 25, 2073.

13. Chiang C.K., Fincher C.R., Park Y.W., Heeger A.J., Shirakawa H. Louis E.J., Gau S.C., MacDiarmid A.G., *Phys. Rev. Lett.*, 1978, 40, 1472.

14. Chiang C.K., Fincher C.R., Park Y.W., Heeger A.J., Shirakawa H., Louis E.J., Gau S.C., MacDiarmid A.G., *Phys. Rev. Lett.*, 1977, 39, 1098.

15. Letheby, H. *Journal of the Chemical Society*, 1862, 15, 61.

16. Jozefowicz M., Buvet R.C., *C. R. Acad. Sc. Fr*., 1961, 253, 1801.

17. Jozefowicz M., Buvet R.C., *C. R. Acad. Sc. Fr.*, 1962, 254, 284.7

18. McNeill R., Siudak R., Wardlaw J.H., Weiss D.E., *Aust. J. Chem.*, 1963, 16, 1056.

19. Bolto B.A., McNeill R., Weiss D.E., *Aust. J. Chem.*, 1963, 16, 1090.

20. Watson W.H.Jr., McMordie W.C. Jr., Lands L.G., *J. Polym. Sci.*, 1961, 55, 137.

21. Hatano M., Kambara S., Shigeharu O., *J. Polym. Sci*,. 1961, 51, S26.

22. Berets D.J., Smith D.S., *Trans. Farad. Soc.*, 1968, 64, 823.

23. Chiang, C.K., Park Y.W., Heeger A.J., Shirakawa H., Louis E.J., MacDiarmid AG., *J. Chem. Phys.*, 1978, 69, 5098.

24. Chiang, C.K., Druy M.A, Gau S.C., Heeger A.J., Louis E.J., MacDiarmid A.G., Park Y.W., Shirakawa H., *J. Am. Chem. Soc.*, 1978, 100, 1013.

25. Reynolds J.R., Chien J.C.W., Karasz F.E., Lillya C.P., Curran D.J., *J. Phys., Coll.*, 1983, 171.

26. Diaz A.F., Kanazawa K.K., Gardini G.P., J. Chem. Soc., *Chem. Commun.*, 1979, 635.

27. Kanazawa K.K., Diaz A.F., Geiss R.H., Gill W.D., Kwak J.F., Logan J.A., Rabolt J. F., Street G.B., J. Chem. Soc., *Chem. Commun.*, 1979, 854.

28. Dall'Olio A., Dascola G., Varacca V., Bocchi V., *Comptes Rendus des Seances de l'Academie des Sciences, Serie C: Sciences Chimiques*, 1968, 267, 433.

29. Facchetti A., *Materials Today*, 2013, 16, 123.

30. Jang J., Chang M., Yoon H., *Adv. Mater.*, 2005, 17, 1616-1620.

31. Levermore P.A., Jin R., Wang X., Chen L., Bradley D.D.C., de Mello J.C., *J. Mater. Chem.*, 2008, 18, 4414-4420.

32. Kang H.S., Kang H.-S., Lee J.K., Joo J., *Nonlin. Opt. Phys. Mater.*, 2004, 13, 633-639.

33. Ng, K. K., *Complete Guide to Semiconductor Devices,* McGraw-Hill: New York, 1995.

34. Roncali, J., *Chemical Reviews,* 1997, 97, 173.

35. Lyons, L. E., *Aust. J. Chem.,* 1980, 33, 1717.

36. Abdulrazzaq M., İçli Özkut M., Gokce G., Ertan S., Tutuncu E., Cihaner A., *Electrochim Acta,* 2017,249, 189-197.

37. Wudl F., Heeger A. J., Patil A. O., *Chem. Rev.*, 1988, 88, 188-200.

38. Reddinger J. L., Reynolds J. R., *Advances in Polymer Science*, 1999 45 59.

39. Cihaner A., Algi F., *Adv. Funct. Mater.*, 2008, 18, 3583.

40. Shirakawa, H., MacDiarmid A. G., Chiang C. K., Heeger A., *J. Chem. Soc., Chem. Commun.*, 1977, 578.

41. Nigrey P. J., MacDiarmid A. G., Heeger A. J., *J. Chem. Soc., Chem. Commun.*, 1979,594.

42. Kroon R., Lenes M., Hummelen J.C., BlomP.W.M., de Boer B., *Polymer Reviews,* 2008,48:531–582.

43. Bredas J. L, Street G. B., Themans B., Andre J. M., *J. Chem. Phys.*, 1985, 83, 1323.

44. Bredas J. L, *J. Chem. Phys.*, 1985, 82, 3808.

45. Andersson M. R., Thomas O., Mammo W., Svensson M., Theander M., Inganas O., *J. Mater. Chem.,* 1999, 9, 1933.

46. Hoffmann K. J., Bakken E., Samuelsen E. J., Carlsen P. H. J., *Synth. Met.*, 2000, 113, 1-2, 39.

47. Guay J., Kasai P., Diaz A., Wu R., Tour J. M., and Dao L. H., *Chem. Mater.*, 1992, 4,1097.

48. Hoffmann K. J., Graskopf A. L., Samulesen E. J., Carlsen P. H. J., *Synth. Met.*, 2000, 113, 1-2, 89.

49. Sato M., and Hiroi, M., *Synth. Met.*, 1995, 71, 2085.

50. Sotzing G. A., Reddinger J. L., Katritzky A. R., Soloducho J., Musgrave R., Reynolds J. R., *Chem. Mater.*, 1997, 9, 1578.

51. Rajca A., Miyasaka M., Pink M., Wang H., Rajca S., *J. Am. Chem. Soc*,. 2004,126, (46), 15211.

52. Witker D., Reynolds J. R., *Macromolecules*, 2005, 38, 18, 7636-7644.

53. Siddiqui S., Spano F. C., *Chem. Phys. Lett.*, 1999, 308, 99.

54. Elschner A., Kirchmeyer S., Lövenich W., Merker U., Reuter K., *PEDOT; Principles and Applications of Intrinsically Conductive Polymer*, CRC Press, Boca Raton, FL, 2011.

55. Stephan O., Schottland P., Le Gall, P.-Y., Chevrot C., Mariet C., Carrier M., *J. Electroanal. Chem.*, 1998, 443, 217-226.

56. Darmanin T., Nicolas M., Guittard F., *Langmiur*, 2008, 24, 9739-9746.

57. Karlsson R. H., Herland A., Hamedi M., Wigenius J. A., Aslund A., Liu X., Fahlman M., Inganas O., Kondradsson P., *Chem. Mater.*, 2009, 21, 1815-1821.

58. Kumar A., Reynolds J. R., *Macromolecules*, 1996, 29, 7629-7630.

59. Patra A., Wijsboom Y.H., Zade S.S., Li M., Sheynin Y., Leitus G., Bendikov M., *J. Am. Chem. Soc.*, 2008, 130 (21), 6734-6736.

60. Byeonggwan Kim, Jeonghun Kim, and Eunkyoung Kim, *Macromolecules*, 2011, 44, 8791–8797.

61. İçli-Özkut M., Mersini J., Önal A.M., Cihaner A., *J. of Polymer Chem.*, 2012, 50, 615.

62. Atak S., Icli-Ozkut M., Önal A.M., Cihaner A., *J. Polym. Sci. Part A: Polym. Chem.*, 2011, 49, 4398-4405.

63. Patra A., Wijsboom Y.H., Leitus G., Bendikov M., *Org. Lett.*, 2009,11, 7, 2009.

64. Pittelkow M., Reenberg T.K., Nielsen K.T., Magnussen M.J., Sølling T.I., Krebs F.C., Christensen J.B., *Angew. Chem. Int. Ed.*, 2006, 45, 5666 –5670.

65. Kaur M., Yang D.-S, Shin J., Lee T.W., Choi K., Cho M.J., Choi D.H., *Chem. Commun.*, 2013, 49, 5495—5497.

66. Carrera E. I. and Seferos D.S., *Macromolecules*, 2015, 48, 297−308.

67. Cihaner A., *Synlett*, 2015, 26, 4, 449.

68. Patra A., Bendikov M., *J. Mater. Chem.*, 2010, 20, 422.

69. Zade S. S., Zamoshchik N., Bendikov M., *Acc. Chem. Res.*, 2011, 44, 14.

70. Wijsboom Y.H., Patra A., Zade S.S., Sheynin Y., Li M., Shimon L.J.W., Bendikov M., *Angew. Chem. Int. Ed.*, 2009, 48, 5443.

71. Wijsboom Y.H., Sheynin Y., Patra A., Zamoshchik N., Vardimon R., Leitus G., Bendikov M., *J. Mater. Chem.*, 2011, 21, 1368.

72. Zade S.S.;,Bendikov M., *Org. Lett.*, 2006, 8, 5243.

73. Zade, S.S., Zamoshchik N., Bendikov M., *Chem. Eur. J.*, 2009, 15, 8613.

74. Aqad E., Lakshmikantham M.V., Cava M.P., *Org. Lett.*, 2001, 3,4283.

75. Li M., Patra A., Sheynin Y., Bendikov M., *Adv. Mater. (Weinheim,Ger.)*, 2009, 21, 1707.

76. Li M., Sheynin Y., Patra A., Bendikov M., *Chem. Mater.*, 2009, 21, 2482.

77. Lu X., Zhang W., Wang C., Wen T.-C, Wei Y., *Progress in Polymer Science*, 2011, 36, 671-712.

78. Gangopadhyay R., De A., *Chem. Mater.*, 2000, 12, 608.

79. Zhan C., Yu G., Wang L., Wujcik E., Wei S., *J. Mater. Chem. C*, 2017, 5, 1569-1585.

80. Cochet M., Maser W. K., Benito A. M., Callejas M. A., Martinez M. T., Benoit J. M., Schreiber J., Chauvet O. *Chem. Commun.*, 2001, 1450-1451.

81. Maser W. K., Benito A. M., Callejas M. A., Seeger T., Martinez M. T., Schreiber J. Muszynski J., Chauvet O., Osvath Z., Koos A. A., Biro L. P., *Mat. Sci. & Eng. C*, 2003, 23, 87-91.

82. Philip B., Xie J., Chandrasekhar A., Abraham J., Varadan V. K., *Smart Mater. Struct.*, 2004, 13, 295-298.

83. Chen J. H., Huang Z. P., Wang D. Z., Yang S. X., Li W. Z., Wen J. G., Ren Z. F., *Synth. Met.*, 2002, 125, 289-294.

84. Chen J. H., Huang Z.P., Wang D.Z., Yang S.X., Wen J.G., Ren Z.F., *Appl. Phys. A*, 2001, 73, 129-131.

85. Wang C., Guo Z.-X., Fu S., Wu W., Zhu D., *Prog. Polym. Sci.*, 2004, 29, 1079-1141.

86. G. Yu, J. Gao, J.C. Hummelen, F. Wudl, A.J. Heeger, *Science*, 1995, 70, 1789-1791

87. Mendez-Vilas A., Solan-Martin A., *Polymer science: research advances, practical applications and educational aspects*, Formatex, Spain, 2016.

88. Zhang J., Zhao X. S., *J. Phys. Chem. C*, 2012, 116, 5420-5426.

89. Bhandari S., Deepa M., Sharma S. N., Joshi A. G., Srivastava A. K., Kant R., *J. Phys. Chem.C*, 2010, 114, 14606–14613.

90. Hartmann-Thompsn C., *Applications of Polyhedral Oligomeric Silsesquioxanes*, Springer, Dordrecht Heidelberg London New York, 2011.

91. Cordes D. B., Lickiss P. D., Rataboul F., *Chem. Rev.*, 2010, 110, 2081-2173.

92. Li G., Wang L., Ni H., Pittman Jr. C. U., *J Inorg Organomet Polym Mater.*, 11, 3, 123-154.

93. Kuo S.-W., Chang F.-C., *Progress in Polymer Science*, 2011, 36, 1649-1696.

94. Koo J. H., *Polymer Nanocomposites; Processing, Characterization and Applications*, McGraw Hill, New York, 2006.

95. Ayandele E., Sarkar B., Alexandridis P., *Nanomaterials*, 2012, 2, 445-475.

96. Gnanasekaran D., Madhavan K., Reddy B. S. R., *J Sci Ind Res*, 2009, 68, 437-464.

97. Xu H., Kuo S.-W., Lee J.-S., Chang F.-C., *Polymer*, 2002, 43, 19, 5117-5124.

98. Haddad T. S., Lichtenhan J. D., *Macromolecules*, 1996, 29, 22, 7302-7304.

99. Wang J., Ye Z., Joly H., *Macromolecules*, 2007, 40, 6150-6163.

100. Milliman H. W., Ishida H., Schiraldi D. A., *Macromolecules*, 2012, 45, 4650–4657.

101. Yang C. C., Chang F. C., Wang Y. Z., Chan C. M., Lim C. L., Chen W. Y., *J Polym Res.*, 2007, 14, 431-439.

102. Lichtenhan J. D., Otonari Y. A., Carr M. J., *Macromolecules*, 1995, 28, 8435.

103. Li G. Z., Yamamoto T., Nozaki K., Hikosaka M., *Polymer*, 2000, 41, 8, 2827.

104. Misra R., Fu B. X., Morgan S. E., *J Polym Sci Part B*, 2007, 45, 2441-2455.

105. Ye Q., Zhou H., Xu J., *Chem. Asian J.*, 2016, 11, 1322-1337.7

106. Xiao S., Nguyen M., Gong X., Cao Y., Wu H., Moses D., Heeger A. J., *Adv. Func. Mater.*, 2003, 13, 25-29.

107. Chi H, Lim SL, Wang F, Wang X, He C, Chin WS, *Macromol. Rapid Comm.*, 2014, 35, 801.

108. Xiong S, Jia P, Mya KY, Ma J, Boey F, Lu X, *Electrochim. Acta,* 2008, 53 3523.

109. Xiaong S, Xiao Y, Ma J, Zhang L, Lu X, *Macromol. Rapid Comm.*, 2007, 28, 281.

110. Ak M, Gacal B, Kiskan B, Yagci Y, Toppare L, *Polymer*, 2008, 49, 2202.

111. Wei B., Liu J., Ouyang L., Martin D.C., *J. Mater. Chem. B*, 2017, 5, 5019-5026.

112. Hoffmann M.R., Martin S.T., Choi W., Bahnemann DW., *Chem. Rev.*, 1995, 95, 69.

113. Pelaez M., Nolan N. T. Pillai S.C., Seery M.K., Falaras P., Kontos A.G., Dunlop P.S.M., Hamilton J.W.J., Byrne J.A., O'Shea K., Entezari M.H., Dionysiou D.D., *Appl. Catal. B*, 2012, 125, 331.

114. Xue M., Huang L., Wang,J.Q., Wang Y., Ga, L., Zhu J H., Zou Z.G., *Nanotechnology*, 2008, 19, 185604.

115. Hernandez-Alonso M.D., Fresno F., Suarez S., Coronado J.M., *Energy Environ. Sci.*, 2009, 2, 1231.

116. Marin M.L., Juanes L.S., Arques A., Amat A.M., Miranda, M.A., *Chem. Rev.,* 2012, 112, 1710.

117. Yanagida, S., Kabumoto, A., Mizumoto, K., Pac, C., Yoshino, K., *J. Chem. Soc., Chem. Commun.*, 1985, 474.

118. Jen K. Y., Miller G. G. and Elsembaumer, R. L. J., *Chem. Soc., Chem. Commun.*, 1986, 1346.

119. Osterholm J.-E., Laakso J., Nyholm P., Isotalo H., Stubb H., Inganas O. and Salaneck W. R., *Synth. Met.*, 1989, 28, C435.

120. Mabbott G. A., *J. Chem. Educ.*, 1983, 60, 9, 697.

121. Zanello P., *Inorganic Electrochemistry: Theory, Practice and Application*, 1st Ed., The Royal Society of Chemistry, 2003, 606 pgs.

122. Granqvist C.G., Avendaño C. G., Azens A., *Thin Solid Films*, 2003, 442, 201-211.

123. Lee E.S., Tavil, A. *Building and Environment*, 2007, 42, 6, 2439-2449.

124. Cirpan A., Argun A. A., Grenier C. R. G., Reeves B. D., Reynolds J. R., *J. Mater. Chem.*, 2003, 13, 2422.

125. Singh B., Parwate D. V., Shukla S. K., *AAPS PharmSciTech*, 2009, 10, 1, 34-43.

126. Wyszecki G., Stiles W. S., *Color Science: Concepts and Methods, Quantitative Data and Formulae*, 2nd ed.; Wiley: Hoboken, NJ, 2000.

127.İçli-Özkut M., Mersini J., Önal A.M., Cihaner A., *J. of Polymer Chem*., 2012, 50, 615.

128. Karabay B., Pekel L. C., Cihaner A., *Macromolecules*, 2015, 48(5), 1352.

129. Patra A., Bendikov M., Chand S., *Accounts Chem. Res.*, 2014, 47, 1465.

130.J. Pommerehne, H. Vestweber, W. Guss, R.F. Mahrt, H. Bässler, M. Porsch, J. Daub, *Adv. Mater.*, 1995, 7, 551.

131.C.M. Cardona, W. Li, A.E. Kaifer, D. Stockdale, G.C. Bazan, *Adv. Mater.*, 2011, 23, 2367.

132. Alarabi-Ahmed, M.M., *Investigation Of The Photocatalytic Activity Of Palladium Nanoparticles Added PEDOT*, Ms Thesis, January 2017.

133. Ertan S., KaynakC., Cihaner A., *J. Polym. Sci. Part A: Polym. Chem.*, 2017, 55 (23), 3935.

134. Zhang T., Wang J., Zhou M., Ma L., Yin G., Chen G., Li Q., *Tetrahedron*, 2014, 70, 2478.

135. Chen K.B., Chang Y.P., Yang S.H., Hsu C.S., *Thin Solid Films*, 2006, 514, 103.

136. Liras M., Pintado-Sierra M., Amat-Guerri F., Sastre R., J. *Mater. Chem.*, 2011, 21, 12803.

137. Ponder Jr. J.F., Österholm A.M., Reynolds J.R., *Macromolecules*, 2016, 49(6), 2106-2111.

138. Krishnamoorthy K., Ambade A.V., Kanungo M., Contractor A.Q., Kumar A., *J. Mater. Chem*., 2001, 11, 2909.

139. Heinze J., Rasche A., Pagels M., Geschke B., *J. Phys. Chem.* B, 2007, 111, 989-997.

140. Le T.-H., Kim Y., Yoon H., *Polymers*, 2017, 9, 150.

141. Hagiwara T., Yamaura M., Sato K., Hırasaka M., Iwata K., *Synth. Met.*, 1989, 32, 367.

142. Szkurlat A., Palys B., Mieczkowski J., Skompska M., *Electrochim. Acta*, 2003, 48, 3665.

143. Welsh D.M., Kumar A., Meijer, E.W., Reynolds J.R., *Adv. Mater.*, 1999, 11, 1379.

144. Gaupp C.L.. Wels D.M., Reynolds J.R., *Macromol. Rapid Commun.*, 2002, 23, 885.

145. Reeves B.D., Grenier C.R.G., Argun A.A., Cirpan A., McCarley T.D., Reynolds J.R., *Macromol.*, 2004, 37, 7559.

146. Mishra S.P., Krishnamoorthy K., Sahoo R., Kumar A., *J. Polym. Sci. A: Polym Chem.*, 2005, 43, 419.

APPENDIX A

NMR DATA OF MONOMERS

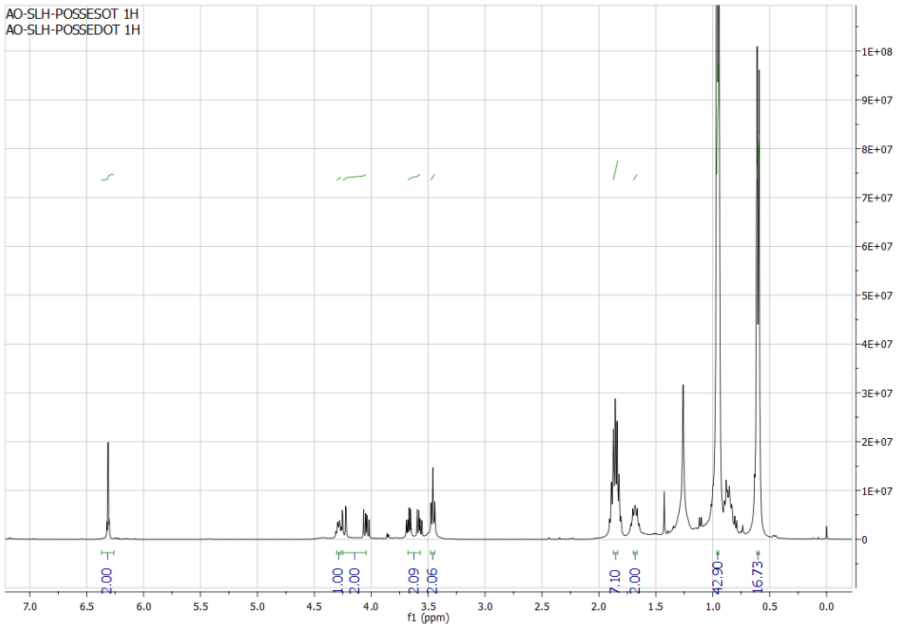

Figure A.1 ^{1}H NMR spectrum of EDOT-POSS in d-$CHCl_3$.

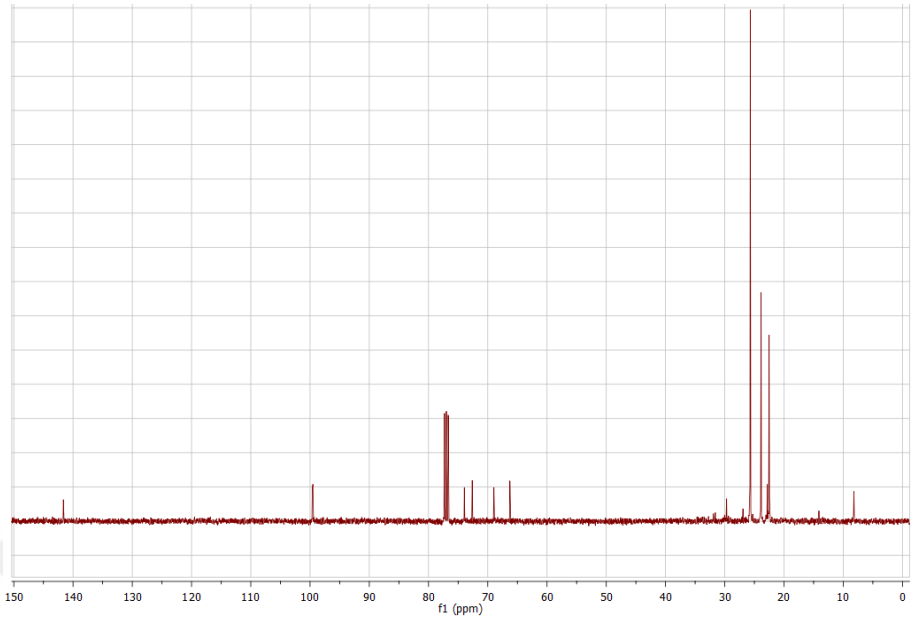

Figure A.2 ^{13}C NMR spectrum of EDOT-POSS in d-$CHCl_3$.

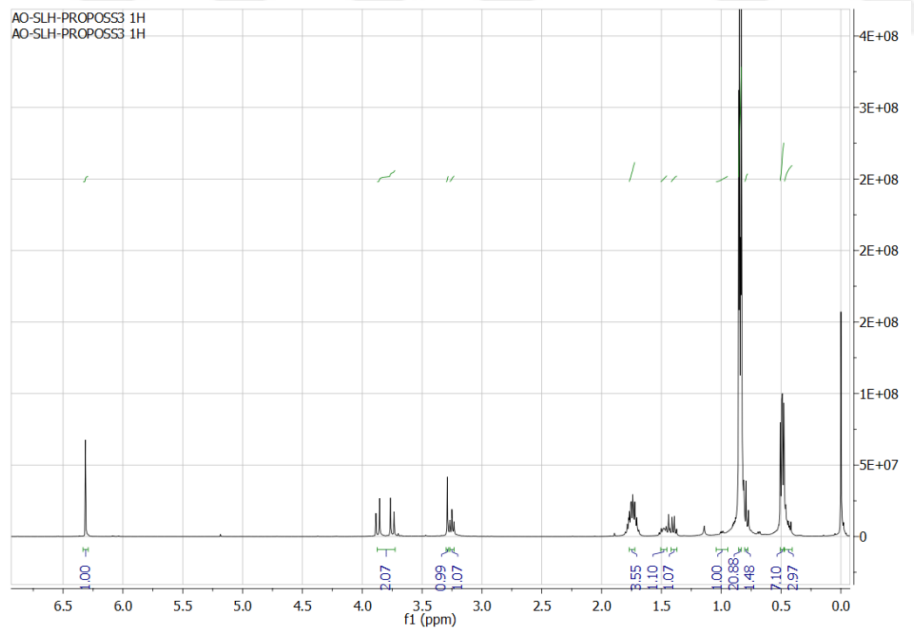

Figure A.3 ^{1}H NMR spectrum of ProDOT-POSS in d-$CHCl_3$.

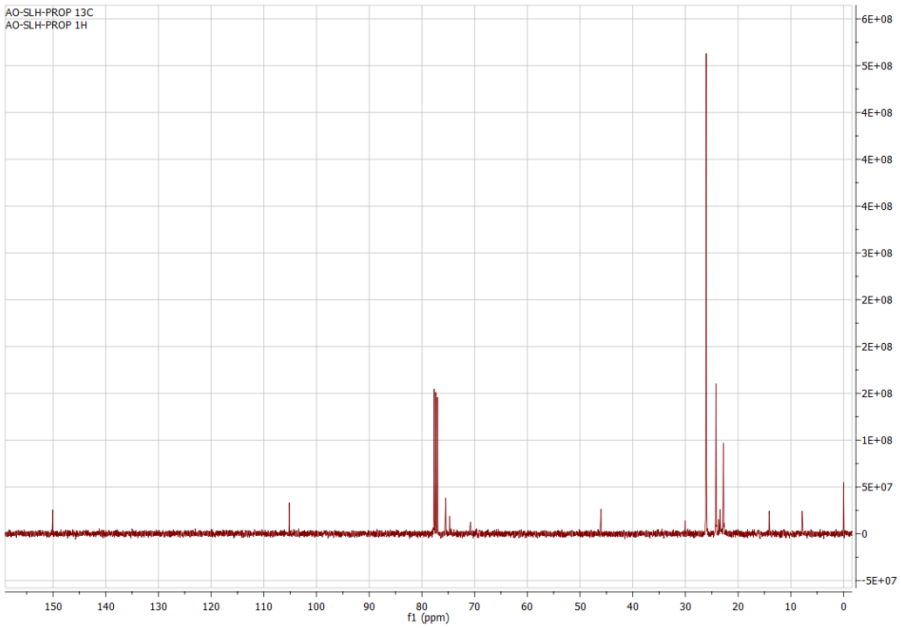

Figure A.4 ^{13}C NMR spectrum of ProDOT-POSS in d-$CHCl_3$.

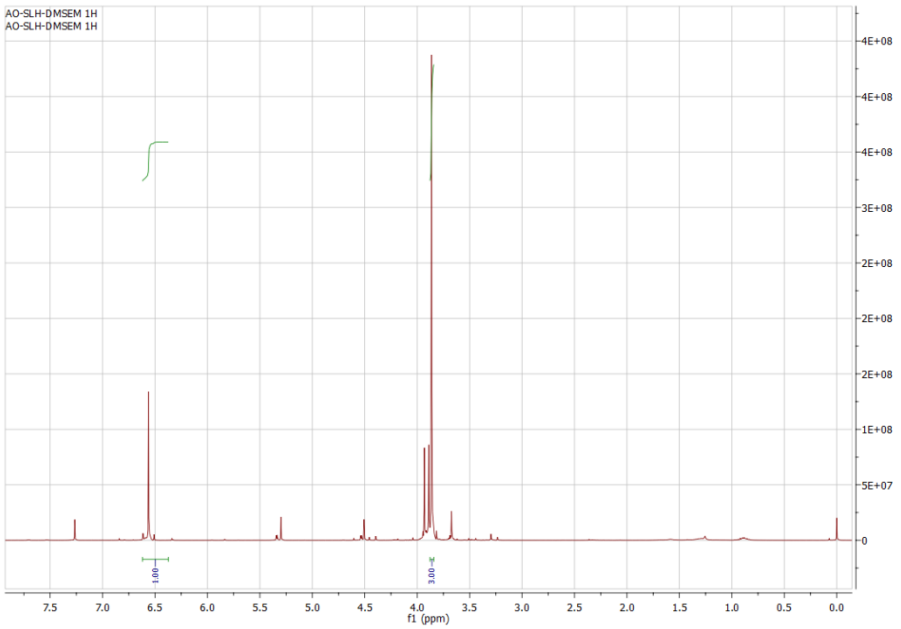

Figure A.5 ^{1}H NMR spectrum of 3,4-dimethoxy selenophene in d-$CHCl_3$.

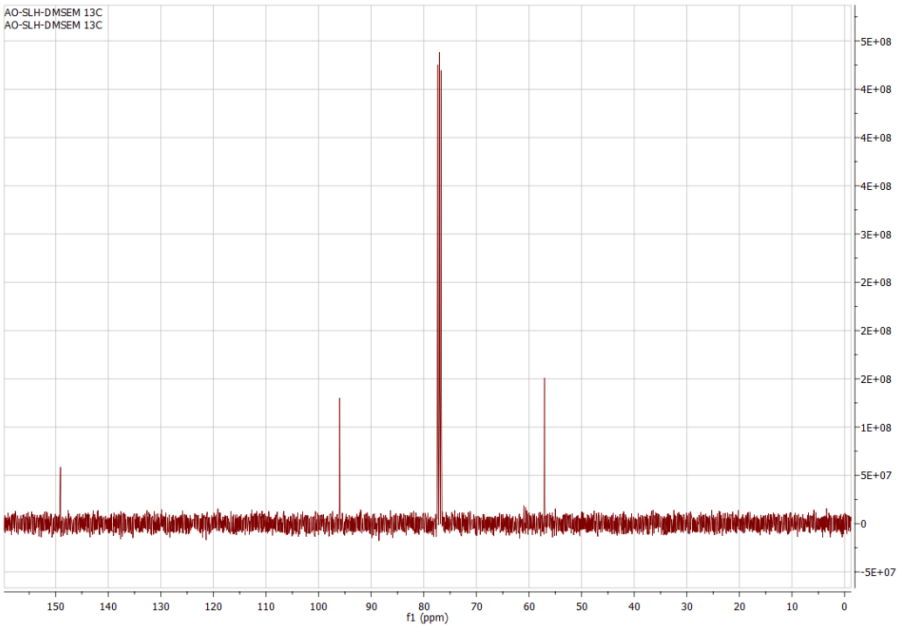

Figure A.6 ^{13}C NMR spectrum of 3,4-dimethoxy selenophene in d-$CHCl_3$.

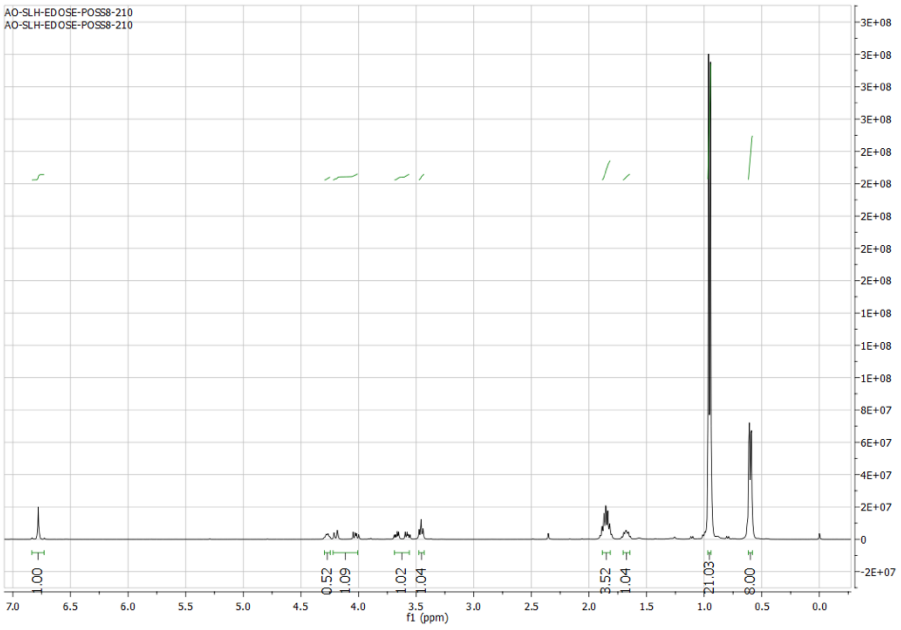

Figure A.7 ^{1}H NMR spectrum of EDOS-POSS in d-$CHCl_3$.

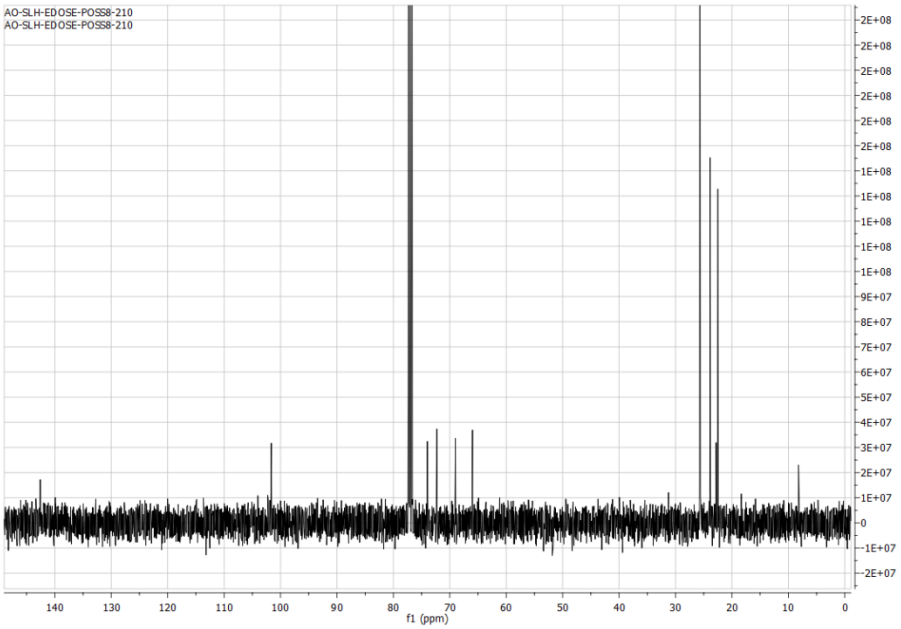

Figure A.8 ^{13}C NMR spectrum of EDOS-POSS in d-$CHCl_3$.

APPENDIX B

FTIR SPECTRA OF MONOMERS

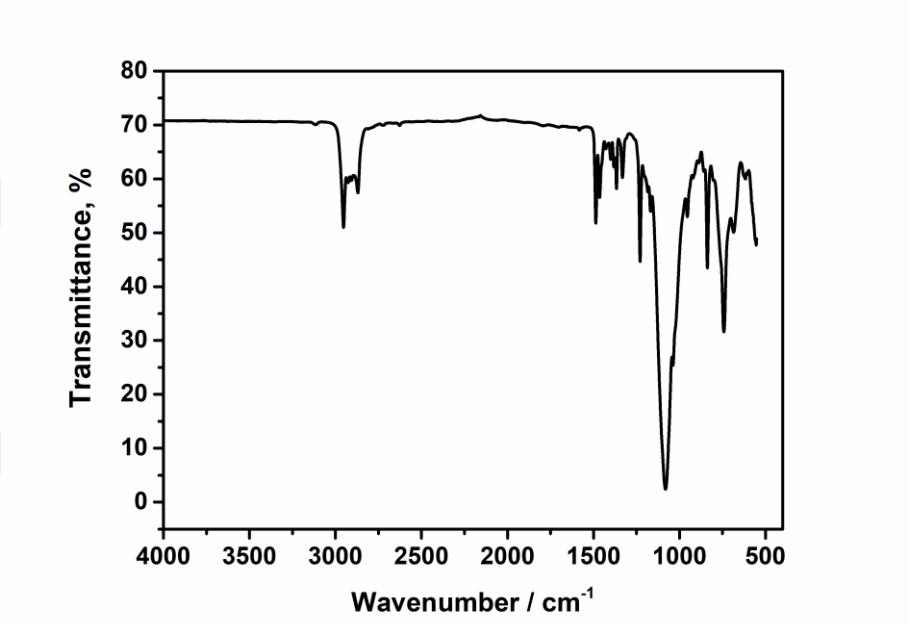

Figure B.1 FTIR spectrum of EDOT-POSS.

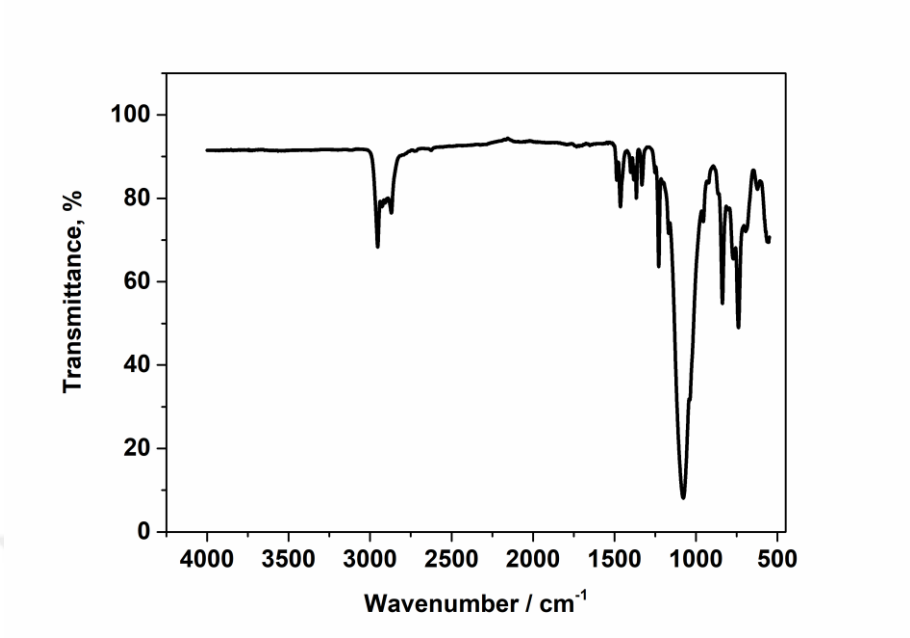

Figure B.2 FTIR spectrum of ProDOT-POSS.

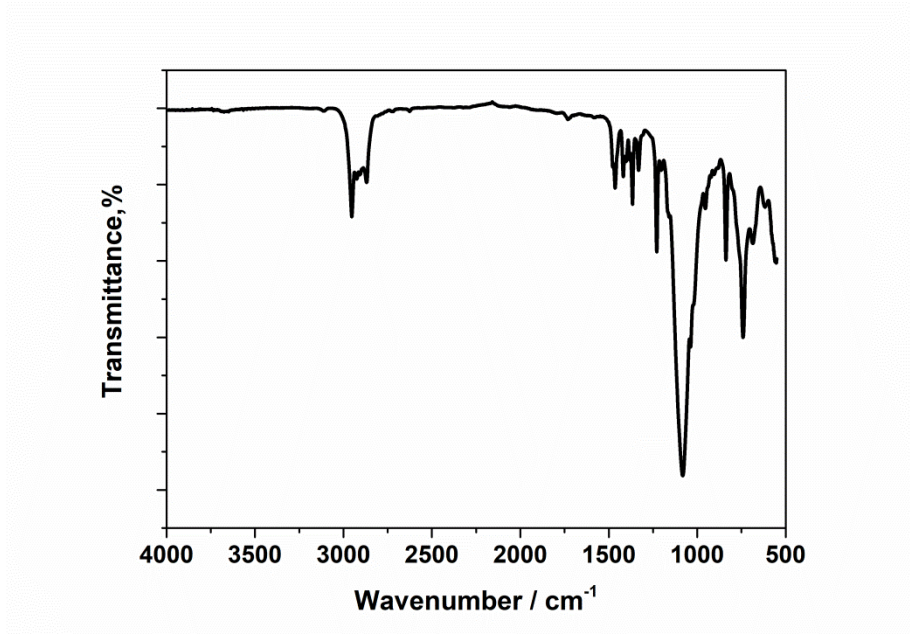

Figure B.3 FTIR spectrum of EDOS-POSS.

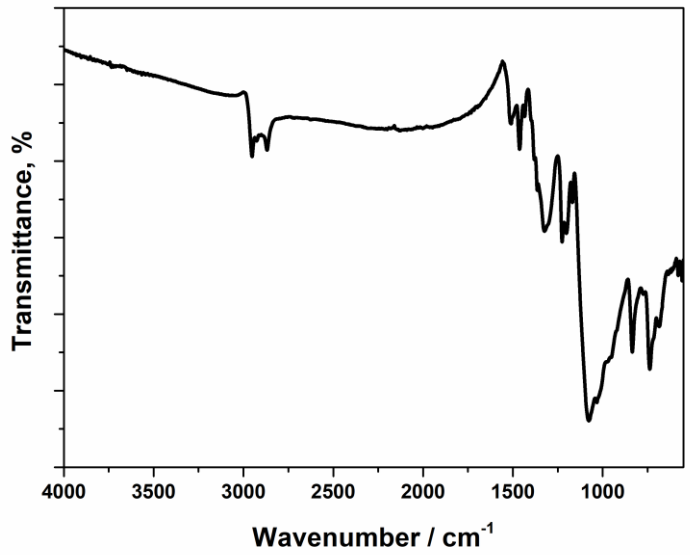

Figure B.4. FTIR spectrum of PEDOT-POSS obtained via constant potential electrolysis at 1.5 V in an electrolyte solution of 0.1 M TBAH dissolved in the mixture of dichloromethane and acetonitrile (1/3: v/v) on ITO electrode.

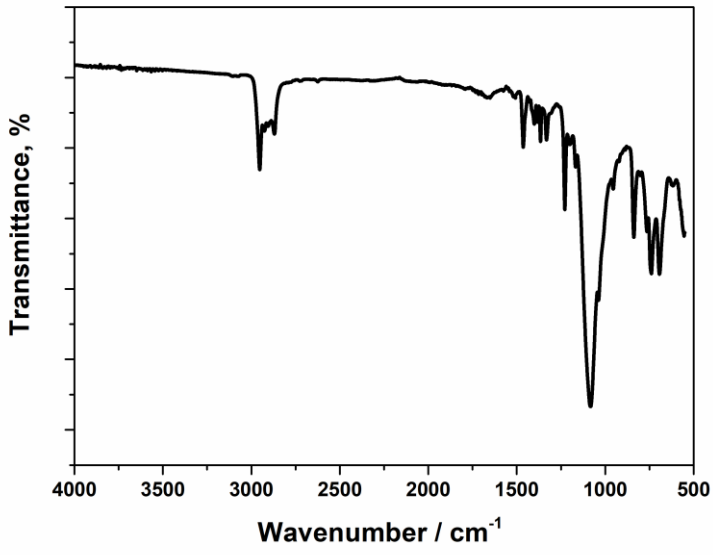

Figure B.5. FTIR spectrum of chemically obtained PEDOT-POSS.

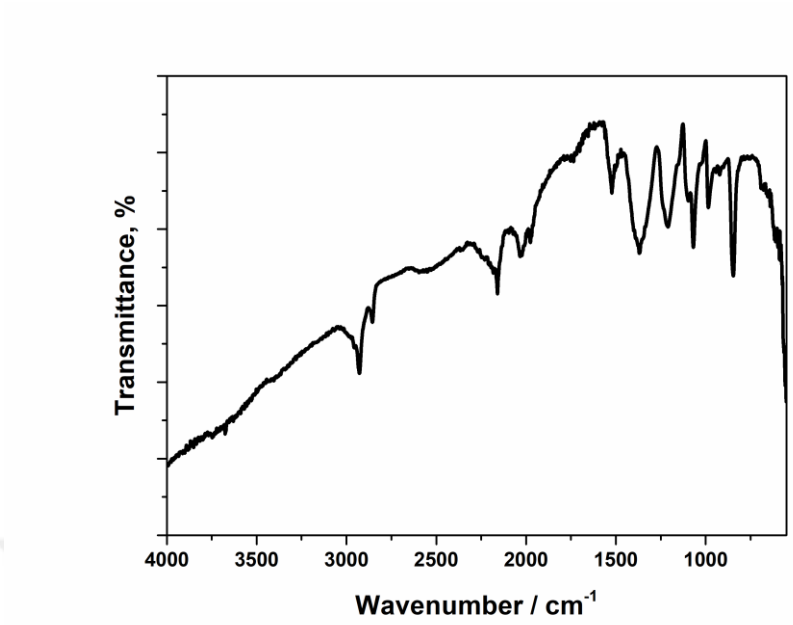

Figure B.6. FTIR spectrum of electrochemically obtained Poly(EDOT-POSS-co-EDOT).

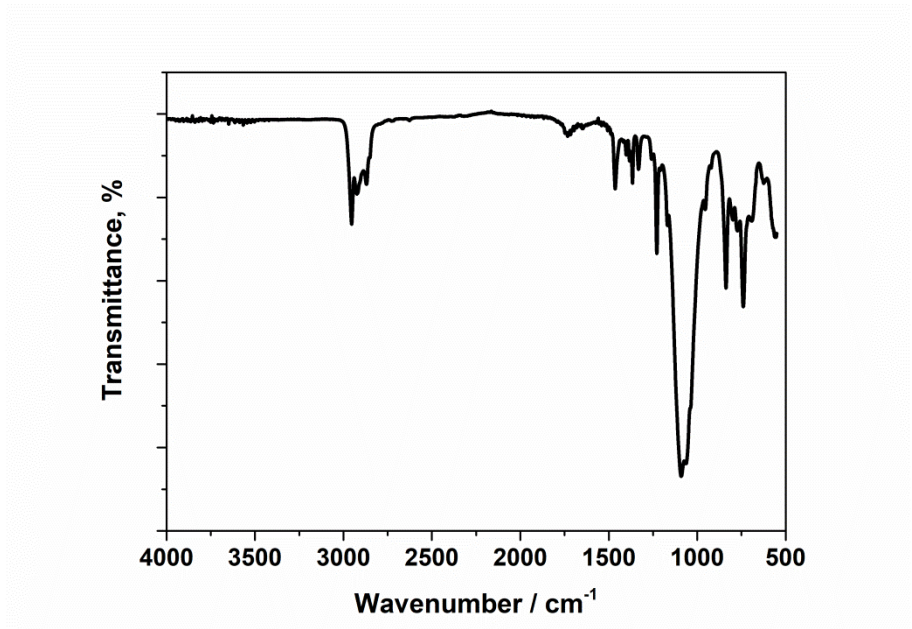

Figure B.7. FTIR spectrum of chemically obtained PProDOT-POSS.

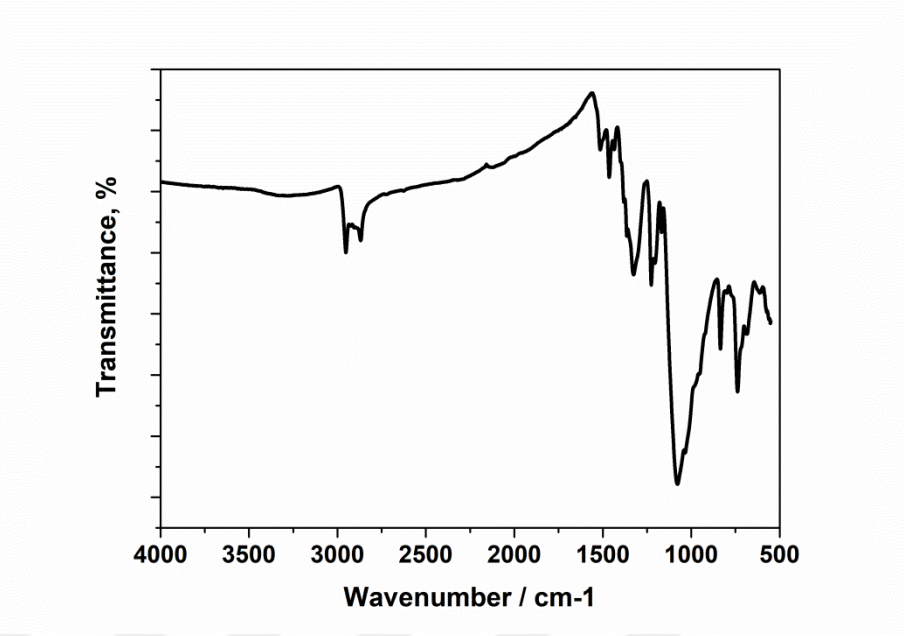

Figure B.8. FTIR spectrum of chemically obtained PEDOS-POSS.

APPENDIX C

HRMS DATA OF MONOMERS

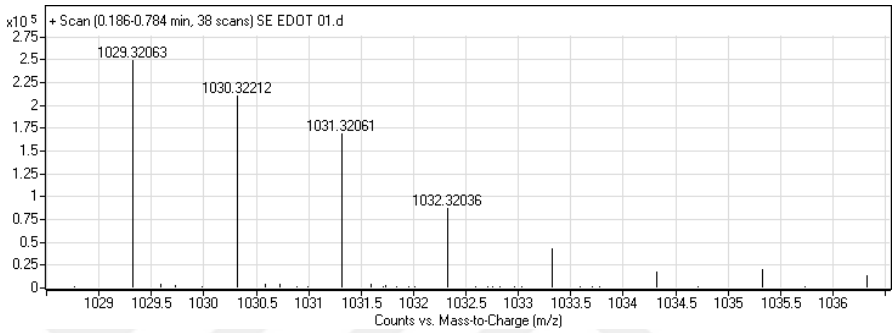

Figure C.1. HRMS data of EDOT-POSS monomer (ESI) *m/z*: calcd for $C_{38}H_{76}O_{15}Si_8$, 1029.31; found 1029.32

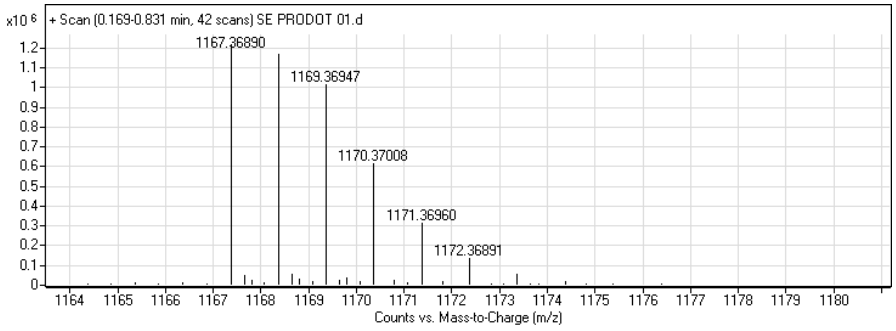

Figure C.2. HRMS data of ProDOT-POSS monomer (ESI) *m/z*: calcd for $C_{43}H_{88}O_{16}Si_9$, 1044.37; found 1067.37. It might capture a Na ion from the solvent.

APPENDIX D

TGA DATA OF POLYMERS

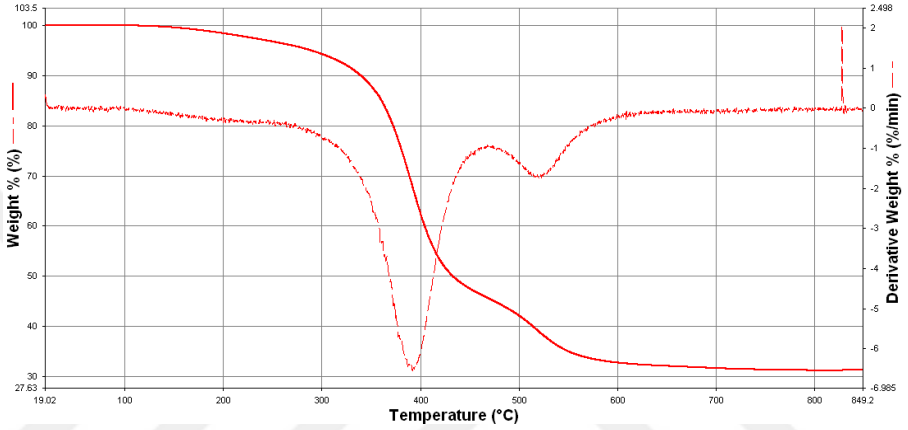

Figure D.1. TGA analysis of chemically obtained PEDOT-POSS.

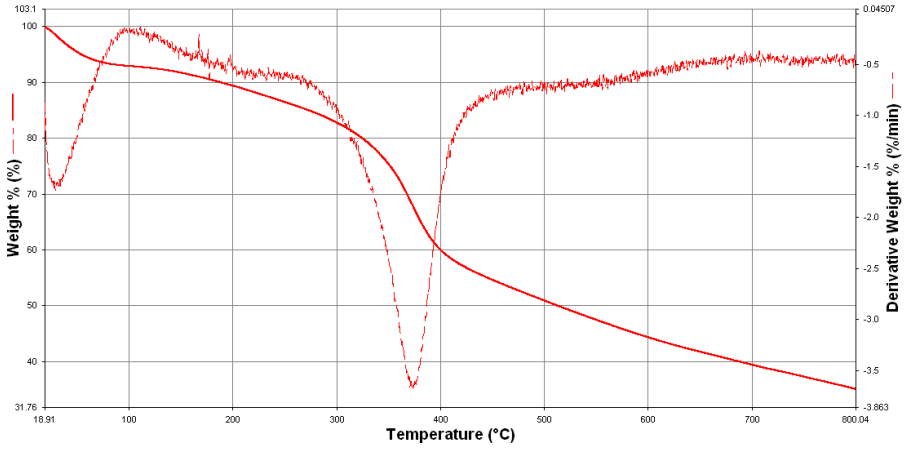

Figure D.2. TGA analysis of chemically obtained PEDOT.

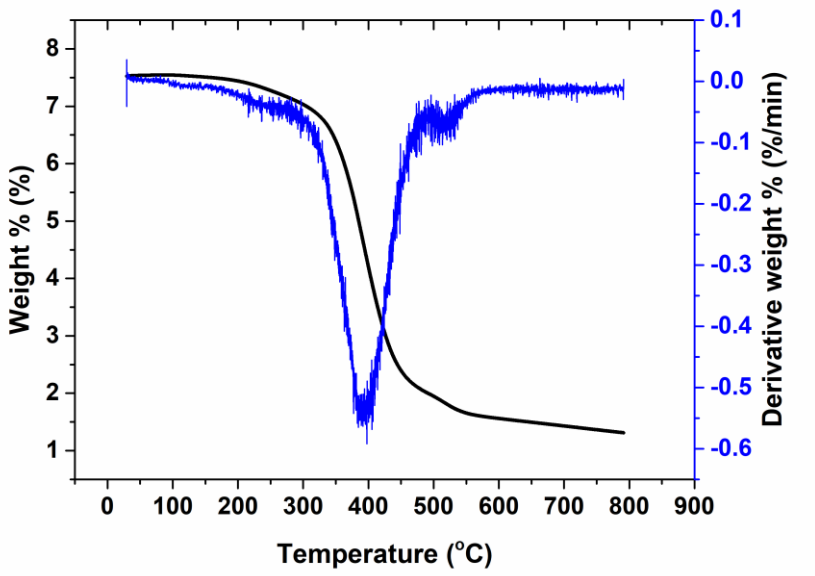

Figure D.3. TGA analysis of chemically obtained ProDOT-POSS.

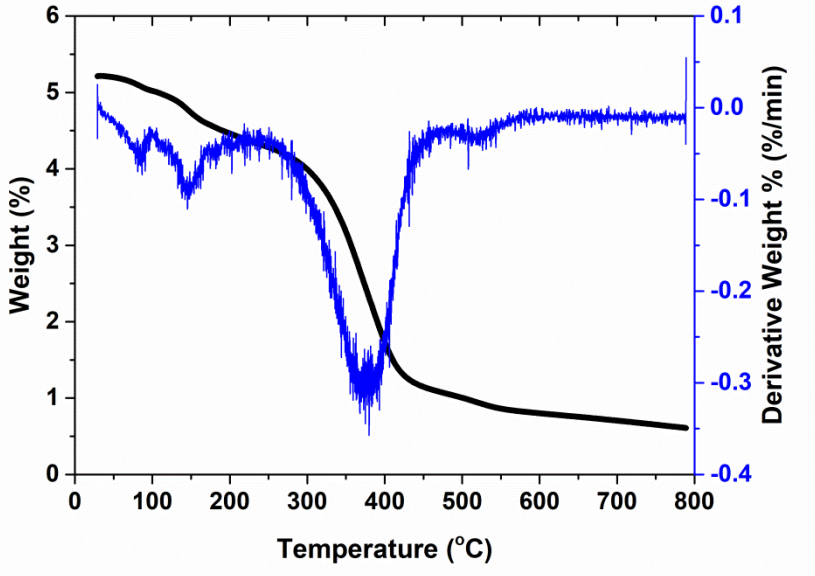

Figure D.4. TGA analysis of chemically obtained PEDOS-POSS.

APPENDIX E

GPC DATA OF POLYMERS

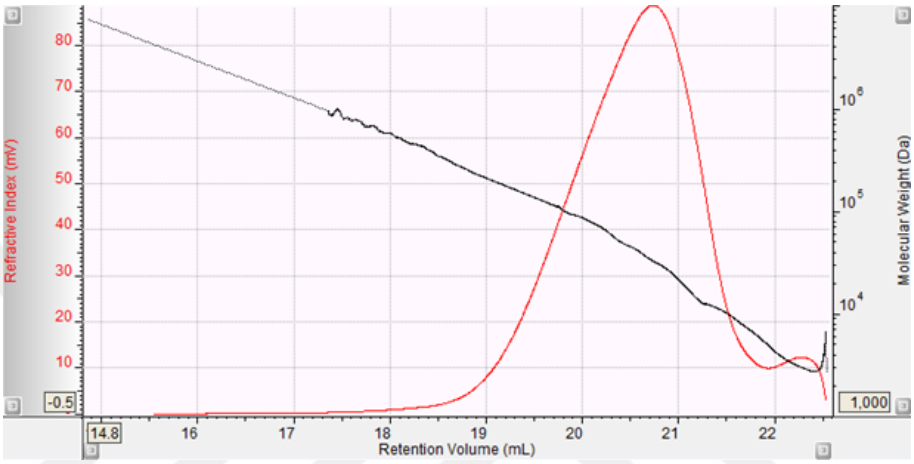

Figure E.1. GPC chromatogram of chemically obtained PEDOT-POSS in tetrahydrofuran.

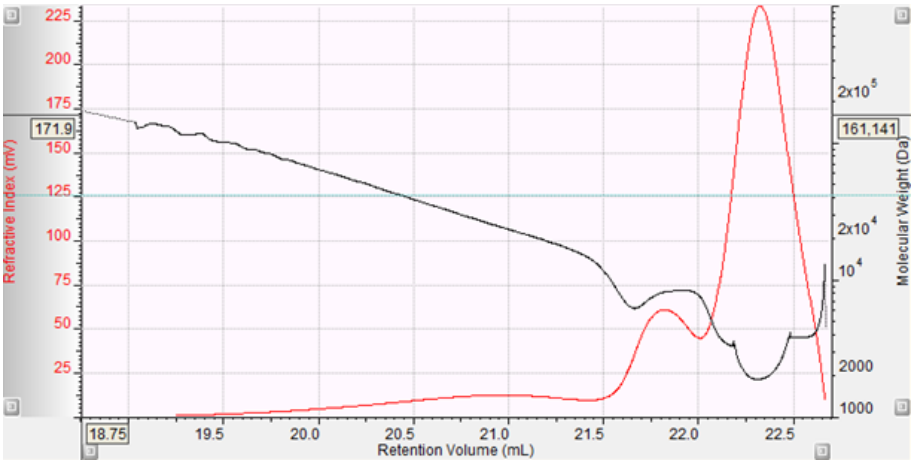

Figure E.2. GPC chromatogram of electrochemically obtained PEDOT-POSS in tetrahydrofuran.

APPENDIX F

CHEMICAL STRUCTURES OF PRODOT DERIVATIVES

Name	Structure
PProDOT-Me_2	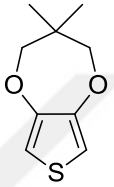
PProDOT-Et_2	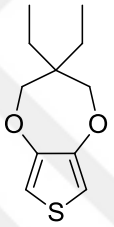
PProDOT-Bu_2	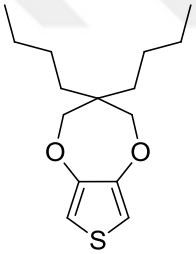
PProDOT-Hex_2	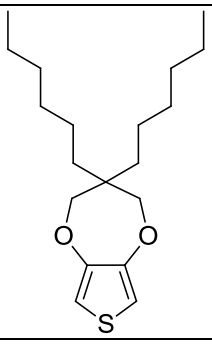

PProDOT-EtHex$_2$	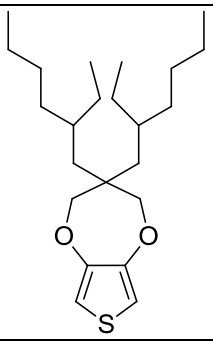
PProDOT-Dec$_2$	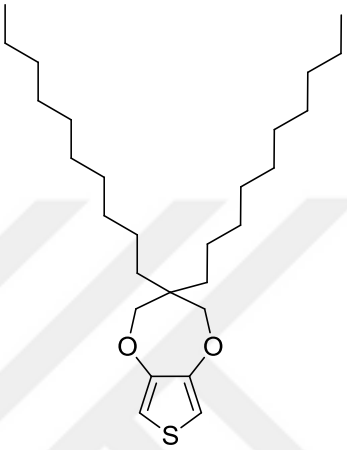
PProDOT-Dodec$_2$	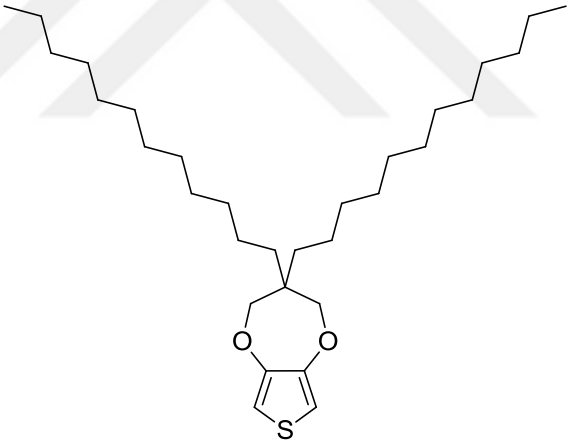
PProDOT-Bz$_2$	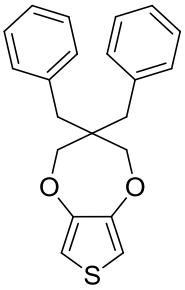

CURRICULUM VITAE

SALİH ERTAN

PERSONAL INFORMATION

Date and Place of Birth : 20.06.1983 SAKARYA

Address : Atılım University, Department of Chemical Engineering and Applied Chemistry, 06836, Gölbaşı, ANKARA.

EDUCATION

2017	Ph.D., Polymer Science and Technology, Middle East Technical University
2011	M.Sc., Chemistry, Middle East Technical University
2008	B.Sc., Chemistry, Middle East Technical University

EXPERIENCE

2010-now	Research Assistant, Atilim University, Ankara, Turkey

2015-2016 Visiting Scholar, Tobin Marks Group, Northwestern University, Illinois, Chicago, USA

2013-2014 Research Scientist, Scientific Research Project ATÜ-BAP-A-1314-01, Department of Chemical Engineering and Applied Chemistry, Atilim University

2008-2011 Research Scientist, Tübitak Project (108T065), Department of Chemistry, Middle East Technical University

PUBLICATIONS

---

[1] Ertan S., Şen F., Şen S., Gökağaç G., Platinum nanocatalysts prepared with different surfactants for C1-C3 alcohol oxidations and their surface morphologies by AFM, *J. Nanopart Res*, 2012, 14, 922-934.

[2] Pamuk-Algı M., Tirkeş S.,Ertan S., Cansu-Ergün E.-G.,Cihaner A., Algı F., Design and synthesis of new 4,4′-difluoro-4-bora-3a,4a-diaza-s-indacene based electrochromic polymers, *Electrochim Acta*, 2013, *109*, 766-774.

[3] Abdulrazzaq, M.; Ozkut, MI.; Gokce, G.; Ertan, S.; Tutuncu, E.; Cihaner, A. (2017), A Low Band Gap Polymer Based on Selenophene and Benzobis (thiadiazole), *Electrochim Acta*, *249*, 189-197.

[4] Ertan S., Kaynak C., Cihaner A., A platform to synthesize a soluble poly(3,4-ethylenedioxythiophene) analogue, J. Polym. Sci. Part A: Polym. Chem. 2017, 55 (23), 3935-3941.

[5] Ertan S., Cihaner A., Improvement of Optical Properties and Redox Stability of Poly(3,4-Ethylenedioxythiophene), *Dyes and Pigments*, **2018**, 149, 437-443.

CONGRESS

2012 4th National Polymer Science and Technology Congress, Çanakkale, Turkey.

2016 28th National Chemistry Congress, Mersin, Turkey.

2016 3rd International Congress on Renewable Energy Technologies, Bangkok, Thailand.

RESEARCH INTERESTS

• Synthesis, purification and characterization of novel electroactive molecules,

• Synthesis, purification and characterization of electroactive polymers,

• Investigation of electroactivity of polymers,

• Investigation of electrochromic behavior of polymers,

• Fabrication of Electrochromic Devices, Light Emitting Diodes, Solar Cells and Sensors.